MOSSY FIBER INPUT TO CA3 INTERNEURONS: BALANCING SHORT TERM PLASTICITY AND REGULATION BY PRESYNAPTIC RECEPTORS

by

Kathleen Elizabeth Cosgrove

B.S., University of Pittsburgh, 2003

Submitted to the Graduate Faculty of

College of Arts and Sciences in partial fulfillment

of the requirements for the degree of

Doctor of Philosophy

University of Pittsburgh

2010

UNIVERSITY OF PITTSBURGH

COLLEGE OF ARTS AND SCIENCES

This dissertation was presented

by

Kathleen Elizabeth Cosgrove

It was defended on

February 11, 2010

and approved by

Alison Barth, Ph.D., Biology, Carnegie Mellon University

Justin Crowley, Ph.D., Biology, Carnegie Mellon University

Nathan Urban, Ph.D., Biology, Carnegie Mellon University

External Examiner: Jean Claude Lacaille, Ph.D., Physiology, Universite de Montreal

Dissertation Chair: Stephen Meriney, Ph.D., Neuroscience, University of Pittsburgh

Dissertation Advisor: German Barrionuevo, M.D., Neuroscience, University of Pittsburgh

Copyright © by Kathleen Elizabeth Cosgrove

2010

MOSSY FIBER INPUT TO CA3 INTERNEURONS: BALANCING SHORT TERM PLASTICITY AND REGULATION BY PRESYNAPTIC RECEPTORS

Kathleen Elizabeth Cosgrove, Ph.D.

University of Pittsburgh, 2010

The hippocampus is a brain structure thought to be critically important for the formation and maintenance of memories. In order do this, the region must process information as both a linear sequence and as discrete events or objects such that representations can be recalled even when the stimulus is incomplete. This is thought to be accomplished in the hippocampus through several streams of serial and parallel processing kept separate and intact by inhibition. These streams of processing take the anatomical form of the three major glutamatergic pathways of the hippocampus: the perforant path, the mossy fibers and the Schaffer collaterals. Inhibition is provided by specialized groups of GABAergic interneurons. Though the hippocampus has been the subject of intense study for decades, there remain populations of cells that are not well understood in terms of their role in the network. Within area CA3, one of these populations is a group of interneurons with soma residing in the str. lacunosum moleculare that provide feedforward inhibition onto CA3 pyramidal cells.

The goal of this thesis was to understand the synaptic physiology of mossy fiber (MF) input to str. lacunosum moleculare interneurons (L-Mi), a connection that has been largely overlooked due to skepticism that an interneuron population ~ 250 μm away could be interacting with the MF pathway. The data presented here describe the functional anatomy of the connection, and define the short term synaptic physiology of MF input to L-Mi including an estimate of the quantal amplitude. I have also documented the modulation of this connection by

a presynaptic metabotropic glutamate receptor not previously thought to have a role in MF physiology, thus expanding the known repertoire of MF target specificity. Most importantly, however, these data provide a mechanism through which feedforward inhibition onto CA3 pyramidal cells is regulated in the short term, under physiologic stimulus patterns, and contribute to our knowledge of the function of the CA3 network.

TABLE OF CONTENTS

LIST OF TABLES

LIST OF FIGURES

PREFACE

The work presented in this thesis is largely based on two manuscripts that have been published or are under review. The functional anatomy work presented in Chapter 3 was published in:

Cosgrove KE, Galvan EJ, Meriney SD, Barrionuevo G. Area CA3 interneurons receive two, spatially segregated mossy fiber inputs. *Hippocampus*. Epub: Oct. 14, 2009.

Much of the remaining work presented is based on:

Cosgrove KE, Meriney SD, Barrionuevo G. High affinity group III mGluRs regulate mossy fiber input to CA3 interneurons. Manuscript submitted to *Hippocampus.*

ACKNOWLEDGEMENTS

This thesis was more than the presentation of my work in the lab. This thesis was, in many ways, evidence of my becoming an adult. As such, there are many people who will not understand the science in these pages, but who can understand and know, perhaps better than I, the steps that it took to get me here. Among those people are my parents. I have been lucky enough to have four exceptional parents in my life, and knowing throughout this process that they were always there with love, support, pep talks and occasional wake-up calls is what made this journey possible. Mom & Dave, Dad & Liz: I hope you know how much I love you and thank you for always being there. Similarly, I have the privilege of being friends with some truly outstanding people, both within the CNUP and in the outside world. You know who you are. And you know that I love you.

My dissertation adviser, German Barrionuevo, has challenged me to become a scientist and not just a graduate student. His matter-of-fact approach tempered by humor has never tolerated excuses and I cannot thank him enough for keeping me on track, even when I was doing my damndest to do anything but. German was exactly the mentor I needed at exactly the right time to finish this work and I have learned so much from working with him both in the lab and in the scientific arena, that I could never repay my debt. I only hope to continue to do good work so that he will be proud to acknowledge me as his former student in the coming years.

My chair, Steve Meriney, was my first mentor as an undergraduate, and my introduction to scientific discovery. From him I learned unabashed questioning of science, and cannot express how much I have appreciated his continued mentoring as I have progressed from an undergraduate to a Ph.D. candidate. Steve has always listened to even my most outlandish ideas, and has helped to teach me how to weed the good from the bad. Thank you.

The other members of my committee, Alison Barth, Justin Crowley and Nathan Urban, have been with me for several years now and I thank them for their considerate feedback in meetings, talks and in response to panicked emails sent in the middle of experiments. My thesis is better because of their input, as am I. I would also like to thank my outside examiner, Jean-Claude Lacaille for being willing to travel to Pittsburgh in February, and for his enthusiasm in discussing my work and what it means to the field. I have admired his work and am honored by his willingness to participate in my defense.

When I interviewed for graduate school, I wanted to join a community, not just a lab. The CNUP community at large has met and exceeded my hopes from a science community and has been generous to me with time, support and advice, and I have appreciated all of it. Lab members past from both the Meriney and Barrionuevo labs, this wouldn't have been possible without you. To Joan Blaney and Marlene Nieri, you are amazing women and I don't know how you do it all. Thank you.

LIST OF ABBREVIATIONS

ACSF – Artificial cerebrospinal fluid

aEPSC – Asynchronous excitatory postsynaptic current

CAMKII – Calcium/calmodulin dependent kinase II

CI-AMPAR – Calcium impermeable AMPA receptor

CP-AMPAR – Calcium permeable AMPA receptor

CV – Coefficient of variation

DG – Dentate gyrus

EC – Entorhinal cortex

EPSC – Excitatory postsynaptic current

EPSP – Excitatory postsynaptic potential

HFS – High frequency stimulation

I/O – Input / output

ISI – Inter-stimulus interval

L-Mi – Str. lacunosum moleculare interneuron

LTD – Long term depression

LTP – Long term potentiation

MF – Mossy fiber

mGluR – Metabotropic glutamate receptor

PKC – Protein kinase C

PP – Perforant path

PPR – Paired-pulse ratio

PSD – Postsynaptic density

PTP – Post-tetanic potentiation

RC – Recurrent collateral

SC – Schaffer collateral

SDG – Suprapyramidal blade of the dentate gyrus

SL – Str. lucidum

SLM – Str. lacunosum moleculare

SP – Str. pyramidale

SO – Str. oriens

SR – Str. radiatum

Sr^{2+} - Strontium

VGCC – Voltage gated calcium channel

1.0 INTRODUCTION

This thesis is the culmination of my work investigating the synaptic physiology of mossy fiber (MF) input to a subtype of feedforward CA3 interneurons. This work grew out of my interest in the ability of cells to tailor release characteristics across boutons depending on the identity of the target cell and what the functional consequences of those specializations are in a network. In theory, presynaptic target-cell dependent specialization has a high metabolic cost. It would follow that the expression of these target specific properties would have a significant impact on the circuit to compensate for that cost. The in vitro slice preparation of CA3 of the hippocampus is an ideal model system to study these kinds of questions. The anatomy of the system is clearly defined, with a limited number of inputs and a tractable number of potential synaptic partnerings. The work I present here focuses on one of these pairings: mossy fiber input to interneurons with soma in the str. lacunosum moleculare (L-Mi) of CA3.

This thesis will first clarify the functional anatomy of MF input to L-Mi, a connection that has been met with skepticism as the soma of L-Mi are found ~250 μm from the MF bundle (Chapter 3). Then, I will discuss the basic properties of transmitter release from the MF onto L-Mi including an estimate of the quantal amplitude, and short term plasticity characteristics of the synapse (Chapter 3). I will then investigate regulation of this synapse by the expression of presynaptic metabotropic glutamate receptors (Chapter 4) and what the functional impact of their expression is on the CA3 network (Chapter 5).

At its most narrow focus, I will define the short term synaptic physiology of MF input to L-Mi and modulation of that connection by a presynaptic metabotropic glutamate receptor not previously thought to have a role in MF physiology. Looking more broadly, I will provide a counter point to published findings describing MF input to another interneuron within CA3, the *str. lucidum* interneurons, thus highlight the target-specificity of the MF system. More broadly still, these data provide a mechanism through which feedforward inhibition onto CA3 pyramidal cells is regulated in the short term, and contribute to our knowledge of the CA3 network.

The purpose of this introduction will be to briefly introduce the reader to the anatomy and function of the hippocampus including the role of feedforward inhibiton from local circuit interneurons in CA3 of the hippocampus. I will then provided a fairly detailed overview of the target specific properties of the mossy fiber system to provide background and identify where the data I will present fit into the literature.

1.1 THE HIPPOCAMPUS: STRUCTURE CONFERS FUNCTION

The hippocampus is thought to be required for memory formation and consolidation. These functions are seemingly a direct result of the anatomy of the system. Through a series of excitatory feedback loops, and independent, yet inter-connected processing centers, cortical information is processed and stored for later retrieval. This has been hypothesized to occur through autoassociative networks, where the connections between cells that represent components of the same memory become stronger, linking them such that the entire memory can be recalled from presentation of a partial stimulus (McNaughton and Morris, 1987; Treves and Rolls, 1992). Within the hippocampal system, four different recurrent excitatory systems have

been documented related to the three major excitatory pathways of the hippocampus (Lisman, 1999).

The excitatory pathways of the hippocampus have been coined the "trisynaptic circuit" based on the apparent flow of information through the structure (Andersen et al., 1971). Extrinsic input enters the hippocampus via the axons of stellate cells in layer II of the entorhinal cortex (EC) that form the perforant path (PP, Fig. 1, red). The excitatory PP synapses on dentate gyrus (DG) granule cells, whose axons come together to form the mossy fiber (MF, Fig. 1, blue). The MF then activates CA3 pyramidal cells, which send axons to CA1 of the hippocampus as the Schaffer collateral (SC, Fig. 1, green). Axons from CA1 pyramidal cells then send axons to out of the hippocampus, back to the subiculum and entorhinal cortex (for review, see Witter, 1993).

These pathways become more complex, however, as the recurrent loops of the hippocampus are considered. The most apparent of these loops is the recurrent collateral projection of CA3 pyramidal cells onto other CA3 pyramidal cells and CA3 interneurons. This connection of CA3 pyramidal cell to CA3 pyramidal cell was the anatomical basis for the hypothesized autoassociated network function of CA3 (McNaughton and Morris, 1987; Treves and Rolls, 1994; Lisman, 1999). With the idea that memories would be formed by synchronous groups of cells becoming active together and then strengthening their connections with one another, the CA3 recurrent collaterals and the Hebbian long term potentiation that the connections undergo, fit perfectly (Lisman, 1999).

The idea that the CA3 is an independent autoassociative network required for pattern separation has been slightly revised in recent years as other recurrent networks in CA3 have been observed. Notably, the dentate gyrus has its own excitatory feedback loop with granule cells forming reciprocal synapses with excitatory mossy cells in the hilus. Recent work has provided

evidence for the hypothesized function of this network being required for pattern separation as an independent autoassociative network (Lisman, 1999; Leutgeb et al., 2007). Additionally, CA3 pyramidal cell axons project back into the dentate gyrus contacting granule cells forming another recurrent loop (Scharfman, 2007). Taken together, the overall function of these systems has been revised such that the dentate gyrus acts as a pattern separator, with further separation happening in CA3, but with the primary function of CA3 being pattern completion, or the retrieval of appropriate memories from incomplete stimuli (Lisman, 1999; Leutgeb et al., 2007; Leutgeb and Leutgeb, 2007). Guiding all of this is yet another excitatory loop. PP input to the hippocampus does not just excite dentate gyrus granule cells, but also travels throughout the str. lacunosum moleculare of CA1 and CA3, contacting pyramidal cells and interneurons in both regions (Amaral et al., 1990; Urban and Barrionuevo, 1998; Calixto et al., 2008). Thus, the PP provides feedforward excitation, and may function to set the sequence of events retrieved from the hippocampal network (Treves and Rolls, 1994; Lisman, 1999).

Throughout all of these systems, inhibition is required to sharpen signals and dampen neighboring excitation through feedforward and lateral inhibition (Treves and Rolls, 1994; Lisman, 1999; Leutgeb and Leutgeb, 2007). Feedforward inhibition functions to narrow the time window for integration of excitatory inputs by pyramidal cells (Pouille and Scanziani, 2001).

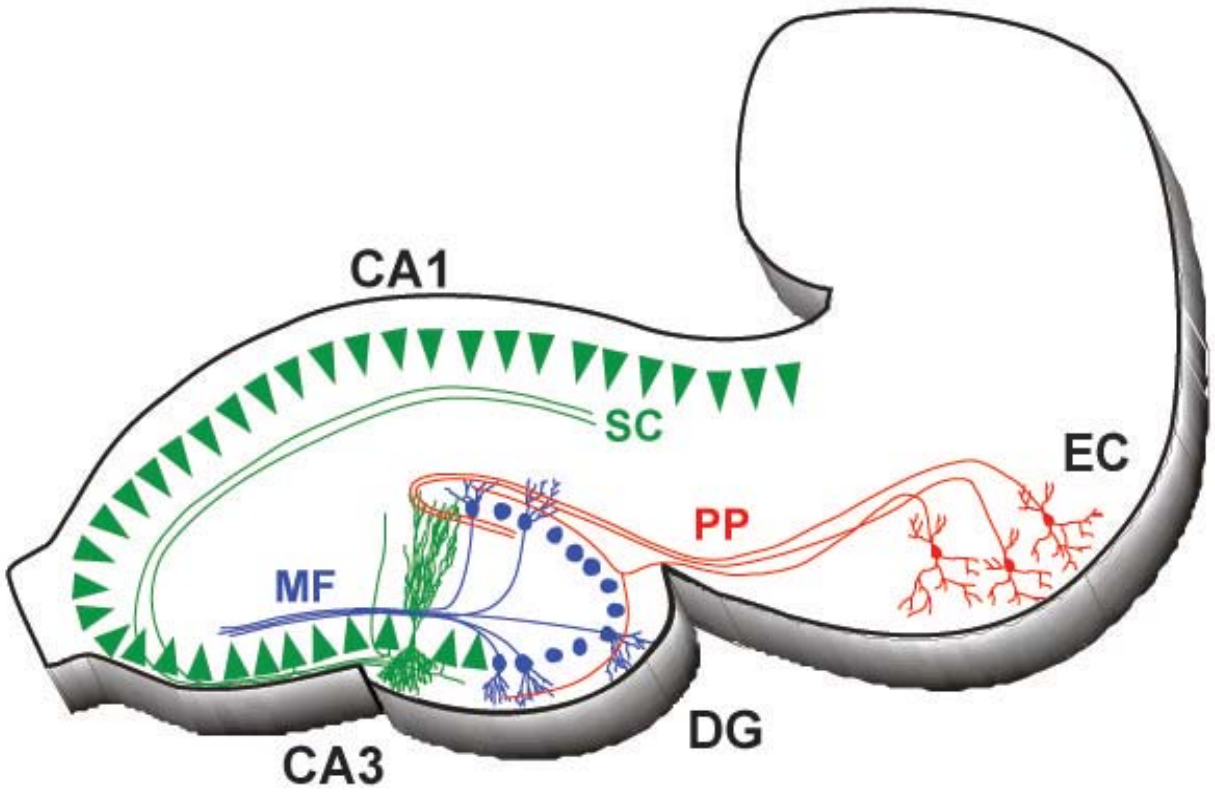

Figure 1. Schematic of the excitatory pathways of the hippocampus

Schematized hippocampus including the entorhinal cortex (EC, red), dentate gyrus (DG, blue), and pyramidal cell layers of CA3 and CA1 (green). Axons of the stellate cells in the EC form the perforant path (PP, red), which synapses on dentate gyrus granule cells whose axons for the mossy fiber (MF, blue). MF axons then synapse on CA3 pyramidal cells, whose projections form the Shafer collateral (SC, green) into CA1.

1.2 CA3 ANATOMY AND FEEDFORWARD INTERNEURONS

A distinctive connectivity feature of hippocampal area CA3 is that it receives two extrinsic excitatory afferent inputs. One input is conveyed via the perforant path (PP), the axons of the stellate cells in entorhinal cortex (EC) layer II. The second extrinsic input is provided by the mossy fibers (MF), the axons of dentate gyrus granule cells, which in turn receive input from the same layer II cells in EC (Tamamaki and Nojyo, 1993). Each projection pathway gains access to area CA3 through compact axonal bundles. The PP enters dorsally near the suprapyramidal blade of the dentate gyrus and the MF enters ventrally at str. lucidum (Fig. 2). Though there are likely other sources of glutamate within area CA3 (e.g. contralateral commissural projections, and input from the thalamus), these inputs are relatively sparse and do not form a coherent bundle. Area CA3 also contains a heterogeneous pool of feed-forward GABAergic interneurons (Freund and Buzsáki, 1996; Ascoli et al., 2009) receiving excitatory drive both from the PP and MF inputs (Buhl et al., 1994; Penttonen et al., 1997).

Interneurons in area CA1 have been extensively categorized based on morphology, somal location, axonal arbor, firing rates and calcium binding proteins (Freund and Buzsáki, 1996; Klausberger and Somogyi, 2008). Though CA3 has not benefitted from such extensive characterization of interneuron populations, independent groups have begun investigating the characteristics of individual populations of interneuron characterized predominantly by somal location and expression of postsynaptic AMPA receptor subtypes. Though it is acknowledged that the interneuron groups may be heterogeneous, the synaptic properties seem consistent within these groups, and progress has been made in understanding the role of these interneurons in the CA3 network (Doherty and Dingledine, 1998; Maccaferri et al., 1998; Toth et al., 2000; Vida and Frotscher, 2000; Lei and McBain, 2002; Lawrence et al., 2004; Pelkey et al., 2005;

Kullmann and Lamsa, 2007; Calixto et al., 2008; Galvan et al., 2008; Ascoli et al., 2009; Cosgrove et al., 2009).

The first interneurons to gain attention in the CA3 network were interneurons with soma located in the str. lucidum. These interneurons have extensive dendrites throughout the str. lucidum and many of these cells target the proximal dendrites and soma of CA3 pyramidal cells (Vida et al., 2006). Additionally, these interneurons receive input from the MF and RC pathways of CA3, putting them in position to mediate both feedforward and feedback inhibition (Lawrence and McBain, 2003). Further discussion of the synaptic properties of MF input to these cells will be discussed below.

Recent work performed by former members of the Barrionuevo lab has uncovered another interneuron subtype in CA3 residing in the str. lacunosum moleculare (L-Mi; Fig. 2). These interneurons have wide spread dendritic and axonal arbors. Dendrites extend horizontally through the str. lacunosum moleculare and ventrally through the str. radiatum and into the str. lucidum (Ascoli et al., 2009) and are thus in position to receive excitatory input from all three excitatory pathways of CA3, the PP, MF and RC (Calixto et al., 2008; Galvan et al., 2008; Ascoli et al., 2009). Axonal arbors of L-Mi are complex and extend throughout the str. radiatum (Ascoli et al., 2009), presumably contacting CA3 pyramidal cells along the apical dendrite, providing feedforward inhibition as is the case with CA1 str. lacunosum moleculare interneurons (Kunkel et al., 1988; Lacaille and Schwartzkroin, 1988; Williams et al., 1994; Bertrand and Lacaille, 2001). Because of this anatomical arrangement, L-Mi may provide feedforward inhibition mediated by both the PP and MF pathways, in addition to the potential for feedback inhibition as a result of activation by the RC pathway. Providing support for this hypothesis is the observation that MF and PP inputs summate supralinearly at short inter-stimulus intervals

(Calixto et al., 2008), allowing L-Mi to serve as coincidence detectors of EC input entering CA3. Additionally, paired recording between CA1 str. lacunosum moleculare interneurons and CA1 pyramidal cells indicates that the unitary amplitude of inhibitiory input onto CA1 pyramidal cells is relatively large, in spite of impinging on distal apical dendrites of the pyramidal cell (Lacaille and Schwartzkroin, 1988; Bertrand and Lacaille, 2001). Thus, though these interneurons are located far from the pyramidal cell soma, the inhibition that they effect may be robust and as a population may exert powerful influence over the firing of pyramidal cells. Excitatory, specifically MF, input to these cells, the CA3 L-Mi, will be the focus of this thesis with the aim of understanding how excitatory input is regulated when targeting these interneurons.

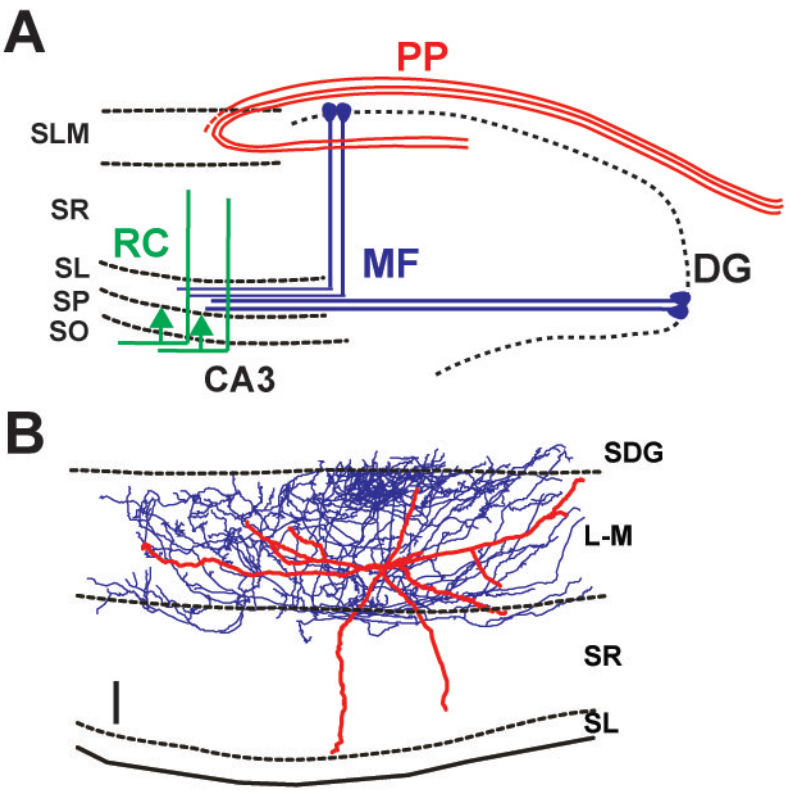

Figure 2. Schematic of lamina in CA3 and reconstruction of L-Mi

A) Schematic of CA3 showing lamina and relative location of pathways. PP: perforant path, red; MF: mossy fiber, blue; RC: recurrent collaterals, green. B) Camera lucida reconstruction of an L-Mi. red: dendrites; blue: axon. Other abbreviations: DG, dentate gyrus; SLM, str. lacunosum moleculare; SR, str. radiatum; SL, str. lucidum; SP, str. pyramidale; SO, str. oriens.

1.3 PROPERTIES OF THE MOSSY FIBER SYSTEM

1.3.1 'Hallmarks' of the MF system

The MF is one of the classic pathways of the central nervous system. Characterized by the giant mossy fiber boutons, or "moss", this pathway has been under scrutiny since it was anatomically described by Ramon y Cajal (1911). As a result of this attention, the synaptic physiology of MF input to CA3 pyramidal cells has been described in detail (Henze et al., 2000). Overall, MF input to CA3 pyramidal cells exhibits robust facilitation across several plasticity parameters. Specifically, MF input to pyramidal cells undergoes robust paired-pulse facilitation, short term facilitation in a train, frequency facilitation, post-tetanic potentiation, and long term potentiation (LTP) (Henze et al., 2000). Additionally, transmitter release from the MF is tightly regulated by presynaptically located metabotropic glutamate receptors (mGluRs), group II in the rat (Kamiya et al., 1996) and group III in guinea pigs (Manzoni et al., 1995). Many of the physiologic features, however, result from the specialized anatomy of the bouton including the multiple active zones, and thus may be specialized only to the mossy fiber to pyramidal cell synapse.

Recently, attention has been drawn to interneurons as targets of the mossy fiber system. Much of this attention was sparked in response to an anatomical paper confirming the hypothesis (Gulyás et al., 1992; Soriano and Frotscher, 1993; Spruston et al., 1997) that interneurons were the targets of filopodial extensions from the giant MF bouton and *en passant* MF boutons (Acsady et al., 1998). Coupled with this, was a physiological paper describing a long term depression (LTD) at MF input to interneurons (Maccaferri et al., 1998) that defied the well-known MF LTP previously described (Harris and Cotman, 1986; Zalutsky and Nicoll, 1990; Henze et al., 2000). Since 1998, a flurry of work has been undertaken aimed at understanding

the physiology of the MF system across targets and whether there are, indeed, “hallmarks” of the mossy fiber system.

1.3.2 Target-specificity of the MF system

Since the observation was made that the MF contacts interneurons as well as pyramidal cells (Acsady et al., 1998), and that the physiology of those connections might be different (Maccaferri et al., 1998), investigations into the physiology of MF input to interneurons with soma in the strs. lucidum (Toth et al., 2000; Lei and McBain, 2002; Lawrence et al., 2004; Pelkey et al., 2005), radiatum (Calixto et al., 2008) and lacunosum-moleculare (Calixto et al., 2008; Galvan et al., 2008; Ascoli et al., 2009) have been performed. Axons of the dentate gyrus granule cells also arborize within the dentate gyrus and input to hilar border interneurons (Doherty and Dingledine, 1998), basket cells (Alle et al., 2001) and mossy cells (Lysetskiy et al., 2005) have been investigated to varying extents. Interestingly, the sum total of this research indicates that the true signature of the MF system may be its ability to uniquely specialize synaptic communication depending on the identity of its postsynaptic partners.

Target specificity, the property where a single presynaptic neuron is capable of expressing different transmitter release properties at its boutons depending on the identity of its postsynaptic partners, has been documented throughout the CNS. Target specific properties generally fall into differences in long term plasticity (Maccaferri et al., 1998; Pelletier et al., 2008), short term plasticity (Thomson, 1997; Markram et al., 1998; Reyes et al., 1998; Toth and McBain, 2000; Rozov et al., 2001; Koester and Johnston, 2005) and distribution of presynaptic proteins including metabotropic glutamate receptors (mGluR) (Shigemoto et al., 1997; Scanziani et al., 1998; Semyanov and Kullmann, 2000; Rusakov et al., 2004) and voltage gated calcium

channels (VGCC) (Reuter, 1995; Reid et al., 1997; Poncer et al., 2000; Millán and Sánchez-Prieto, 2002; Ali and Nelson, 2006). Perhaps the most dramatic and simplest example of the impact of target-cell dependent short term plasticity is a demonstration from Markram et al. (1998), where a short burst of action potentials in a presynaptic neocortical pyramidal neuron contacting a second pyramidal neuron and an interneuron, elicited an action potential in the interneuron, but not the postsynaptic pyramidal cell. Consequently, the output of that microcircuit was inhibition in spite of a pyramidal cell also being a synaptic partner. If only one synapse or the other had been studied, predictions about the output of that microcircuit would have been false. Thus, to understand the network dynamics of a system, it is not enough to know which cells contact each other and what the properties of one connection are. To be able to make accurate predictions about a circuit, the connections between all the players must be identified, or at the very least, the range of neuronal communications must be identified.

1.3.2.1 Long term plasticity of the MF system

Long term plasticity is defined as a persistent change in the synaptic strength of a connection – long term potentiation is an increase in synaptic strength (Bliss and Lomo, 1973), and long term depression is a weakening of the synaptic connection (Dudek and Bear, 1992; Malenka, 1993). Though long term plasticity is not the focus of the work presented here, I will quickly summarize the different forms of long term plasticity the MF exhibits to highlight the target specificity of the system. This information is also presented in Table 1.

High frequency stimulation (HFS) of MF input to CA3 pyramidal cells was the first documented form of presynaptic, NMDA receptor (NMDAR) - independent LTP (Harris and Cotman, 1986; Zalutsky and Nicoll, 1990; Henze et al., 2000). Following this discovery, other forms of long term plasticity including LTD were documented at this synapse as investigators

used different protocols to induce long term changes (Nicoll and Schmitz, 2005). In considering other postsynaptic targets of the MF, long term plasticity characteristics of the MF have a considerable range.

Within the hilus, several different forms of long term plasticity have been observed. MF input to glutamatergic mossy cells undergo a presynaptic NMDAR – independent form of LTP in response to HFS that is reminiscent of the LTP seen at the MF to pyramidal cell connection (Lysetskiy et al., 2005). MF input to basket cells also undergoes LTP, but can express a presynaptic form of LTD if the basket cell is hyperpolarized throughout the HFS (Alle et al., 2001).

Similarly, MF input to CA3 interneurons expresses several different forms of long term plasticity. When HFS is delivered to the MF targeting a str. lucidum interneuron expressing CP-AMPA receptors, for example, the connection is strongly depressed due to activation of mGluR 7 on the presynaptic terminals contacting those cells (Pelkey et al., 2005). If mGluR 7 is internalized, however, the connection displays LTP instead, though LTP is not expressed if mGluR 7 is simply blocked pharmacologically (Pelkey et al., 2006). At str. lucidum interneurons expressing CI-AMPA receptors, a different form of LTD is observed that is due to activation of postsynaptic NMDAR (Lei and McBain, 2004). Additionally, MF input to str. radiatum interneurons has been shown to undergo LTD in response to HFS (Ascoli et al., 2009). In contrast to these intereneurons, HFS of MF input to L-M interneurons displays a robust LTP as the predominant form of plasticity that is NMDAR-independent (Galvan et al., 2008). The connection is bidirectional, however, and LTD can be observed if postsynaptic mGluR 1α activation is prevented or the intracellular cascade is disrupted (Galvan et al., 2008).

Table 1: Long term plasticity characteristics at MF targets

	LTP	LTD
Pyramidal	Yes, presynaptic[a], NMDAR-independent	Yes, mGluR + LFS
Str. lucidum, CP-AMPA	Yes, presynaptic, internalization of mGluR 7[b]	Yes, presynaptic, mGluR 7 – mediated[c]
Str. luciducm, CI-AMPA	--	Yes, postsynaptic, NMDAR – mediated[d]
Str. radiatum	--	Yes[e]
Str. lacunosum-moleculare[f,g]	Yes, pre & postsynaptic, NMDAR–independent[f,g]	Yes, blockade of mGluR1α[f]
Hilar border interneuron	--	--
Hilar basket cell[h]	Yes, presynaptic, associative HFS	Yes, presynaptic, nonassociative HFS
Mossy cell[i]	Yes	No

[a] Harris and Cottman, 1986
[b] (Pelkey et al., 2006)
[c] (Pelkey et al., 2005)
[d] (Lei and McBain, 2004)
[e] (Ascoli et al., 2009)
[f] (Galvan et al., 2008)
[g] Galvan et al., 2010
[h] (Alle et al., 2001)
[i] (Lysetskiy et al., 2005)

1.3.2.2 Short term plasticity of the MF system

"Short term plasticity" is a term used to group together rapid, transient changes in synaptic strength usually resulting from a change in the frequency of input. These short term changes provide information about the relative strength of a synapse and the capacity of the synapse to integrate information over durations of seconds to minutes (Zucker and Regehr, 2002). One measure that is frequently used is the determination of the paired-pulse ratio (PPR) of a synapse. A pair of stimuli is delivered at a short interstimulus interval (ISI) and the amplitude of the second response is divided by the first. If the ratio is greater than 1, the synapse undergoes paired-pulse facilitation, whereas a ratio of less than 1 is termed paired-pulse depression. A similar measure is determined through a short train of stimuli (often five to ten) at varying frequencies, and the overall ratio is determined by dividing the n^{th} response by the first. For both paired-pulse ratios and short train ratios, the hypothesized mechanisms are similar. Both paired-pulse and short train facilitation patterns are thought to result from the buildup of residual calcium in the presynaptic terminals of synapses with low initial probabilities of release (Katz and Miledi, 1968; Zucker and Regehr, 2002). An extreme example of short term facilitation is post tetanic potentiation (PTP), a phenomenon that can occur following a longer tetanus of high frequency activity. The mechanisms of PTP are also thought to rely on a buildup of calcium in the presynaptic terminal, as buffering calcium in the presynaptic terminal can prevent PTP (Kamiya and Zucker, 1994; Zucker and Regehr, 2002). Conversely, paired-pulse and short train depression are thought to result from depletion of the readily-releasable pool of synaptic vesicles at synapses with high initial probabilities of release (Betz, 1970; Zucker and Regehr, 2002), through postsynaptic receptor desensitization (Jones and Westbrook, 1996), or through inhibition by a presynaptic receptor (Wu and Saggau, 1997).

At MF input to CA3 pyramidal cells, the paired-pulse ratio can exceed three (Salin et al., 1996), and short trains of high frequency input result in robust train facilitation (Henze et al., 2000; Toth and McBain, 2000). Similarly, MF input to mossy cells and hilar basket cells undergo robust paired-pulse and short train facilitation at short ISIs (Alle et al., 2001; Lysetskiy et al., 2005). In contrast, hilar border interneurons display short train depression (Doherty and Dingledine, 2001). At MF input to str. lucidum interneurons, a roughly 50 / 50 mix of short term facilitation and depression is observed (Toth and McBain, 2000). Interestingly, however, even when MF input to str. lucidum interneurons expresses short term facilitation, the amount of facilitation is much smaller than that seen at MF input to pyramidal cells (Toth and McBain, 2000).

MF input to CA3 pyramidal cells undergoes a robust PTP that is likely due, at least in part, to a buildup of residual calcium in the giant MF bouton (Regehr et al., 1994; Henze et al., 2000). PTP is observed at other MF targets as well, including hilar mossy cells (Lysetskiy et al., 2005; Lee et al., 2007), basket cells (Alle et al., 2001), and str. lacunosum moleculare interneurons (Galvan et al., 2008). Recent work in the hilus indicates that the mechanisms of calcium buildup during a tetanus are more complex than simply calcium entry through voltage-gated calcium channels, but that mitochondria may be involved in releasing calcium stores into the cytosol at giant boutons and PKC activation is required at *en passant* boutons (Lee et al., 2007). As intracellular calcium can be viewed as a signaling molecule, these differences in PTP mechanisms may provide insight into the mechanisms of presynaptically localized long term changes as well.

The MF expresses another form of short term plasticity, frequency facilitation, an increase in postsynaptic amplitude as presynaptic activity increases from very low (0.05 Hz) to

moderate frequencies (1 Hz) (Salin et al., 1996; Henze et al., 2000; Toth et al., 2000). In contrast to the robust frequency facilitation observed at MF input to CA3 pyramidal cells, RC input undergoes only a slight facilitation of ~ 20% (Salin et al., 1996). It was found that frequency facilitation was dependent on a rise in intracellular calcium in the presynaptic terminal, and activation of CAMKII (Salin et al., 1996). It was further hypothesized that a factor in the expression of robust frequency facilitation was an initial low probability of release, as increased frequency facilitation corresponded with a decrease in the paired-pulse ratio (Salin et al., 1996). More recently, a mechanism for keeping the probability of release low at the MF to pyramidal cell synapse has been uncovered. G-protein coupled A1 adensosine receptors have been shown to be tonically active at the synapse, profoundly decreasing the probability of release, such that blockade of the receptor, degradation of extracellular adenosine and knocking out the A1 receptor have all revealed an increase in the initial probability of release, and a decrease in frequency facilitation observed at the synapse (Moore et al., 2003; Klausnitzer and Manahan-Vaughan, 2008).

Low probability of release is not the complete mechanism for expression of frequency facilitation, however. With the hypothesis that low probability of release was causal to the expression of frequency facilitation, Salin et al. (1996) attempted to reveal frequency facilitation at the RC synapse by altering the ratio of divalent ions such that the probability of release would be low. Though this manipulation did increase frequency facilitation at Schaffer collateral synapses onto CA1 pyramidal cells, the facilitation did not approach levels observed at MF input to CA3 pyramidal cells (Salin et al., 1996). Similarly, if other targets of the MF are considered, it becomes clear that probability of release cannot fully explain the phenomenon.

MF input to str. lucidum interneurons undergoes a robust frequency facilitation (~ 400 %) at 4 Hz when compared to 0.05 Hz (Toth et al., 2000). Though this facilitation is not as large as what is observed in the pyramidal cell synapse (~ 1000% increase; Toth et al., 2000), the effect is still much larger than what is seen at RC inputs. Interestingly, the probability of release at the MF input to str. lucidum interneurons has been calculated to be ~ 0.4, which is a mid-range value for the probability of release from an active zone (Lawrence and McBain, 2003; Lawrence et al., 2004). Thus, in spite of a mid-range probability of release, robust frequency facilitation was still observed at this synapse.

Other targets of the MF system also show frequency-dependent short term plasticity. MF input to mossy cells shows strong frequency facilitation, at times exceeding 600% (Lysetskiy et al., 2005). In contrast, hilar border interneurons show frequency-dependent depression at 5 Hz (Doherty and Dingledine, 2001). As MF input to these cells undergoes both short train and frequency depression, it is likely that MF input to hilar border interneurons has a high probability of release. Together, though MF input to pyramidal cells can be summarized as having an overall facilitating synaptic profile, it is clear from these results that the MF is capable of demonstrating a high degree of target specificity in both short and long term plasticity mechanisms (Table 2). Thus, in order to understand the role of the L-M interneuron in the CA3 network, it is important to assess the short term plasticity characteristics of the synapse.

Table 2. Short term plasticity characteristics of MF targets

	Train facilitation ($EPSC_5$ / $EPSC_1$)	Frequency Facilitation	PTP
Pyramidal[a]	Yes, ~300%	Yes, ~1000%	Yes
Str. lucidum, CP-AMPA	50/50 ratio of cells show facilitation / Depression[b]	Yes, ~400%[b]	No[c]
Str. lucidum, CI-AMPA	60/40 ratio of cells show facilitation / depression[b]	Yes, ~400%[b]	No[c]
Str. radiatum,	--	--	No[d]
Str. lacunosum-moleculare	?	?	Yes
Hilar border interneuron[e]	depression	No, depression	--
Hilar basket cell[f]	Paired-pulse facilitation	--	Yes
Mossy cell[g]	Yes, ~700%	Yes, ~650%	Yes

[a]Henze et al., 2000
[b]Toth et al., 2000
[c]Maccaferri et al., 1998
[d]Ascoli et al., 2009
[e]Doherty and Dingledine, 2001
[f]Alle et al., 2001
[g]Lysetskiy et al., 2005

1.3.2.3 Presynaptic protein distribution across MF boutons

Though various presynaptic proteins are capable of modulating release characteristics, I restricted my focus to voltage-gated calcium channels and presynaptic metabotropic glutamate receptors, as both proteins are notoriously differentially distributed across boutons and have been shown to affect short term plasticity characteristics (Scanziani et al., 1998; Inchauspe et al., 2004; Ali and Nelson, 2006). Within the mammalian central nervous system, transmitter release is generally linked to calcium entering through either P/Q- or N-type VGCCs, with smaller contributions from R- and L-type VGCCs (for review, see Catterall and Few, 2008). Different calcium channels can confer short term plasticity characteristics (Inchauspe et al., 2004), and are differentially modulated by kinases and G-protein coupled receptors (Evans and Zamponi, 2006). Because of this, an important step in defining the physiology of a synapse is defining the VGCCs linked to release at that synapse.

Glutamate release from the giant MF boutons onto pyramidal cells is primarily linked to P/Q-type VGCCs with lesser contributions from N- and R-type channels (Castillo et al., 1994; Breustedt et al., 2003; Pelkey et al., 2006; Li et al., 2007). These channels have different gating characteristics, with P/Q- and N-type channels having high activation thresholds and fast gating mechanisms, and R-type channels having a lower activation threshold and slower gating (Li et al., 2007). These characteristics become important because R-type channels are sensitive to slower, broader, subthreshold changes in membrane voltage (Li et al., 2007) that occur during theta oscillations in granule cells (Ylinen et al., 1995), and during action potential broadening that occurs with trains of activity (Geiger and Jonas, 2000; Li et al., 2007). At MF input to str. lucidum interneurons, a similar complement of VGCCs is observed, with predominantly P/Q-

type VGCCs linked to transmitter release at that synapse, with a lesser contribution from N-type VGCCs.

Metabotropic glutamate receptors fall into three distinct groups based on amino acid sequence and sensitivity to specific agonists (Conn and Pin, 1997). Group I mGluRs increase phospholipase C activity, and groups II and III inhibit adenylyl cyclase activity (Conn and Pin, 1997; Cartmell and Schoepp, 2000). When expressed presynaptically, mGluRs reduce synaptic transmission through a variety of mechanisms including modulation of ion channels, and phosphorylation of proteins in the release machinery (Anwyl, 1999; Cartmell and Schoepp, 2000). Additionally, mGluRs are frequently expressed differentially on axon terminals based on the identity of the target (Scanziani et al., 1998; Semyanov and Kullmann, 2000; Toth and McBain, 2000; Rusakov et al., 2004). To date, all known targets of the MF are sensitive to group II mGluR agonists. Variability arises, however, in the sensitivity to agonists of presynaptically expressed group III mGluRs, and these results are summarized in Table 3.

MF boutons are known to express many different presynaptic receptors (for review, see Henze et al., 2000), and group III mGluRs have been shown to be intricately linked with the expression of synaptic physiology at MF synapses (Pelkey et al., 2005). The expression pattern of group III mGluRs in the hippocampus has been documented anatomically with the finding that the low affinity mGluR 7 is predominantly expressed in the hippocampus, but in a target specific pattern (Bradley et al., 1996; Shigemoto et al., 1997; Bradley et al., 1999). Shigemoto (1997), in particular, has demonstrated the selective expression of mGluR 7 on terminals contacting interneurons. Furthermore, functional demonstrations of the selective targeting of mGluR 7 on MF boutons contacting interneurons, but not pyramidal cells, have been performed (Pelkey et al., 2005; Pelkey et al., 2006). However, not all MF boutons targeting interneurons express mGluR

7 (Shigemoto et al., 1997), and granule cells have been shown to express mRNA for mGluRs 4 and 8 as well (Tanabe et al., 1993; Ohishi et al., 1995; Saugstad et al., 1997; Ferraguti et al., 2005). Furthermore, granule cell input to hilar border interneurons is sensitive to low concentrations of agonist, indicating the presence of mGluR 4 or 8, not mGluR 7 (Doherty and Dingledine, 1998). This demonstrates the possibility that MF input to some interneurons are either not modulated by group III mGluRs, or are modulated by mGluRs 4 and/or 8.

Interestingly, the interaction of VGCC expression and presynaptic mGluR expression is important for the plasticity seen at MF input to str. lucidum interneurons, as mGluR 7 has been shown to target P/Q-type VGCCs at that synapse to effect its actions (Pelkey et al., 2006). Consequently, in an attempt to understand the spectrum of MF synaptic plasticity properties, the VGCCs linked to release and the expression of presynaptic mGluRs that may target those channels are important aspects of the physiology of the synapse.

Table 3. Distribution of presynaptic proteins across MF boutons contacting different targets

	Group II mGluR?	VGCC	Group III mGluR?
Pyramidal	Yes[a]	P/Q dominant[b]	High affinity (guinea pig)[c]
Str. lucidum, CP-AMPA	Yes[d]	P/Q dominant[e]	mGluR 7[f]
Str. lucidum, CI-AMPA	Yes[d]	--	--
Str. radiatum,	Yes[g]	--	--
Str. lacunosum-moleculare	Yes[h]	?	?
Hilar border interneuron[i]	Yes	--	High affinity
Hilar basket cell	Yes[j]	--	--
Mossy cell	Yes[k]	--	--

[a]Kamiya et al., 1996
[b]Castillo et al., 1994
[c]Manzoni et al., 1995
[d]Maccaferri et al., 1998
[e]Pelkey et al., 2006
[f]Pelkey et al., 2005
[g]Calixto et al., 2008
[h]Calixto et al., 2008
[i]Doherty and Dingledine, 1998
[j]Alle et al., 2001
[k]Lysetskiy et al., 2005

1.4 GENERAL GOALS OF THIS THESIS

With this thesis, I will provide insight into the regulation of MF input to L-Mi. Though the long term plasticity characteristics have been characterized (Galvan et al., 2008), other aspects of the connection remain undescribed. Thus, it is my aim to clarify these synaptic characteristics in light of recent literature surrounding MF input to CA3 interneurons. Chapter 3 will first clarify the functional anatomy of the MF input to L-Mi, and then describe the quantal amplitude, identify the VGCCs linked to release, and determine the short term plasticity profile of the synapse. In Chapter 4, I will determine which group III mGluRs are present at the synapse, and determine whether that receptor has a pre- or postsynaptic localization, as well as offer up a mechanism through which the receptor effects its actions. The functional implications of the expression of this receptor will be identified in Chapter 5, with particular emphasis on what a physiologic pattern of activity might be to activate the receptor.

Throughout these experiments, I would like to emphasize that the data gathered here are interesting in their own right because they describe a synaptic connection that may be critical to the proper balance of excitation and inhibition in the CA3 network. Beyond that, these data become even more interesting when put in the context of the literature such that the capability of the MF to express target-cell specific synaptic properties is highlighted. Thus, I will frequently compare my results to those found at other synapses in order to provide this context and deepen the impact of these findings. Together, these data will present an interesting synapse that emphasizes the impact the expression of a single protein can have on a network.

2.0 GENERAL MATERIALS AND METHODS

All experiments were performed in the *in vitro* hippocampal slice preparation. Additionally, experiments were performed using whole cell patch clamp, except where noted. This chapter will provide the general methods used with specific methods detailed throughout the text.

2.1 IN VITRO SLICE PREPARATION

Slices were prepared as described previously (Calixto et al., 2008). Briefly, Male Sprague-Dawley rats (21 -28 days old; Charles River) were deeply anaesthetized (Nembutal, I.P., 5mg per 100 g body weight) and perfused intracardially with cold (4^{o}C) modified artificial cerebrospinal fluid (ACSF) in which sodium chloride was replaced with sucrose (concentration in mM: 210 sucrose, 2.8 KCl, 2 $MgSO_4$, 1.25 Na_2PO_4, 26 $NaHCOO_3$, 10 glucose, 1 $CaCl_2$, 1 $MgCl_2$, pH 7.3, continuously bubbled with 95% O_2 / 5% CO_2). Following 30 sec to 1 min of perfusion, animals were decapitated and the brain removed. The brains were sliced using a Leica VT1000S vibratome and were cut in 320-340 µm sections. Slices were transferred to an incubation solution (in mM: 125 NaCl, 2.5 KCl, 1.25 Na_2PO_4, 25 $NaHCOO_3$, 10 glucose, 1 $CaCl_2$, 4 $MgCl_2$, 0.4 L-ascorbic acid, pH 7.3), continuously bubbled with 95% O_2 / 5% CO_2 at 32^{o}C for 30 min, and then allowed to return to room temperature for at least 30 min before beginning

recording. The slices were then transferred to a submersion recording chamber and superfused at a constant flow (2.5 mL / min) with ACSF (in mM: 125 NaCl, 2.5 KCl, 1.25 Na_2PO_4, 25 $NaHCO_3$, 10 glucose, 2 $CaCl_2$, 2 $MgCl_2$, pH 7.3) via a peristaltic pump (Watson Marlow 400 series). All recording were made at 32 – 34^oC and in the presence of 10 µM bicuculine and 50 µM D-2-amino-5-phosphonopentanoic acid (D,L–AP5) unless otherwise noted. All animal use was in accordance with the University Institutional Animal Care and Use Committee at the Univ. of Pittsburgh.

2.2 ELECTROPHYSIOLOGIC RECORDINGS

Whole cell recordings were made from the soma of putative interneurons in the str. lacunosum moleculare of CA3b of the hippocampus. Cell bodies were localized 50 – 100 µm from the slice surface and identified visually using infrared video microscopy and differential interference contrast optics. Patch pipettes with resistances of 2 – 5 MΩ were pulled from borosilicate glass and filled with a solution containing (in mM): 120 $KMeSO_4$, 10 KCl, 10 HEPES, 0.5 EGTA, 4 MgATP, 0.3 Na_2GTP, 8 phosphocreatine. Biocytin (0.2%) was routinely added to the pipette solution to allow subsequent morphological identification and reconstruction of the neurons. All recordings were obtained using an Axopatch 200B amplifier (Axon Instruments, Foster City, CA, USA). Signals were low pass filtered at 2 kHz, digitized at 10 kHz and stored on disk for off-line analysis. Data acquisition and analysis were performed using the pClamp 10 suite of software (Moleculare Devices). Series resistance was monitored throughout recordings and experiments were discontinued if resistance increased by > 15%. Whole cell voltage-clamp

recordings were held at -60 mV and in current clamp the cell was maintained within ~ 3 mV of rest unless otherwise noted.

The mossy fiber was stimulated extracellularly using a concentric bipolar electrode (FH-US) positioned either at the medial extent of the suprapyramidal blade of the dentate gyrus (MF_{SDG}) or within the s. lucidum dorsal to the ventral tip of the dentate gyrus (MF_{SL}; Fig. 3A). In every experiment, the group II metabotropic glutamate receptor agonist (2S,2'R,3'R) – 2 – (2',3' – dicarboxycyclopropyl) glycine (DCG-IV; 1 – 2.5 μM) was applied and responses were classified as of MF origin if DCG-IV decreased the postsynaptic response by > 50% (Alle et al., 2001; Lawrence et al., 2004; Galvan et al., 2008). The recurrent collaterals were stimulated by an electrode positioned within the str. oriens of CA3. When the perforant path was used, the stimulation electrode was positioned in the str. lacunosum moleculare of CA1. Synaptic responses were evoked by low intensity stimulation (10 to 300 μA intensity, 100 μs duration) via a constant-current isolation unit (Wesco, SC-100). Responses were included in analysis only if the rate of rise could be fit with a single exponential that lacked any obvious multiple EPSC or polysynaptic waveforms. Paired pulse ratio was determined using the calculation $EPSC_2$ / $EPSC_1$.

Table 4. Pharmacologic Agents

Agent	Concentration	Target	Effect
CNQX	50 µM	AMPAR	antagonist
L-AP4	10 – 20 µM	mGluR 4/8	agonist
L-AP4	100 – 400 µM	mGluR 7	agonist
DCG-IV	1 – 2.5 µM	mGluR 2/3	agonist
MSOP	100 µM	mGluR 4/8	antagonist
ω – conotoxin GVIA	1 µM	N-type VGCC	antagonist
ω – agatoxin IVA	250 nM	P/Q-type VGCC	antagonist
Ni^{2+}	100 µM	R-type VGCC	antagonist
Nitrendipine	10 µM	L-type VGCC	antagonist

2.3 ANALYSIS AND STATISTICS

Significance was determined as $p < 0.05$ using Student's t-test and ANOVA with multiple comparisons.

3.0 CHARACTERISTICS OF GLUTAMATE RELEASE FROM MOSSY FIBER ONTO L-M INTERNEURONS

3.1 INTRODUCTION

Dentate gyrus granule cell axons are unique because they form three different specialized presynaptic structures: the giant mossy fiber bouton, filopodial extensions from the bouton, and small, *en passant* boutons (Amaral, 1979; Claiborne et al., 1986; Acsady et al., 1998). Of these structures, the giant bouton contacts CA3 pyramidal cells while the filopodia and *en passant* boutons contact interneurons (Acsady et al., 1998). These structural specializations and the target specificity of bouton type suggest that specialized presynaptic properties depend on the type of nerve terminal, and the identity of the target cell. Indeed, previous investigations of mossy fiber release properties onto pyramidal vs. str. lucidum interneuron targets have revealed target-cell dependent differences that are in keeping with the differences in terminal structure (Toth et al., 2000; Lawrence et al., 2004). If these structural specializations do confer different synaptic properties, the location of the synapse becomes important since the entire length of the axon does not contain the same presynaptic structures. Since the mossy fiber travels in a tight bundle, filopodial extensions from the giant boutons are restricted to the bundle in the str. lucidum, extending up to 60 μm (Acsady et al., 1998). Thus for a cell to receive input from a filopodial extension, the dendrite presumably must cross into the str. lucidum. In contrast, *en*

passant boutons are present throughout the axon from its origination in the dentate gyrus through CA3 proper. The goals of this chapter are to determine the synaptic location of MF input to a subtype of CA3 interneurons, the str. lacunosum moleculare interneurons (L-Mi), and then define the basic release properties of the MF onto that cell with the hypothesis that target-cell dependent differences will be present.

Target-cell specific differences have been observed throughout the CNS and specializations have been observed in short term plasticity characteristics (Thomson, 1997; Markram et al., 1998; Reyes et al., 1998; Scanziani et al., 1998; Toth et al., 2000; Rozov et al., 2001; Patenaude et al., 2005), long term plasticity characteristics (Maccaferri et al., 1998; Lei and McBain, 2004), and the distribution of presynaptic proteins including voltage-gated calcium channels and presynaptic receptors (Reid et al., 1997; Scanziani et al., 1998; Rusakov et al., 2004; Ali and Nelson, 2006). Though MF input to CA3 pyramidal cells has been well characterized (for review, see Henze, 2000), the characterization of MF input to other cell types has only recently been undertaken. One interneuron subtype that has received much attention is the str. lucidum interneuron, which is logical because the interneuron somata reside in the direct path of the mossy fiber. When compared to MF to pyramidal cell synapses, differences in short term plasticity (Toth and McBain, 2000) and quantal amplitude (Lawrence et al., 2004) have been documented at MF synapses on to str. lucidum interneurons. Furthermore, the long term plasticity characteristics of MF input to pyramidal cells and to str. lucidum interneurons are markedly different, with MF input to str. lucidum interneurons undergoing either long term depression or no plasticity (Maccaferri et al., 1998; Lei and McBain, 2002, 2004) rather than the classic presynaptic long term potentiation seen at MF input to pyramidal cells (Harris and Cotman, 1986; Zalutsky and Nicoll, 1990).

Other interneurons also exist in CA3, however, and recent work has begun to elucidate the role of a second interneuron subtype in the mossy fiber system, the str. lacunosum moleculare interneuron (L-Mi; Calixto et al., 2008; Galvan et al., 2008; Ascoli et al., 2009). L-Mi are feedforward interneurons with somata in the str. lacunosum moleculare and wide reaching dendritic and axonal arbors (Ascoli et al., 2009). The first clue that MF input to L-Mi is not the same as MF input to str. lucidum interneurons came from the long term plasticity characteristics of the connection. MF input to L-Mi is capable of undergoing a robust LTP that is in stark contrast to what is observed at MF input to str. lucidum interneurons which undergo LTD (Maccaferri et al., 1998; Lei and McBain, 2004; Galvan et al., 2008). Because of this difference in long term plasticity at MF input to L-Mi vs. str. lucidum interneurons, it was my hypothesis that MF input to L-Mi had several target-cell dependent differences. Though the long term plasticity characteristics of MF input to L-Mi have been defined, the short term plasticity characteristics and presynaptic release characteristics have not yet been investigated. Thus, I determined the basic release characteristics of MF input to L-Mi including the quantal amplitude and the complement of voltage-gated calcium channels linked to release. Additionally, I determined the short term plasticity characteristics of the connection including the paired-pulse ratio, the response of the connection to a short high frequency train, and whether the connection undergoes frequency-dependent facilitation, a "hallmark" of the mossy fiber to pyramidal cell connection that is conserved at other MF targets (Salin et al., 1996; Toth et al., 2000; Lysetskiy et al., 2005).

Since L-Mi somata are located far (~250 μm) from the str. lucidum, it was important to determine where synaptic inputs to L-Mi occurred – within the str. lucidum or near the dentate gyrus as granule cell axons travel *en route* to form the mossy fiber bundle proper. L-Mi have

wide spread dendritic arbors that extend throughout CA3, potentially encountering the MF in several anatomical locations. Thus I used focal application of CNQX to selectively silence AMPAR-mediated synapses in the str. lacunosum moleculare in order to determine the location of MF synapses onto L-Mi.

Together, these data will explore the extent to which MF terminals are specialized and whether the target-cell specific properties extend from pyramidal cell vs. interneuron to further specialization across subgroups of interneurons. Further, these data will provide additional information about the functional anatomy of the mossy fiber system and the potential for various inhibitory interneurons in CA3 to contribute to the circuit.

3.2 RESULTS

3.2.1 Characteristics of MF-evoked synaptic responses

Before discussing experiments aimed at understanding the components and modulation of MF input to L-Mi, it is important to first define the basic characteristics of MF-evoked synaptic responses recorded in L-Mi. Furthermore, throughout many of the experiments discussed herein, two different MF stimulation locations were utilized. One stimulating electrode was positioned at the medial extent of the suprapyramidal blade of the dentate gyurs (SDG; Fig. 3; blue), the other was positioned within the str. lucidum of CA3 (SL; Fig. 3; green), where the MF bundle travels. To minimize the potential of recruiting additional glutamatergic fibers in the slice, the stimulation intensity was kept low (10 to 300 μA intensity, 100 μs duration). Additionally, for all MF responses, the group II mGluR agonist DCG-IV (1 – 2.5 μM) was applied to

pharmacologically confirm MF origin (Alle et al., 2001; Lawrence et al., 2004; Galvan et al., 2008). Furthermore, the use of two different MF stimulation locations alleviates concerns of contamination by either the RC (for the MF_{SL} stimulation location) or PP (for the MF_{SDG} stimulation location) inputs. As an example, the PP has been shown to be sensitive to group II mGluR agonists like DCG-IV (Macek, 1996), thus it might be a concern that a PP fiber might be contaminating the MF_{SDG} stimulation location as both synaptic responses are affected by DCG-IV. If, however, identical results are seen at the MF_{SL} stimulation location located far away from the PP, it can be concluded that the effects of MF_{SDG} stimulation to L-Mi are independent of the PP.

Table 5 details the pooled characteristics of EPSCs recorded from all cells. Importantly, there were no detectable differences in the amplitude or kinetics of the postsynaptic responses. Furthermore, no detectable differences were noted in the response of either input to any pharmacologic agent and the data were pooled throughout, except where noted. The table below details the amplitude, kinetics, PPR and response to pharmacologic agents, including DCG-IV.

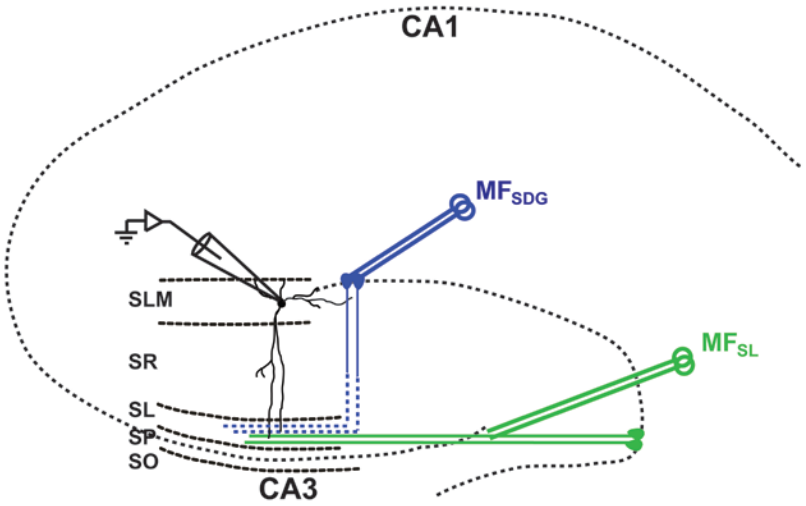

Figure 3. Schematic of recording configuration.

Schematic diagram of area CA3 of hippocampus showing typical soma location of L-M interneurons relative to the suprapyramidal blade of the dentate gyrus (SDG) and the arrangement of stimulating electrodes in the slice. Mossy fibres were activated from two locations: 1) the suprapyramidal blade of the dentate gyrus (blue, MF_{SDG}); and 2) from the s. lucidum dorsal to the ventral tip of the DG (green, MF_{SL}). Abbreviations: SO, s. oriens; SP, s. pyramidale; SL, s. lucidum; SR, s. radiatum; SLM, s. lacunosum moleculare; DG, dentate gyrus; PP, perforant path; MF_{SDG}, mossy fibre originating from the suprapyramidal blade of the dentate gyrus; MF_{SL}, mossy fibre bundle in s. lucidum.

Table 5. Comparison of MF_{SDG} and MF_{SL} synaptic characteristics.

	MF_{SDG} (N = 70)	MF_{SL} (N = 38)	"p value"
Amplitude (pA)	33.92 ± 5.02	36.67 ± 2.72	0.700
Rise Time (ms)	1.31 ± 0.06	1.39 ± 0.13	0.493
Decay Tau (ms)	7.40 ± 0.42	8.33 ± 1.06	0.342
PPR ($EPSC_2$ / $EPSC_1$)	1.72 ± 0.09 (N = 51)	1.75 ± 0.16 (N = 24)	0.836
Sensitivity to 10 µM L-AP4 (% of control)	58.4 ± 3.34 (N = 17)	53.7 ± 6.08 (N = 11)	0.462
Sensitivity to 1-2.5 µM DCG-IV (% of control)	30.2 ± 2.48 (N = 34)	37.5 ± 4.29 (N = 12)	0.140

3.2.2 Anatomy of MF input to L-M interneurons

Interneurons with soma residing in str. lacunosum moleculare (L-M interneurons) are known to mediate the influence of the entorhinal cortex on pyramidal cell activity by providing strong feed-forward inhibition (Lacaille and Schwartzkroin, 1988; Williams et al., 1994; Khazipov et al., 1995; Freund and Buzsáki, 1996; Chitwood and Jaffe, 1998; Savic et al., 2001; Cope et al., 2002). The somata of the majority of L-M interneurons are bipolar, with primary dendrites arising from the polar extremes of the cells. When viewed in a coronal section, dendrites extend dorsally throughout the str. lacunosum moleculare of CA3 where they overlap with the trajectory of PP fibers (Ascoli et al., 2009). Ventrally, the dendritic branches of L-M interneurons arborize within the str. lucidum and can extend into the pyramidal cell layer (Ascoli, 2009). The MF travels through the str. lucidum and contacts interneurons via *en passant* synapses arising from the main axonal trunk and filipodial extensions from the giant MF boutons on CA3 pyramidal cells (Acsady et al., 1998). However, MFs exiting the dentate gyrus *en route* to the str. lucidum form extensive collateral plexuses within the polymorphic layer and hilus of the dentate gyrus (Claiborne et al., 1986; Acsady et al., 1998; Calixto et al., 2008; Galvan et al., 2008). Some of the dorsally extending dendrites of L-M interneurons coexist with MF collateral plexus axons near the suprapyramidal blade of the dentate gyrus (SDG), and the ventrally extending dendrites overlap the str. lucidum and MF bundle proper.

MF-evoked EPSCs can be recorded from L-Mi when stimulating electrodes are positioned in both the SDG (MF_{SDG}) and str. lucidum (MF_{SL}; Fig. 3). The ability to evoke MF-mediated EPSCs from both stimulating electrode positions does not, however, confirm that the two locations are activating different sets of synapses impinging on different dendrites. In order to understand the anatomical arrangement of MF input to L-Mi, I wanted to determine whether

the two stimulation locations did, in fact, impinge on dorsal vs. ventral dendritic branches of the L-Mi. On the basis of the anatomy of the dendritic arbors (Ascoli et al., 2009) coupled with the known anatomy of the MF system (Amaral, 1979; Acsady et al., 1998), I predicted that focal blockade of AMPAR-mediated synaptic transmission in the str. lacunosum moleculare (and dorsal dendritic branches of the L-Mi) would suppress the MF_{SDG} input while sparing the MF_{SL} input.

3.2.2.1 Specific Methods: Focal application of CNQX

A pressure ejection pipette was filled with ACSF, CNQX (50 µM), and Fast Green (3%, to visualize the spread of the plume; (Perkins, 2002). After a stable whole-cell recording from an L-Mi was achieved, the pressure ejection pipette was lowered to within ~20 µm from the cell soma and ~10 µm above the surface of the slice. CNQX was then gently puffed (2-4 mmHg) onto the str. lacunosum moleculare using a pneumatic transducer (Model number DPM-13; Bio-Tek Instruments Inc.; Winooski, VT, USA) and visually monitored to ensure that the application was focal. Approximate dimensions of the visualized plume were 50 µm along the medial-lateral axis, and 150 µm along the dorsal-ventral axis. The direction of flow of ACSF in the recording chamber was adjusted so that any excess CNQX along the dorsal-ventral axis was directed towards area CA1, away from the s. lucidum (Fig. 4A). The duration of CNQX application was at least two minutes and did not exceed six minutes.

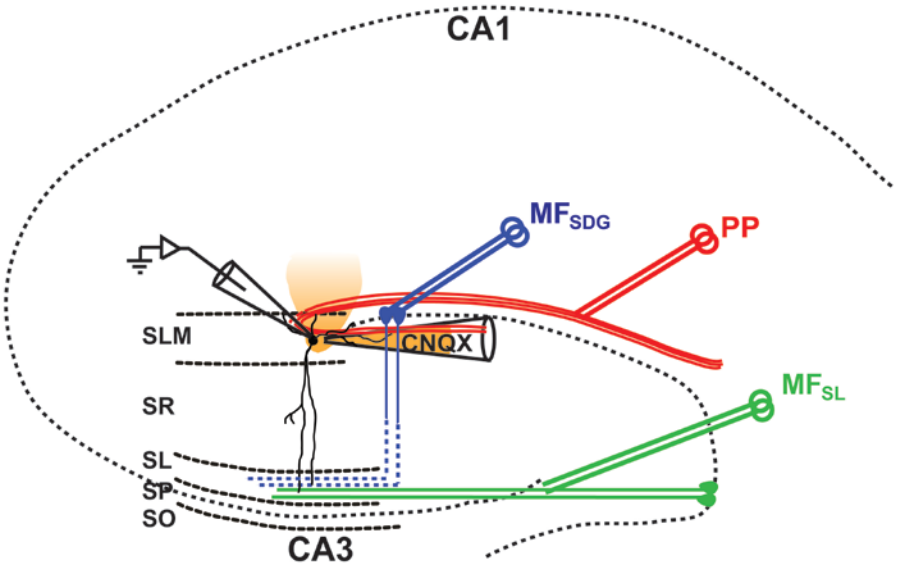

Figure 4. Schematic of stimulating electrode position and CNQX focal application.

Schematic diagram of area CA3 of hippocampus showing typical soma location of L-M interneurons relative to the suprapyramidal blade of the dentate gyrus (SDG) and the arrangement of stimulating electrodes and pressure ejection pipette in the slice. Perforant path fibres (red, PP) were activated from the s. lacunosum moleculare in area CA1. Mossy fibres were activated from two locations: 1) the suprapyramidal blade of the dentate gyrus (blue, MF_{SDG}); and 2) from the s. lucidum dorsal to the ventral tip of the DG (green, MF_{SL}). The pressure ejection pipette was placed within 20 µm of the soma, and the plume of CNQX was visually monitored to restrict CNQX application to the s. lacunosum moleculare.

3.2.2.2 MF_{SDG} input is selectively silenced with focal application of CNQX to str. lacunosum moleculare of CA3.

To test the hypothesis that focal application of CNQX in the str. lacunosum moleculare would suppress the MF_{SDG} input while sparing the MF_{SL} input, EPSCs were recorded from the soma of L-M interneurons at a holding potential of -70 mV in the presence of bicuculline and AP5. Since the PP input traverses the str. lacunosum moleculare of CA3 in a tight bundle (Calixto et al., 2008), the PP was also activated as a control to determine if the focal application of CNQX in a constantly perfusing bath was sufficient to suppress AMPAR-mediated responses within the s. lacunosum molecular of area CA3 (Fig. 4A). PP EPSCs (40.02 ± 9.48 pA; N = 6; Fig. 5C) were evoked from str. lacunosum moleculare in hippocampal area CA1. MF EPSCs (Fig. 5C) were evoked using stimulation locations described above (MF_{SDG}; 26.28 ± 2.75 pA; N = 7; and MF_{SL}; 28.43 ± 7.88 pA; N = 6; Fig. 5A). The site of MF_{SL} stimulation was ~200 µm from the str. lacunosum moleculare, the site of the presumed location of PP and MF_{SDG} synapses. There was no significant difference in EPSC amplitude or kinetics among the pathways. DCG-IV reduced PP EPSC amplitude by 21.84 ± 3.15% ($p<.05$; N = 6; Fig. 5C) but produced an inhibition greater than 50% on MF_{SDG} and MF_{SL} EPSC amplitudes (61.89 ± 3.65%; $P<0.001$; N = 7; and 67.82 ± 6.87%; $P<0.001$; N = 6, Fig. 5C), respectively. The slight decrease in PP EPSC amplitude with the application of DCG-IV is consistent with previous reports in CA1 demonstrating inhibition of glutamate release from the PP following application of group II mGluR agonists (Macek et al., 1996; Price et al., 2005). Following DCG-IV application, a pressure ejection pipette containing CNQX (50 µM) was positioned within 20 µm of the interneuron soma. CNQX was then focally applied with a pulse of pressure (2-4 mmHg) for ~2 to 4 minutes, creating a plume that

encompassed the s. lacunosum moleculare (Fig. 5A). The pressure pipette solution contained Fast Green (3%, or in some cases fluorescein; Fig 5A) to allow visual confirmation that the application of the CNQX solution was restricted to the s. lacunosum moleculare. CNQX further reduced the EPSC amplitudes from PP by 77.46 ± 4.26% ($P<0.001$; N = 6, Fig. 5) and MF_{SDG} by 61.72 ± 4.78% ($P<0.05$; N = 7, Fig. 5) such that the remaining response was only 17.69 ± 3.64% ($p<0.001$; N = 6) and 14.44 ± 2.23% ($P<0.001$; N = 7) of control values, respectively. In contrast, CNQX did not significantly decrease the MF_{SL} EPSC amplitude ($P>0.05$; N=6; Fig. 5). These data demonstrate the spatial segregation of the two MF inputs to L-M interneurons – one within the str. lacunosum moleculare, and the other more ventral, likely near the str. lucidum.

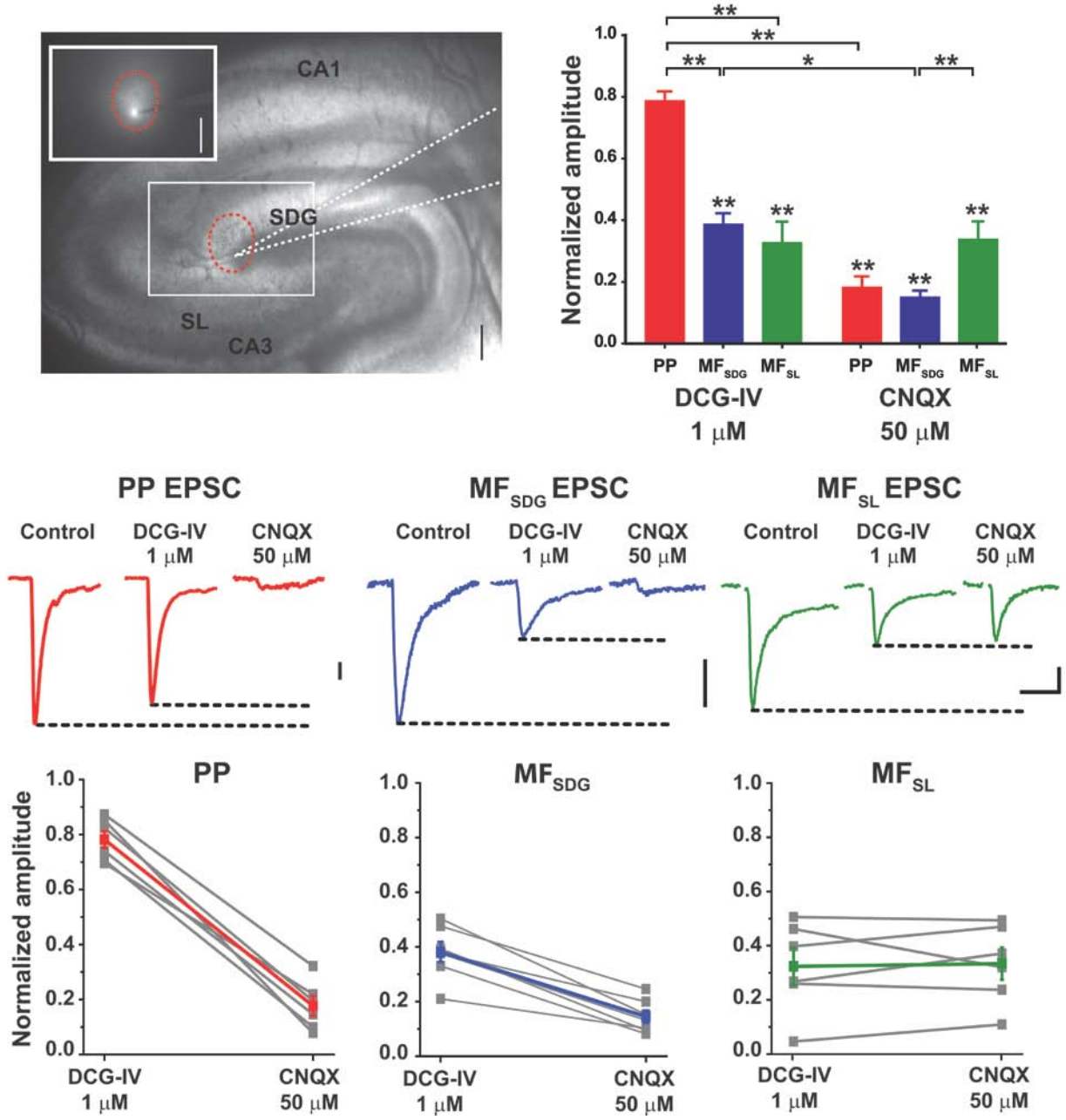

Figure 5. PP and MF_{SDG} synapses on L-M interneurons coexist within the s. lacunosum moleculare far from MF_{SL} synapses.

A. Bright field image of hippocampal slice and typical placement of pressure ejection pipette (dashed lines). (*Inset*) Fluorescence image demonstrating the spread of drug application using fluorescein as a marker. Dashed outline marks region estimated to be affected by drug application. Scale bar, 200 µm. B. Summary graph illustrating EPSC amplitude changes after bath application of DCG-IV (left), and subsequent focal application of CNQX to the s. lacunosum moleculare (right). EPSC amplitudes were normalized to control. DCG-IV (1 µM) significantly decreased the amplitude of MF_{SDG} and MF_{SL} relative to control. Additionally, CNQX (50 µM) significantly

decreased the amplitudes of MF_{SDG} and PP EPSCs, but did not change the amplitude of MF_{SL}EPSCs . *p<.01; **p<.001. C. Average EPSCs (N = 10 to 30) from three L-M interneurons illustrating the reduction of EPSCs by DCG-IV (1 µM) and the selective suppression of PP and MF_{SDG} EPSC amplitudes by focal application of CNQX (50 µM) to str. lacunosum moleculare. Scale bars, 10 pA, 25 ms. C. Scatter plots displaying individual normalized values (grey symbols and lines) following bath application of 1 µM DCG-IV and focal application of 50 µM CNQX to the str. lacunosum moleculare. Mean values overlaid in color (PP: left; MF_{SDG}: middle; MF_{SL}: right). Error bars indicate S.E.M.

3.2.3 Quantal amplitude of glutamate release from mossy fiber onto L-M interneurons

Having determined the anatomical organization of MF input to L-Mi, it was important to next understand the relative strength of that input. One way to measure the relative strength of an input is to gauge the quantal amplitude of the input. Thus, I next determined the quantal amplitude of MF input to L-Mi.

Previous investigations into the quantal amplitude of MF input to CA3 interneurons indicates that the value is larger than the quantal amplitude of MF input to CA3 pyramidal cells (Jonas et al., 1993; Lawrence et al., 2004). It was hypothesized that this large quantal amplitude (mean ~24.5 pA; Lawrence et al., 2004) may be linked to synapses arising from filopodial extensions (Lawrence et al., 2004) because filopodial active zones are relatively large and the postsynaptic densities in apposition are longer (Acsady et al., 1998). Since filopodial extensions stem from the giant mossy fiber boutons contacting CA3 pyramidal cells and extend for only 60 µm (Acsady et al., 1998), the MF_{SDG} input to L-Mi within the str. lacunosum moleculare (~250 µm from the str. lucidum) could not result from this type of presynaptic structure. The MF_{SL} input to L-Mi, however, could arise from filopodial extensions as the ventral input presumably occurs within range of the str. lucidum. Consequently, I was interested in determining what the

quantal amplitude of MF input to L-Mi is at each MF stimulation location and whether there is a difference between the two that would indicate a difference in the presynaptic structure.

Quantal amplitude was determined using strontium (8 mM) to de-synchronize release into putative single quanta (Goda and Stevens, 1994; Bekkers and Clements, 1999; Lawrence et al., 2004). These data also provided a measure of the quantal variance of the MF to L-Mi synapse, providing information on the variability of the quantal amplitude that may provide information on the number of release sites or amount of transmitter in each vesicle. Additionally, I was interested in obtaining an estimate of the convergence rate of MF input to L-Mi as the convergence rate also contributes to determinations of the strength of an input. Though determining the absolute convergence rate of an input onto a cell is difficult, it is possible to get a rough estimate of convergence by dividing a "macro" synaptic response by the quantal value.

3.2.3.1 Specific Methods: Quantal analysis and selection of aEPSCs.

Experiments using strontium to determine the quantal amplitude of the MF response were performed with a modified internal solution that replaced K^+ with Cs^+ (in mM): 120 $CsMeSO_4$, 10 KCl, 10 HEPES, 0.5 EGTA, 4 MgATP, 0.3 Na_2GTP, 8 phosphocreatine. Bath solution was altered to contain 0 Ca^{2+} and 8mM Sr^{2+} (Goda and Stevens, 1994; Bekkers and Clements, 1999; Lawrence et al., 2004). The MF was stimulated and asynchronous EPSCs (aEPSCs) were selected as follows. The time from the stimulus to the beginning of each event was calculated and plotted in a histogram, excluding the synchronous event (Fig. 6). The histogram was then fit with a single exponential decay, and the value of the offset was considered to be the background frequency (indicated by the arrow in Fig. 6B). The 95% confidence interval of the offset was calculated and extrapolated horizontally back to the y-axis (Fig. 6B, red line). The time at which

the fitted decay crossed the 95% confidence interval of the offset was considered to be the cutoff time (Fig. 6B, t_c). Only events that occurred prior to t_c were considered to be aEPSCs evoked by MF stimulation and included in the analysis. To determine the mean quantal amplitude, the peak amplitudes of each aEPSC were plotted in a histogram (Fig. 6C). This histogram was then fit with a single Gaussian function to determine the quantal amplitude (mean) for each input (Bekkers and Clements, 1999).

3.2.3.2 Quantal amplitude of MF input to L-Mi is small and has a small quantal variance.

To determine the mean quantal amplitude, the peak amplitudes of each aEPSC were plotted in a histogram (Fig. 6C). This histogram was then fit with a single Gaussian function to determine the mean and standard deviation for each input (Bekkers and Clements, 1999). No difference was observed in the quantal amplitudes resulting from stimulation of the MF_{SDG} vs. the MF_{SL} input to L-Mi and the values are presented in Table 6. The mean quantal amplitude for pooled MF input to L-Mi was determined to be 7.88 ± .29 pA (range: 6.70 pA to 9.59 pA; N = 10; Fig. 6D), a value similar to those from other central synapses (Jonas et al., 1993; Bekkers and Clements, 1999) but significantly smaller than the quantal amplitude for the mossy fiber input to str. lucidum interneurons (mean: 24.5 pA; Lawrence et al. 2004).

In considering the Gaussian fits of the data, there appeared to be the possibility of a slight skew of the data toward larger amplitude responses. Part of this is due to the thresholding of the amplitude of the synaptic events where the event needed to be at least 3 to 4 pA in order to be visible above the noise of the recording. Additionally, though efforts were made to minimize contamination of the analysis by spontaneous events not linked to stimulation, since these experiments were not carried out in tetrodotoxin to prevent spontaneous activity in the slice, it is possible that larger amplitude spontaneous events were included in the analysis. Indeed, when

spontaneous events were recorded a separate group of cells, and the same analysis was performed, the average amplitude of spontaneous EPSCs was 12.48 ± 0.92 pA (N=6), which is larger than the calculated quantal amplitude from MF-evoked aEPSCs ($p < 0.001$). Thus, any skew to the distribution of aEPSCs observed may be due to spontaneous glutamatergic activity from the slice.

Additionally, the coefficient of variation (S.D. of the Gaussian fit / mean) was calculated to determine the variability of each quantal amplitude (0.330 ± 0.02; N = 10; Fig. 6D). This quantal variance is consistent with what has been reported for the MF – PYR synapse (Jonas et al., 1993), Shafer collateral input to CA1 pyramidal cells (Stricker et al., 1996) and EPSCs evoked from distal inputs to dentate gyrus granule cells (Bekkers and Clements, 1999). Large quantal variances (CV > 0.4) (Jonas et al., 1993; Stricker et al., 1996) were only observed in two out of ten cells. Mossy fiber origin was confirmed after Sr^{2+} washout with the application of 2 μM DCG-IV (39.09 ± 6.02% of control; N = 6). In a subset of cells, DCG-IV was applied in the continued presence of Sr^{2+} and aEPSCs were analyzed for changes in frequency and amplitude. In the continued presence of Sr^{2+}, DCG-IV decreased the frequency (control: 14.83 ± 1.37 Hz; DCG-IV: 10.50 ± 1.16 Hz; N = 4; $p < 0.05$) without changing the amplitude of the aEPSC (control: 7.60 ± 0.42 pA; DCG-IV: 7.26 ± 0.81 pA; N = 4; $p = 0.467$), consistent with what has been observed as a result of activation of a presynaptic receptor (Price et al., 2005).

Given that the average quantal amplitude is ~ 8pA, the average amplitude of evoked MF EPSCs (~35 pA; Table 5) indicates that several MF terminals likely converge onto L-Mi. Consistent with this interpretation, we found that MF EPSCs evoked from both MF_{SDG} and MF_{SL} stimulation locations can be observed in a single L-Mi (Cosgrove et al., 2009). Therefore, even though individual MF to L-Mi synapses are relatively weak, with small quantal amplitudes,

many individual MF terminals may converge onto L-Mi creating a strong overall input. Though multiple inputs could arise from multiple points of contact form a single MF axon, the anatomy indicates that this is a rare occurrence (Shigemoto et al., 1997). Alternatively, it is possible that multi-vesicular release occurs from a single boutons, though this is also unlikely based on the anatomical reconstructions of presynaptic boutons (Shigemoto et al., 1997).

Table 6. Comparison of quantal properties for MF_{SDG} and MF_{SL} inputs to L-Mi

	MF_{SDG} (N = 6)	MF_{SL} (N = 4)	p value
Quantal Amplitude (pA)	7.72 ± 0.44	8.12 ± 0.36	0.541
Quantal Conductance (pS)	128.67 ± 7.32	135.27 ± 6.07	0.542
Quantal Variance	0.33 ± 0.02	0.33 ± 0.03	0.973

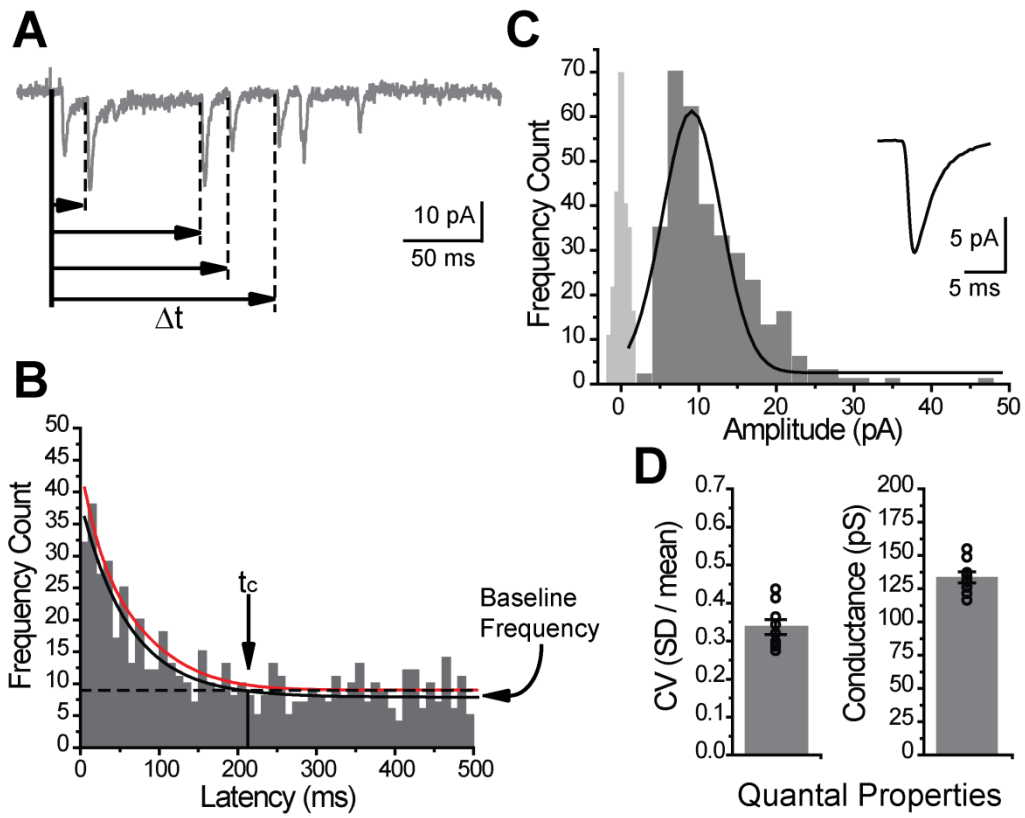

Figure 6. Selection of aEPSC and determination of quantal amplitudes using Sr2+.

A and B) Demonstration of method used to select asynchrounous EPSCs. Latency to each event (omitting the synchronous event) was determined from the time of stimulus to the start of each event (Δt) as illustrated in (A). Latencies were then plotted in a histogram (B) and fitted with a single exponential (black curve). The offset of the exponential decay was considered to be the background frequency (indicated by arrow). A horizontal line (dashed line) was plotted back from the 95% confidence interval of the offset of the decay (light grey line) and the point at which that line crossed the decay was considered the cutoff time (t_c). Only events that occurred before that time were considered linked to the stimulus and aEPSCs. C) The amplitude of the aEPSCs were then plotted in a histogram and fitted with a single Gaussian (black line). The distribution of the noise is plotted in light grey. Inset is the average quantal aEPSC for this cell. D) Summary plots of the coefficient of variation (left) and the quantal conductance (right) for nine cells**.**

3.2.4 Short term plasticity characteristics of the mossy fiber to L-M interneuron synapse

Though the long term plasticity characteristics of MF input to L-Mi have been characterized, the short term plasticity characteristics have yet to be investigated. The MF to pyramidal cell connection is known for displaying robust paired-pulse facilitation and robust frequency facilitation, an increase in the amplitude of the postsynaptic response as the stimulation frequency increases from very low (.05 Hz) to more moderate (1 – 4 Hz; Salin et al., 1996; Henze et al., 2000). These properties are thought to make MF input to pyramidal cells very strong by allowing the pyramidal cell reach action potential threshold in response to small changes in the frequency of MF input.

Short term plasticity characteristics have been repeatedly shown to exhibit target-cell specificity (Thomson, 1997; Markram et al., 1998; Reyes et al., 1998; Toth and McBain, 2000; Rozov et al., 2001; Koester and Johnston, 2005). Indeed, MF input to str. lucidum interneurons does not display robust paired-pulse facilitation, and instead commonly displays paired-pulse depression (Toth et al., 2000), though the connection does display frequency facilitation (Toth et al., 2000). Thus, I wanted to determine the short term plasticity characteristics of MF input to L-Mi.

MF input to L-Mi undergoes both paired-pulse and short term facilitation in response to short trains of five stimuli at 20 Hz. Specifically, the paired-pulse ratio of MF input to L-Mi is 1.73 ± 0.08 (N = 75; Table 5), which demonstrates a more robust paired-pulse facilitation than the MF to str. lucidum interneuron connection (Toth, et al., 2000) but less strong facilitation than at MF input to CA3 pyramidal cells (Henze et al., 2000). Additionally, MF input to L-Mi facilitates throughout a train of five MF stimuli at 20 Hz, though the facilitation accommodates by the fifth stimulus ($EPSC_5$ / $EPSC_1$: 1.28 ± 0.10; N = 12; Fig. 7). This facilitation also differs

from the pattern of short term plasticity observed at MF input to str. lucidum interneurons, as that synapse tends to undergo short term depression (Toth et al., 2000).

MF input to pyramidal cells undergoes robust facilitation at low and moderate frequencies that can exceed 600% at 4 Hz vs. 0.05 Hz (Salin et al., 1996; Scanziani et al., 1997; Henze et al., 2000; Toth et al., 2000). Similaraly, it has been reported that mossy fiber input to str. lucidum interneurons exhibits strong frequency facilitation (~400% increase at 4 Hz vs. 0.05 Hz) (Toth et al., 2000). To investigate whether glutamate release by low to moderate frequencies of MF activity at undergoes facilitation at MF input the L-Mi, stimulation frequencies from 0.05 to 4Hz were tested (Henze et al., 2000). In contrast to the MF to PYR and MF to str. lucidum interneuron connections, I did not detect a significant increase in amplitude at 4 Hz compared to the .05 Hz control (1.09 ± 0.12 normalized to 0.05 Hz control; $p = 0.460$; $N = 8$; Fig. 7B).

These data demonstrate a new synaptic phenotype for the MF that contrasts with what has been observed at other MF synapses. MF input to L-Mi undergoes short term facilitation in response to high frequency input, but not frequency facilitation at low to moderate frequencies. Another contributor to short term plasticity at other MF synapses onto interneurons is the presence of a calcium-permeable AMPA receptor (CP-AMPAR; Toth et al., 2000). L-Mi have been shown to rarely express CP-AMPARs (Galvan et al., 2008; Galvan et al., 2010; personal observations), thus making it unlikely that CP-AMPARs are contributing to the short term plasticity seen at MF input to L-Mi.

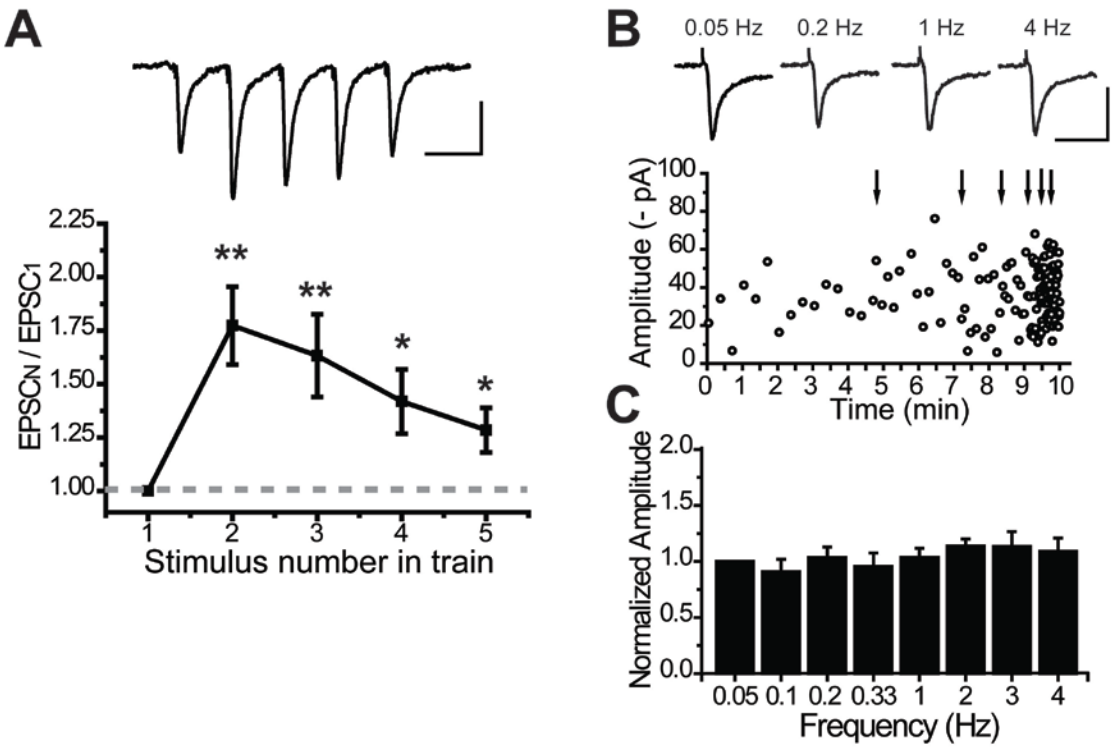

Figure 7. MF input to L-Mi undergoes short term, but not frequency facilitation.

A. MF EPSCs facilitate during short, high frequency trains. The top panel shows an averaged trace (N = 20 sweeps) from a representative cell to demonstrate the facilitation pattern in response to a short train at 20 Hz. The bottom panel shows summary data of the ratio of $EPSC_N$ to $EPSC_1$ of a short train of MF input to L-Mi. A train of five stimuli were delivered at 20 Hz, and facilitation was observed throughout the train. (N = 12; ** $p < 0.01$; * $p < 0.05$) B and C. MF input to L-Mi does not undergo frequency facilitation. B. Averaged traces (N = 15) from a representative cell (top), and a scatter plot of EPSC amplitudes over time across all test frequencies (bottom). Arrows indicate a change in stimulation frequency to 0.1, 0.2, 0.33, 1, 2, and 4 Hz. C. Plot of summary data showing the EPSC amplitude of MF input to L-Mi at frequencies ranging from 0.1 to 4 Hz and normalized to 0.05 Hz. None of the test frequencies were significantly different than 0.05 Hz (N = 8; $p > 0.05$). Scale bars: 20 pA; 25 ms

3.2.5 Voltage-gated calcium channels linked to glutamate release from the mossy fiber

The voltage-gated calcium channel linked to transmitter release can impact short term plasticity characteristics as well as susceptibility to modulation by presynaptic receptors. For example, in P/Q-type VGCC knockout animals, it has been shown that N-type VGCC expression is increased at the Calyx of Held which displays short term facilitation in wild type animals. As a result of the shift in VGCC population mediating release, however, the Calyx displays short term depression (Inchauspe et al., 2004). In contrast, in the neocortex, pyramidal cell synapses expressing predominantly N-type VGCCs onto burst firing cells showed facilitation, whereas synapses onto fast spiking interneurons and linked to predominantly P/Q-type VGCCs showed depression (Ali and Nelson, 2006). Furthermore, N-type VGCCs seem to be more susceptible to modulation by G-protein coupled receptors (Catterall and Few, 2008). Consequently, the identification of the VGCC linked to release at a particular synapse is an important part of defining the presynaptic physiology of that synapse.

In order to determine the complement of VGCCs linked to glutamate release at MF to L-Mi synapses, specific antagonists were bath-applied while recording MF-evoked EPSCs. Using specific toxins to isolate the P/Q- and N-type calcium channels, we found that glutamate release at the MF to L-Mi connection is largely dependent on P/Q-type VGCCs, as previously reported for the MF to pyramidal cell, and MF to str. lucidum interneuron connections (Castillo et al., 1994; Breustedt et al., 2003; Miyazaki et al., 2005; Pelkey et al., 2006; Li et al., 2007). Specifically, we found that glutamate release was predominantly linked to P/Q-type channels (ω-agatoxin IVA decreased EPSC amplitude by 83.1 ± 2.4%; N = 13; $p < 0.0001$) with a variable but significant contribution from N-type VGCCs (ω-conotoxin GVIA decreased EPSC amplitude by 27.29 ± 5.5%; N = 18; $p < 0.001$; Fig. 8A). Using 100 µM Ni^{2+} to block R-type channels, a

small, but significant contribution was observed (12.01 ± 4.49% decrease; N = 5; $p < 0.05$). However, there was no evidence to indicate that L-type VGCCs were linked to release at the MF to L-Mi synapse (10 µM Nitrendipine did not change EPSC amplitude: 12.31 ± 8.31%; N = 3; $p = 0.282$)

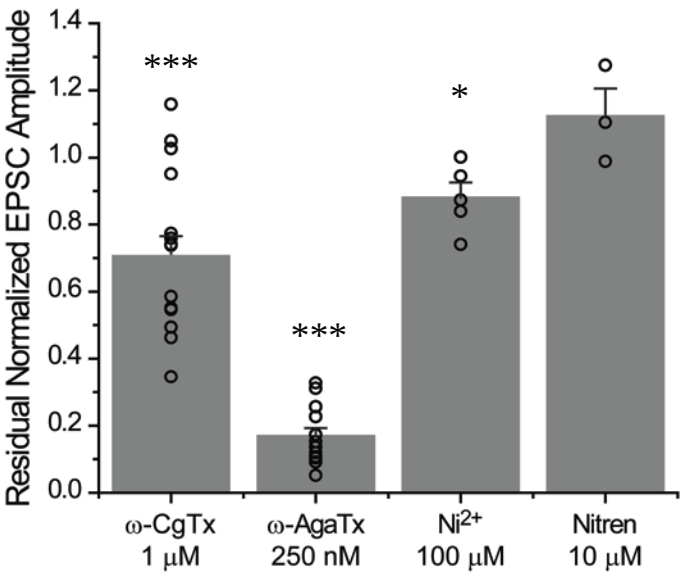

Figure 8. Voltage-gated calcium channels linked to release at MF to L-Mi.

Summary plot of normalized EPSC amplitude following each voltage-gated calcium channel blocker. Open circles represent individual cell data, bars represent mean numbers. ω-Cgtx: N-type VGCC; N = 18. ω-AgaTx: P/Q-type VGCC; N = 13. Ni^{2+}: R-type VGCC; N = 5. Nitren: L-type VGCC; N = 3. *** $p < 0.001$; * $p < 0.05$.

At other synapses, the short term plasticity observed has been linked to the population of VGCCs present at the synapse (Ali and Nelson, 2005; Inchauspe et al., 2004). Though the complement of VGCCs present at MF input to L-Mi is similar to that seen at both MF input to CA3 pyramidal cells and str. lucidum interneurons, there was considerable variability in both the paired-pulse ratio and the contribution of N-type VGCCs to release at the MF to L-Mi synapse. Thus, it may be possible that a higher proportion of N-type VGCCs may shift the synapse to be more or less facilitating. Thus, to gain an understanding of whether the short term plasticity characteristics at this synapse are linked to the VGCC-subtype mediating transmitter release (Ali and Nelson, 2005) I plotted the percent decrease in EPSC amplitude as a result of ω-conotoxin GVIA (CgTx) application against the PPR of the cell. Since some synapses have a large proportion of N-type VGCCs (~50% reduction in EPSC amplitude with CgTx) and some had very few N-type VGCCs (less than 15% reduction in EPSC amplitude with CgTx), if the short term plasticity of the synapse is dependent on the VGCC population, there should be a trend. As Fig. 9 shows, however, no relationship was found between the contribution of N-type VGCC to release and the PPR. Thus, at this synapse, short term plasticity characteristics are as a result of some other presynaptic attribute that remains undetermined, and not affected by the proportion of N-type VGCCs present at the terminal.

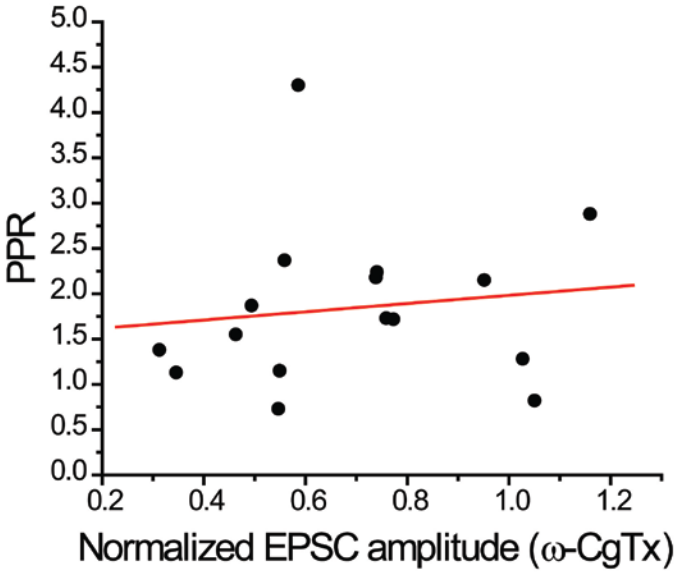

Figure 9. Complement of VGCCs does not dictate short term plasticity.

Plot of the normalized EPSC amplitude following application of ω-CgTx (1 μM) against the paired-pulse ratio of the connection. Filled circles represent individual cell data. Red line is the linear fit of the data. No relationship was found between the effect of CgTx and the PPR ($R = 0.131$; $p = 0.629$).

3.3 DISCUSSION

This chapter has presented data which serve to further our understanding of the synaptic physiology of MF input to CA3 interneurons. Together these data indicate that MF target-specificity extends beyond the pyramidal cell vs. interneuron delineation to also distinguish between different subgroups of interneurons. Short term plasticity of MF input to CA3 interneurons and the quantal amplitude of that input differ between L-Mi and str. lucidum interneuron targets. Interestingly, the complement of VGCCs linked to release is similar at all three synapses, indicating that some synaptic characteristics are conserved across targets. Further, since responses elicited from MF_{SDG} and MF_{SL} stimulation sites have identical synaptic properties, but impinge on different dendritic branches of the L-Mi, one near the SDG and one likely within the str. lucidum, it is unlikely that these target specific differences are a by-product of synaptic location. Instead, the target specificity arises from some characteristic of the postsynaptic cell that is, as yet, unknown. These results add to our knowledge of the CA3 circuit and highlight synaptic specializations of the MF system.

3.3.1 Anatomy of MF input to L-Mi: small but many?

MF input to L-Mi occurs both in a dorsal location, near the suprapyramidal blade of the dentate gyrus, and in a more ventral position, likely within the str. lucidum. These inputs have similar amplitude and decay kinetics (indicating that the corresponding synapses were positioned at similar distances from the interneuron soma), but target spatially segregated domains on the interneuron dendrites. The current data demonstrate that L-Mi are entrained by two convergent MF inputs to spatially separated regions of the dendritic tree. This anatomical arrangement could

also make these interneurons considerably more responsive to the excitatory drive from dentate granule cells.

The range of quantal amplitudes recorded from L-Mi are significantly smaller than those reported in str. lucidum interneurons (Lawrence et al., 2004), and are closer to the range of amplitudes at the MF to pyramidal cell connection (Jonas et al., 2003) or the synaptic input to dentate gyrus granule cells (Bekkers and Clements, 1999). Though occasional aEPSC had amplitudes up to ~50 pA, those instances were rare, and most aEPSC amplitudes fell between 5 and 20 pA, making the quantal variance for the MF – L-Mi connection fairly small. In trying to understand the discrepancy in quantal amplitude between L-Mi and str. lucidum interneurons, one proposed explanation for the relatively large quantal amplitude observed at the MF to str. lucidum interneuron connection was that the presynaptic structure may be a filopodial extension (Lawrence et al., 2004).

MF filopodial extensions have been shown to be in apposition to larger postsynaptic densities (PSDs) than those seen at MF input to pyramidal cells via the giant bouton. Comparing the two presynaptic structures contacting interneurons, the filopodial and *en passant* boutons, the PSDs in apposition to filopodia are usually perforated, whereas synapses made by *en passant* boutons generally have shorter, nonperforated PSDs. Interestingly, it has been demonstrated that perforated PSDs have a much higher concentration of AMPA receptors than nonperforated synapses (Ganeshina et al., 2004), a characteristic that is permissive of larger synaptic conductances. Consequently, it may be that the relatively large quantal amplitude aEPSCs observed in str. lucidum interneurons is a result of these larger, perforated PSDs in apposition to filopodia. It then follows, that the smaller quantal amplitude reported here for L-Mi maybe a result of the presynaptic structure being an *en passant* bouton. This hypothesis is consistent with

the MF_{SDG} and MF_{SL} inputs having the same quantal amplitude, as filopodial extensions are absent near the SDG.

Certainly this arrangement may not be true for every synapse. Indeed, small quantal amplitudes are occasionally observed at MF input to str. lucidum interneurons (Lawrence et al., 2004). Similarly, I occasionally observed very large amplitude EPSCs that were all-or-none in normal recording conditions. These instances were rare, however. In general, the data demonstrate that MF input to L-Mi has a smaller quantal conductance than that seen at MF input to str. lucidum interneurons. This claim is supported by the observation that MF input to L-Mi has a small quantal variance. Further, the data support the hypothesis that MF input to L-Mi is via small, *en passant* boutons both near the SDG and within the str. lucidum.

Small quantal variance can indicate a variety of synaptic characteristics including: a small number of release sites, little variation in the amount of transmitter per vesicle, or postsynaptic differences including the availability of receptors and dendritic filtering (Jonas et al., 1993; Bekkers and Clements, 1999). For example, it has been shown that distal inputs to a cell have a smaller quantal variance than proximal inputs (Bekkers and Clements, 1999). Interestingly, there was no difference in quantal amplitude or variance between the MF_{SDG} and MF_{SL} stimulation locations, indicating that the inputs may be equidistant and far from the soma. This hypothesis is further supported by the lack of difference between rise and decay times of macro EPSCs for the two inputs.

Possibly compensating for the relatively small quantal amplitude is a high convergence ratio from the MF onto L-Mi. Based on the average EPSC amplitude that is approximately four to five times larger than the quantal amplitude, many individual MF inputs converge onto single L-Mi. Furthermore, MF EPSCs that are between 4 and 5 times larger than the calculated quantal

amplitude can be evoked in L-Mi from both the MF_{SDG} and MF_{SL} stimulation locations simultaneously (Cosgrove et al., 2009), indicating a greater degree of input convergence. Thus, in my recordings, when both MF inputs were found in a single cell, 8 to 10 individual MF boutons may have been active (i.e. two inputs, each with amplitudes 4 to 5 times larger than the quantal amplitude). Alternatively, it is possible that boutons were release multiple quanta, and / or a single axon made multiple contacts with each L-Mi, though the anatomy do not indicate that granule cell axons frequently contact a postsynaptic target more than once or twice (Acsady et al., 1998). Thus, it would seem that multiple granule cell axons converge onto L-Mi. It is interesting to note that failures were evident even with these EPSC amplitudes, indicating a very low probability of release at each individual MF synapse. Together, these data indicate that MF input to L-Mi is comprised of many terminals that are probably *en passant* with small quantal amplitudes, low variance and low probabilities of release.

3.3.2 The MF to L-Mi connection is insensitive to small frequency changes

MF synapses on pyramidal cells and str. lucidum interneurons undergo frequency facilitation (Salin et al., 1996; Scanziani et al., 1998; Toth et al., 2000; Henze et al., 2000) which is thought to allow for temporal integration of stimuli across a broad range of frequencies (Salin et al., 1996; Lawrence and McBain, 2003). Since baseline firing of granule cells is usually low (Jung and McNaughton, 1993; Henze et al., 2002), frequency facilitation allows the MF connection to be sensitive to small changes in activity patterns (Salin et al., 1996; Lawrence and McBain, 2003). Since MF synapses on L-Mi do not facilitate at low or moderate frequencies, this connection appears to be responsive to the number rather than the frequency of individual inputs.

At high frequencies, however, MF input to L-Mi undergoes short term facilitation, which amplifies the integration of MF input. The short term facilitation at high frequencies of input indicate that these interneurons may utilize temporal summation to integrate inputs, requiring a barrage of high frequency input to reach action potential threshold. Indeed, we have shown that L-Mi summate inputs at short interstimulus intervals (Calixto et al., 2008; Cosgrove et al., 2009). As a result, it is possible that L-Mi integrate input from both the PP and MF in order to reach firing threshold, thus providing feedforward inhibition onto the pyramidal cell that is representative of both entorhinal cortex inputs to CA3. Interestingly, however, the inputs needed to converge on a dendritic compartment to allow supralinear summation – if the inputs occurred far apart, there was no supralinearity (Cosgrove et al., 2009).

Since L-Mi show facilitation only at high frequencies and dentate gyrus granule cells fire at high frequencies only occasionally, it is possible that these interneurons become active only during periods of high frequency dentate gyrus activity as brought about by exploratory behavior and memory formation (Hughes, 2008). Furthermore, since these interneurons undergo short term facilitation, rather than depression (as seen at the str. lucidum interneurons) it can be hypothesized that the interneurons serve complimentary functions. Str. lucidum interneurons respond relatively quickly to MF excitation because of their relatively large quantal amplitude and depolarized membrane potential (Lawrence et al., 2004), but then may cease firing due to the lack of short term facilitation at the synapse. Conversely, L-Mi may have a longer delay before first firing due to small quantal amplitude, thus exerting an inhibitory influence over CA3 pyramidal cells as activity from the str. lucidum interneurons in response to MF input wanes. Consequently, feedforward inhibition in area CA3 may result from the combined output of these two cell types, and others (i.e. str. radiatum interneurons).

4.0 MODULATION OF MOSSY FIBER INPUT TO L-M INTERNEURONS BY METABOTROPIC GLUTAMATE RECEPTORS

4.1 INTRODUCTION

The main sources of extrinsic excitatory input to area CA3 of the hippocampus are the perforant path (PP) from the entorhinal cortex, and the mossy fibers (MF) from the dentate gyrus. In addition, the CA3 network receives a strong intrinsic excitatory input from the associational connections via the recurrent axon collaterals (RC) of CA3 pyramidal cells. Under normal conditions, the excitatory drive from these three inputs is regulated by feedforward and feedback inhibition mediated by local GABAergic interneurons. Under pathological conditions like epilepsy, the balance between excitation and inhibition is disrupted (Avoli et al., 2002). Recent epilepsy research indicates that metabotropic glutamate receptors (mGluRs) may be a therapeutic target because they modulate both excitatory and inhibitory circuits in the hippocampus (Schoepp, 2001; Tang, 2005).

Metabotropic glutamate receptors fall into three distinct groups based on amino acid sequence and sensitivity to specific agonists (Conn and Pin, 1997). Group I mGluRs increase phospholipase C activity, and groups II and III inhibit adenylyl cyclase activity (Conn and Pin, 1997; Cartmell and Schoepp, 2000). Group III mGluRs are mGluRs 4, 6, 7 and 8 which are sensitive to the agonist L-(+)-2-amino-4-phosphnobytyric acid (L-AP4) at varying

concentrations (Conn and Pin, 1997), and of those, mGluRs 4, 7 and 8 are expressed in the hippocampus. Group III mGluRs 4 and 8 have a high affinity for both L-AP4 and glutamate, becoming active with concentrations in the tens of μM (Conn and Pin, 1997). In contrast, mGluR 7 has a very low affinity for both L-AP4 and glutamate, requiring concentrations of near 1 mM to become active. Anatomical data indicate that within the hippocampus, group III mGluRs are commonly found presynaptically within the active zone of asymmetric synapses (Shigemoto et al., 1997; Bradley et al., 1999). When expressed presynaptically, mGluRs reduce synaptic transmission through a variety of mechanisms including modulation of ion channels, and phosphorylation of proteins in the release machinery (Anwyl, 1999; Cartmell and Schoepp, 2000). Additionally, mGluRs are frequently expressed differentially on axon terminals based on the identity of the target cell (Scanziani et al., 1998; Semyanov and Kullmann, 2000; Toth and McBain, 2000; Rusakov et al., 2004).

Previous investigations into the functional role of group III mGluRs in CA3 of the hippocampus have focused on mGluR 7 (Shigemoto et al., 1997; Corti et al., 2002; Pelkey et al., 2005). MF boutons containing mGluR 7 target interneurons within the str. lucidum, but not pyramidal cells (Shigemoto et al., 1997; Pelkey et al., 2005). The presence of mGluR 7 on MFs targeting str. lucidum interneurons facilitates the expression of long term depression at that synapse in response to high frequency MF activity (Pelkey et al., 2005). MF input to L-Mi, however, generally undergoes postsynaptically expressed long term potentiation in response to high frequency stimulation. Because not all MF terminals targeting interneurons express mGluR 7 (Shigemoto et al., 1997), and MF to L-Mi connection does not express presynaptic long term depression, I hypothesized that mGluR 7 is not present on MF terminals contacting L-Mi, and

that presynaptic expression of group III mGluRs on MF boutons contacting interneurons is target-cell specific.

In order to test this hypothesis, the group III mGluR agonist L-AP4 was utilized at varying concentrations. First, a dose-response curve was performed in order to gauge the sensitivity of the synapse to varying concentrations of L-AP4. Then, having identified the receptor that is present, a series of experiments were performed using a single concentration (10 μM) to gain a deeper understanding of the localization of the receptor and its mechanisms.

This chapter will demonstrate the presence of a high affinity group III mGluR at the MF to L-Mi synapse that is in contrast to the low affinity mGluR 7 at the MF to str. lucidum interneuron synapse described previously (Pelkey et al., 2005). Additionally, I will provide evidence that localizes the receptor to the presynaptic terminal and I will offer a mechanism through which the receptor effects its actions.

4.2 RESULTS

4.2.1 High affinity, but not low affinity group III mGluRs are present at MF to L-Mi synapses.

Receptors belonging to group III mGluRs are mGluRs 4, 6, 7 and 8 and are activated by the agonist L-AP4 (Conn and Pin, 1997). Of those receptors, mGluRs 4, 7 and 8 are expressed in the hippocampus (Tanabe et al., 1993; Saugstad et al., 1994; Shigemoto et al., 1997). Previous reports indicate that MF input to str. lucidum interneurons is modulated by mGluR 7, the low affinity group III mGluR (Pelkey et al., 2005) which binds glutamate in the 1 mM range and L-

AP4 at 160 to 500 µM (Conn and Pin, 1997). To determine whether this receptor is also present on MF terminals contacting L-Mi, I performed a dose-response curve using the group III mGluRs agonist L-AP4 (Fig. 10B). Since there is a ten-fold difference in the affinity mGluRs 4/8 and mGluR 7 for L-AP4, it is possible to parse the group III mGluRs into high (mGluRs 4/8) and low (mGluR 7) affinity receptors. As a result of the dose-response curve, I found no evidence for the presence of mGluR 7, but did find evidence for the presence of high affinity group III mGluRs 4 and 8, which have an affinity for glutamate near 3 -38 µM, and for L-AP4 in the 1 – 2 µM range (Conn and Pin, 1997). Specifically, the dose response curve shows that L-AP4 at 400 µM produced no further decrease in EPSC amplitude compared to L-AP4 at 20 µM, a saturating dose for mGluRs 4/8 that is insufficient to activate mGluR 7 (400 µM: 31.93 ± 7.13% of control, N = 5; 20 µM: 32.30 ± 6.47% of control, N = 9; p = .971; Fig. 10B). These data indicate that mGluR 7 is not present at MF terminals contacting L-Mi, but that mGluRs 4/8 are present, confirming the hypothesis that these receptors are distributed in a target-specific manner across MF boutons targeting interneurons.

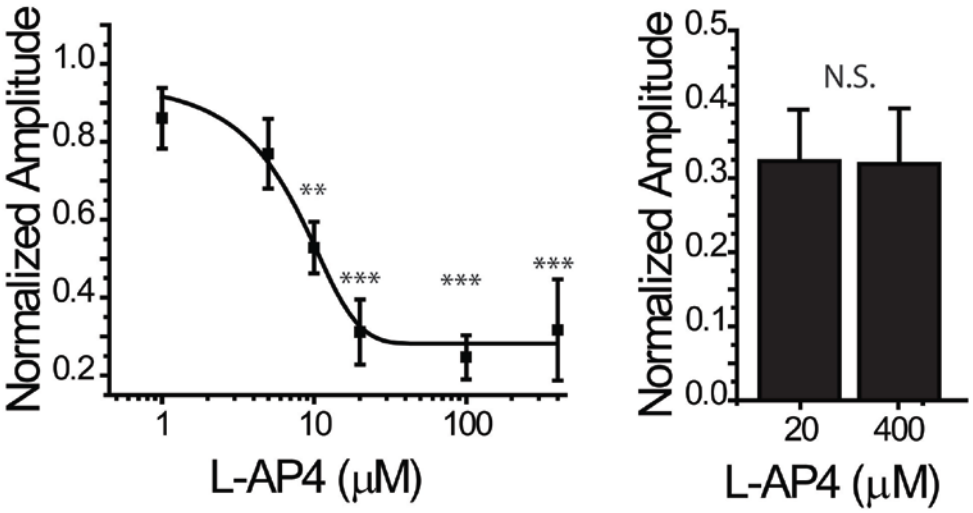

Figure 10. MF input to L-Mi is modulated by low, but not high affinity group III mGluRs.

The left panel shows a plot of normalized EPSC amplitude at varying concentrations of L-AP4 from 1 to 400 μM. The right panel is a summary bar graph demonstrating no difference in the amount of inhibition by 20 vs. 400 μM – AP4. $N \geq 5$ at each point. ** $p < 0.01$; *** $p < 0.001$

4.2.1.1 Effect of mGluRs 4/8 activation at the MF to L-Mi synapse

Though the dose response curve indicates the presence of mGluRs 4/8 at MF input to L-Mi, a more careful series of experiments was required to elucidate the localization of the receptor and the mechanisms through which it effects its actions. Thus, in the next series of experiments, I applied 10 μM L-AP4 to ensure that I was selectively activating mGluRs 4/8, and also stimulated the RC pathway of CA3, which has been shown to be relatively insensitive to mGluRs agonists (Kamiya et al., 1996; Toth and McBain, 1998) but see (Doherty and Dingledine, 1998; Laezza et al., 1999). The RC pathway was included for two reasons. First, the inclusion of a second, independent pathway allows for a rudimentary assessment of pre- vs. postsynaptic localization of a receptor as the bath application of the agonist could affect all inputs if the receptor was expressed postsynaptically. Though a postsynaptic expression does not guarantee that an effect would be observed at all inputs, if the RC input was also affected in the absence of evidence for a presynaptic effect, it would provide evidence that the receptor was postsynaptically expressed. Additionally, the RC pathway allowed me to determine if all excitatory inputs to L-Mi were modulated by mGluRs 4/8, or if the expression pattern was restricted to the MF input.

EPSCs evoked by MF stimulation decreased by 45.65 ± 5.47% ($N = 12$, $p < 0.001$) in the presence of 10 μM L-AP4, an effect that was fully reversible with a washout period (93.38 ± 4.34% of control, $p = 0.183$; Fig. 11C and 11F, blue bars). The effect of the group II mGluRs agonist DCG-IV (1 μM) for this group of cells was a decrease of 67.75 ± 4.34% ($N = 12$, $p < 0.001$), which is similar to the effect of DCG-IV on MF-evoked responses in other interneurons (Toth et al., 2000; Alle et al., 2001; Lawrence et al., 2004). In contrast, EPSCs evoked by RC stimulation did not change in response to either L-AP4 or DCG-IV application (L-AP4: 2.71 ± 5.92% decrease, $p = 0.666$; DCG-IV: 4.45 ± 5.14% decrease, $p = 0.426$; $N = 6$; Fig. 11D and

11F, red bars). Interestingly, the decrease in MF-evoked EPSC amplitude with 10 µM L-AP4 is similar to that previously reported at the MF to pyramidal cell synapse of the guinea pig (Manzoni et al., 1995; Yoshino et al., 1996) and at granule cell input to hilar border interneurons (Doherty and Dingledine, 1998). Consequently, though the anatomical data indicate that the predominant group III mGluR present within CA3 of the hippocampus is mGluR 7, this physiologic demonstration of the presence of a high affinity group III mGluR at this synapse is not unprecedented, and will require further study.

In a subset of these cells, the control MF recordings had a failure rate of at least 10%. For these cells, I analyzed the failure rate, paired-pulse ratio and coefficient of variation before and after the application of 10 µM L-AP4. As would be expected from a presynaptically mediated depression, application of L-AP4 increased the failure rate (21.0 ± 6.23% control to 66.45 ± 11.47% L-AP4; $p < 0.01$; $N = 6$), paired-pulse ratio (1.04 ± .05 control to 1.54 ± .14 L-AP4; $p < 0.01$; $N = 5$) and coefficient of variation (0.535 ± 0.08 control to 0.857 ± 0.208; $p < 0.05$; $N = 6$) indicating that activation of mGluRs 4/8 decreases the probability of transmitter release (Fig. 11E). Coupled with the observation that L-AP4 application did not affect the amplitude of the RC input recorded from L-Mi, these data support the hypothesis that mGluRs 4/8 are located presynaptically at the MF to L-Mi connection.

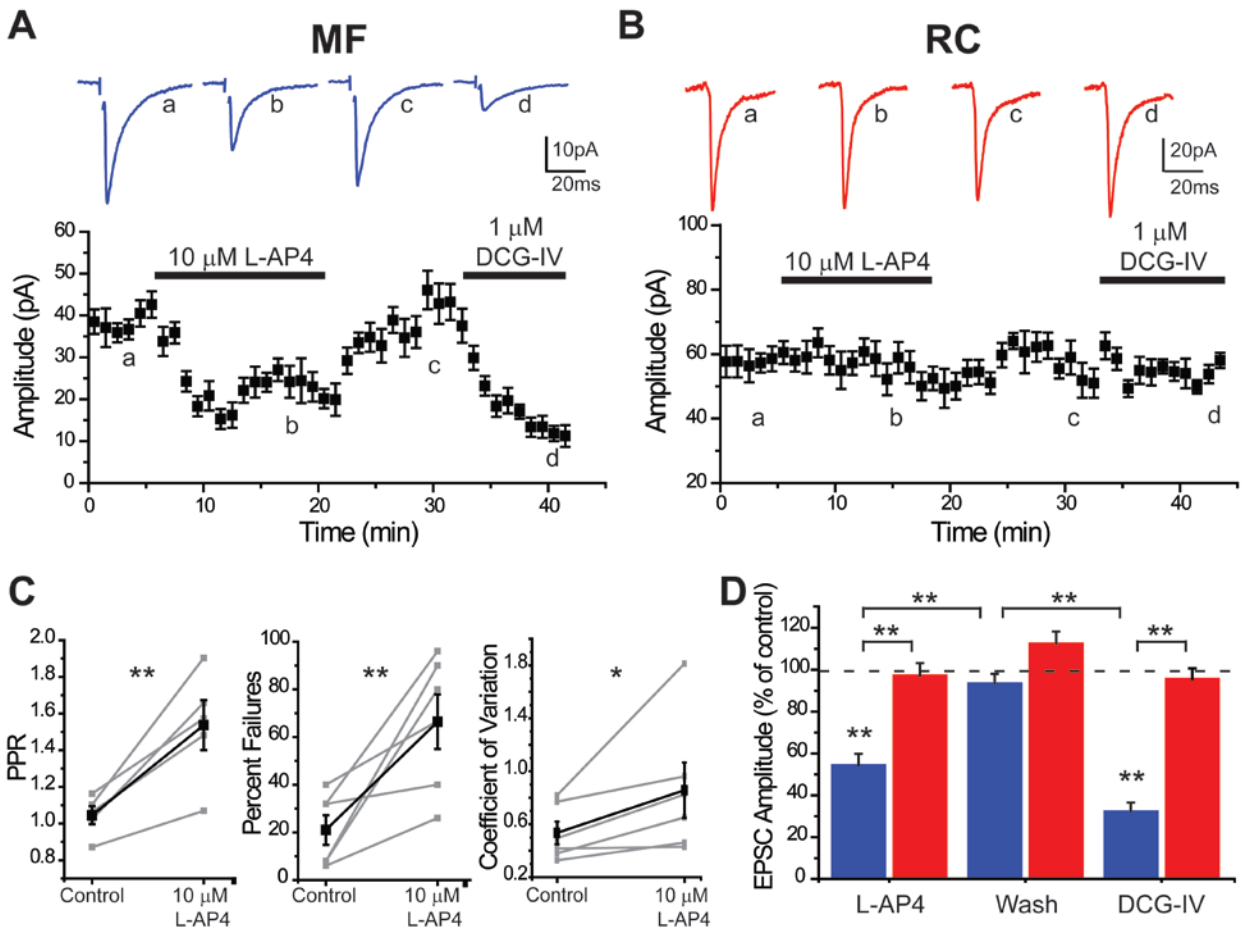

Figure 11. High affinity group III mGluRs are present on MF terminals contacting L-Mi.

A) Example cell showing the effect of 10 µM L-AP4 on MF evoked EPSCs. Averaged traces (N = 30) are inset; a = control, b = L-AP4, c = washout, d = DCG-IV. B) Same as in A, but as a result of RC stimulation. C) Summary data for paired-pulse ratio (left), failure rate (middle) and coefficient of variation (right) of a subset of the data. D) Summary data showing the effect of 10 µM L-AP4 on MF evoked (blue bars, N = 11) and RC evoked (red bars, N = 6) EPSCs. *p < 0.05; **p < 0.01.

Since MFs are pharmacologically identified through the application of the group II mGluRs agonist DCG-IV (Kamiya et al., 1996), and both group II and group III mGluRs have been shown to inhibit adenylyl cyclase (Conn and Pin, 1997; Cartmell and Schoepp, 2000), I wanted to know whether L-AP4 occluded the actions of DCG-IV. In a separate group of cells I performed a simple occlusion experiment, first applying L-AP4 and then applying DCG-IV without a washout period. L-AP4 did not occlude the actions of DCG-IV. Following application of 10 μM L-AP4 (38.28 ± 4.2% decrease, N = 10), DCG-IV caused a further decrease of 66.08 ± 5.32% in EPSC amplitude ($p < 0.001$; N = 10; Fig. 12). Additionally, since 10 μM L-AP4 was not a maximal concentration (see Fig. 10), I compared the effect of DCG-IV after L-AP4 application to the effect of DCG-IV alone (previous experiment). There was no significant difference in the effect of DCG-IV (DCG-IV alone: 67.75 ± 4.34%; N = 12; DCG-IV after L-AP4: 66.08 ± 5.32%; N = 10; $p = 0.967$; Fig 12C).

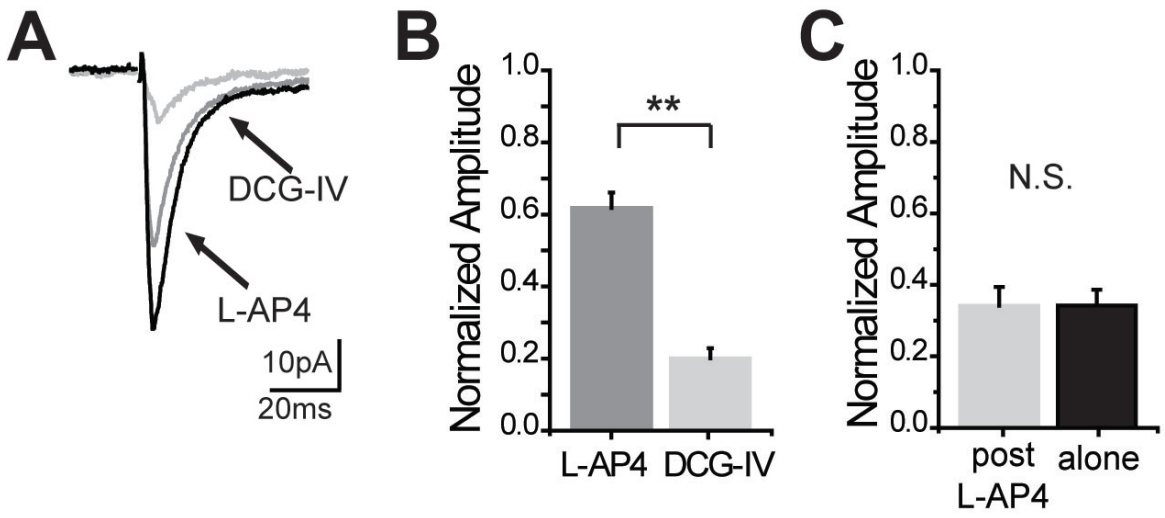

Figure 12. Group III mGluR activation does not occlude group II mGluRs.

A) Averaged traces (N = 30) of a mossy fiber evoked EPSC after application of 10 µM L-AP4 (dark grey) and then 1 µM DCG-IV (light grey) in the continued presence of L-AP4. B) Summary data showing the average normalized values following L-AP4 (dark grey bar) and DCG-IV (light grey bar) in the continued presence of L-AP4. C) Summary data comparing the effect of DCG-IV (light grey bar) after L-AP4 vs. alone (black bar, data re-presented from Fig. 11) on the normalized value of EPSC amplitude. There was no difference in the effect of DCG-IV ($p > 0.001$). **$p < 0.01$

4.2.2 mGluRs 4/8 are localized on MF terminals contacting L-Mi

The increase in failure rate and PPR suggests a presynaptic localization of mGluRs 4/8 at the MF – L-Mi synapse, an interpretation supported by anatomical studies (Shigemoto et al., 1997; Bradley et al., 1999; but see Bradley et al., 1996). To obtain a direct confirmation of the presynaptic localization of the receptor, I used Sr^{2+} (see section 3.2.3.1) to de-synchronize the evoked release into putative single quanta (Goda and Stevens, 1994; Bekkers and Clements, 1999; Lawrence, 2004). To confirm that activation of mGluRs 4/8 had a presynaptic effect, I assessed the effect of L-AP4 (10 µM) on the amplitude and frequency of aEPSCs (Price et al., 2005). In the presence of 3 mM Sr^{2+}, L-AP4 application decreased the frequency of aEPSCs following stimulation (3.72 ± 0.72 Hz control to 2.30 ± 0.30 Hz L-AP4; $p < 0.05$; $N = 7$) without changing the amplitude (7.09 ± 0.40 pA control to 7.73 ± 0.61 pA L-AP4; $p = 0.389$; $N = 7$; Fig. 13). The effect on frequency was fully reversible (3.84 ± 0.33 Hz after washout). This was also true when the frequency was normalized to the frequency of spontaneous events (2.39 ± 0.48 Hz control; 1.49 ± 0.34 Hz L-AP4; 2.01 ± 0.55 Hz wash out; Fig. 13). The MF origin of the pathway stimulated in this experiment was confirmed with application of DCG-IV (1 µM) following washout of Sr^{2+} (41.5 ± 5.8% of control). The lack of change in aEPSC amplitude combined with a significant decrease in frequency indicates that activation of mGluRs 4/8 decreases the probability of release without affecting postsynaptic receptors (Price et al., 2005), providing direct evidence that mGluRs 4/8 are localized presynaptically on MF terminals contacting L-Mi.

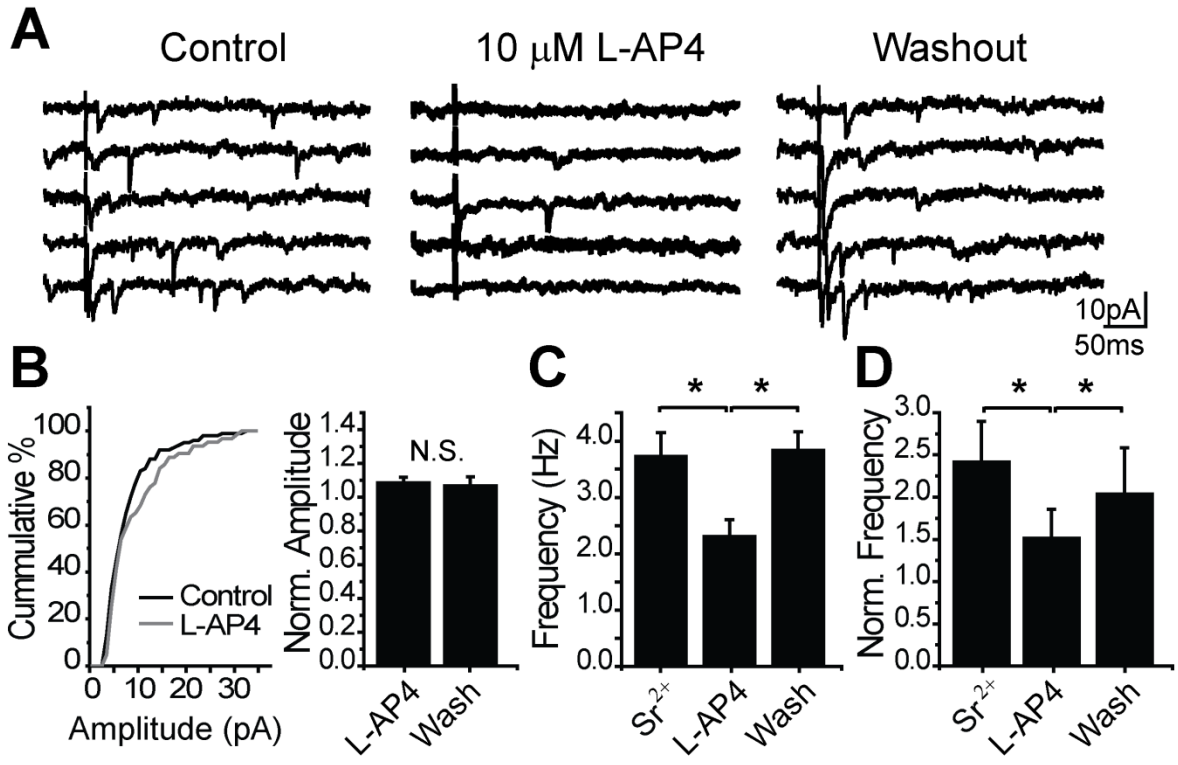

Figure 13. L-AP4 decreases frequency but not amplitude of aEPSCs.

A) Sample traces recorded from a representative L-Mi in the presence of 3 mM Sr^{2+} (left), 10 μM L-AP4 (middle), and following L-AP4 wash out (right). B) Left, plot of the cumulative amplitude of aEPSCs before (control, black line) and after L-AP4 (grey line) for the example cell. Right, summary data of the average amplitude of aEPSCs normalized to the amplitude of aEPSCs in the control condition. There is no significant difference in amplitude with L-AP4, or washout. C and D) L-AP4 decreases both the actual frequency of aEPSC (C) and the frequency of aEPSCs when normalized to the spontaneous frequency (D). *$p < 0.05$

4.2.3 The N-type calcium channel is a target of high affinity mGluRs at MF input to L-Mi

Having demonstrated the presynaptic localization of the high affinity mGluRs at MF input to L-Mi, I assessed whether N-type or P/Q-type VGCCs were downstream targets of mGluRs 4/8 activation. Previous reports have demonstrated that a common mechanism through which presynaptic receptors effect their actions is inhibition of a VGCC (Catterall and Few, 2008). Specifically, it has been demonstrated that group III mGluRs inhibit N-type VGCC function (Millán and Sánchez-Prieto, 2002; Rusakov et al., 2004; Guo and Ikeda, 2005) though inhibition of P/Q-type VGCCs has also been documented (Takahashi et al., 1996). At the MF filopodial extension, activation of the low affinity group III mGluR, mGluR 7, inhibits P/Q-type VGCC function (Pelkey et al., 2006), as application of the P/Q-type channel blocker occludes the effects of mGluR7 in str. lucidum interneurons. There is evidence, however, that low and high affinity group III mGluRs target different populations of VGCCs (Millan et al., 2002).

In order to determine whether N- or P/Q-type VGCCs are inhibited by activation of mGluRs 4/8 at MF input to the L-Mi, I again performed an occlusion experiment. L-AP4 (10 μM) was applied after selectively blocking the N- or P/Q-type VGCCs with the specific toxins ω-conotoxin GVIA (ω-CgTx) or ω-agatoxin IVA (ω-AgaTx), respectively. L-AP4 decreased EPSC amplitude by 28.05 ± 4.90% (N = 10) in the presence of ω-CgTx, but caused a decrease of 62.0 ± 11.69% (N = 7; $p < 0.01$; Fig. 14B) in the presence of ω-AgaTx. These data indicate that activation of mGluRs 4/8 results in inhibition of N-type VGCCs, which is a similar to what has been reported at other synapses (Rusakov et al., 2004). Additionally, when these data are compared to the effect of 10 μM L-AP4 in the absence of a VGCC, the effect of L-AP4 after blockade of N-type VGCCs is significantly smaller, indicating that ω-CgTx partially occludes

the effects of L-AP4 (L-AP4 after CgTx: 28.05 ± 4.90% decrease; N = 10 vs. L-AP4 alone: 45.65 ± 5.47% decrease; N = 11; $p < 0.05$; value from previous experiment, see 4.2.1.2).

Since the variability of the effect of ω-CgTx was high, determining whether the effect of L-AP4 was occluded by blocking N-type VGCCs was difficult, since in some cells N-type VGCCs were not linked to release. Consequently, I determined whether there was a relationship between the effect of L-AP4 and CgTx. If many N-type VGCCs were present (a large effect of ω-CgTx), would L-AP4 cause a further decrease (indicating N-type VGCCs are not a target of mGluRs 4/8 activation) or would the effect of L-AP4 be small (indicating that N-type VGCCs were a target). To do this, I plotted the percent decrease as a result of L-AP4 application after ω-CgTx vs. the percent decrease in EPSC amplitude resulting from application of ω-CgTx (Fig. 14E). As the figure demonstrates, the two values were significantly correlated (slope: -41.55 ± 4.64; N = 10; R = -0.807; $p < 0.01$) such that when ω-CgTx had its largest effect (% decrease near 50%), L-AP4 application resulted in no further decrease in EPSC amplitude (% decrease near 10%). Thus, it can be concluded that when N-type VGCCs are linked to transmitter release at the MF to L-Mi connection, activation of mGluRs 4/8 target N-type VGCCs to decrease transmitter release.

I was also interested in determining whether the group II agonist DCG-IV targeted either N- or P/Q-type VGCCs. Since L-AP4 and DCG-IV did not occlude one another, indicating that the two receptors do not converge on a common mechanism, it was my hypothesis that N-type VGCCs were not a downstream target of group II mGluRs activation. The actions of DCG-IV were not occluded by either the application of ω-CgTx (63.35 ± 5.94% decrease; N = 7; $p > 0.05$) or ω-AgaTx (63.74 ± 7.14% decrease; N = 6; $p > 0.05$) when compared with the effect of DCG-IV alone (67.75 ± 4.34% decrease; N = 11; Fig. 14; DCG-IV value from previous

experiment, see: 4.2.1.2). From these data, it can be concluded that group II mGluRs do not target either N- or P/Q-type VGCCs, which is not unprecedented (Takahashi et al., 1996) as group II mGluRs have been shown to target release machinery proteins to effect their actions (de Jong and Verhage, 2009).

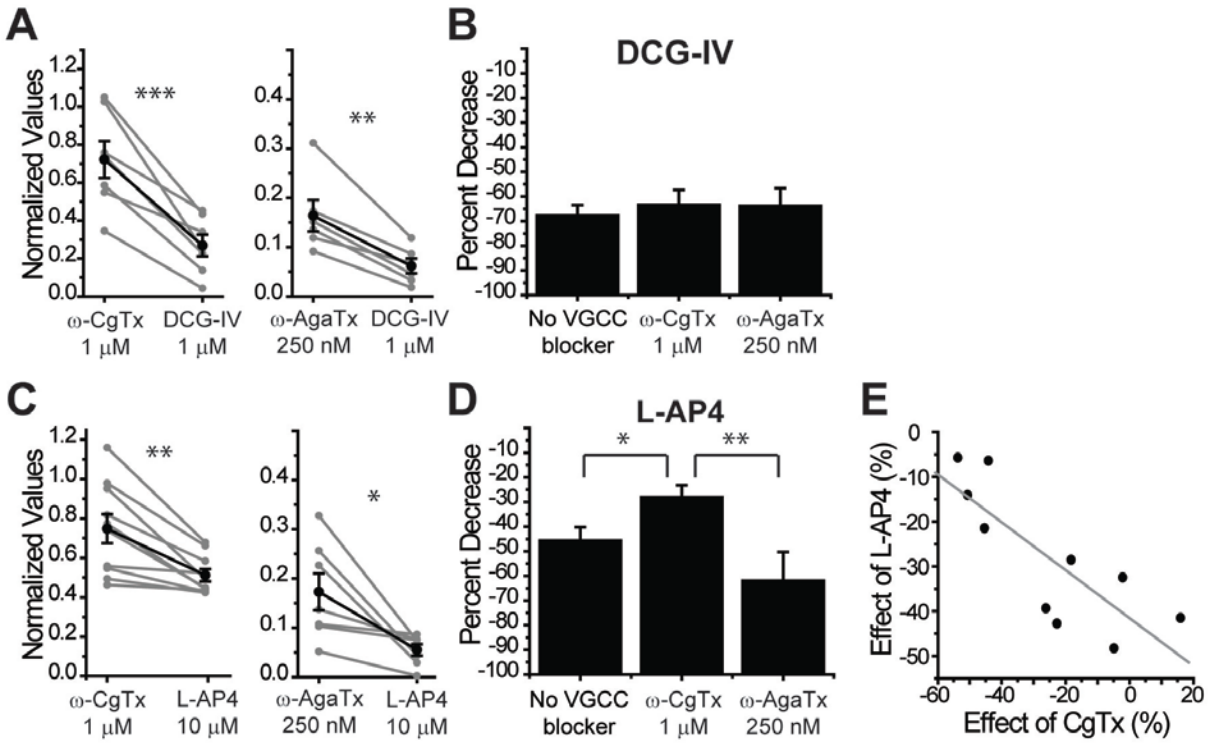

Figure 14. Blockade of N-type VGCCs occludes group III mGluR actions.

A. Plot of the normalized MF EPSC amplitude following application of ω-conotoxin GVIA (left; N = 10) or ω-agatoxin IVA (right; N = 7), and subsequent application of 1 μM DCG-IV. Grey symbols and lines represent individual cell data, black symbols and lines represent mean ± SEM. B. Summary data showing the percent decrease in EPSC amplitude following application of 1 μM DCG-I alone (No VGCC blocker) and after blockade of either N-type (ω-CgTx) or P/Q-type (ω-AgaTx) VGCCs. C and D. Same as in A and B, but using the group III mGluR agonist L-AP4. E. Plot of the percent decrease in EPSC amplitude resulting from application of CgTx vs. L-AP4. Black symbols are individual cell data. The grey line is a linear fit, showing the negative relationship of the two values. N = 10; R = -0.807; $p < 0.01$. * $p < 0.05$; ** $p < 0.01$; *** $p < 0.001$.

4.3 DISCUSSION

In this chapter, I have presented data demonstrating the presence of a high affinity group III mGluR on the presynaptic terminals of MF input to interneurons within str. lacunosum moleculare of CA3. Furthermore, I have provided evidence that mGluRs 4/8 mediated suppression of glutamate release through inhibition of N-type VGCCs. These results indicate that MF input to CA3 interneurons displays target specificity not only of short term plasticity characteristics (Chapter 3), but also the distribution of presynaptic proteins that regulate transmitter release.

This finding that MF input to L-Mi is modulated by high, but not low affinity group III mGluRs, is surprising. Previous reports detailing the mechanisms of MF input to str. lucidum interneurons as well as anatomical data detailing the cellular localization of group III mGluRs in area CA3 indicate that mGluR 7 is the predominant group III mGluR in CA3. Importantly, these data also indicate that mGluR 7 is not the only group III mGluR in CA3 of the hippocampus.

4.3.1 Addressing the anatomical location of mGluRs in the hippocampus

A previous electrophysiological report did not indicate the presence of mGluRs 4/8 at the MF to str. lucidum interneuron synapse but showed that this connection is specifically modulated by mGluR 7 activation (Pelkey et al., 2005; but see Doherty and Dingledine, 1998). Consistent with these electrophysiological data, a Ca^{2+} imaging study of the MF filopodial extensions, which are known to preferentially target interneurons (Acsady et al., 1998), showed that high concentrations of L-AP4 decreased fluorescence, indicating that VGCCs are targets of mGluR 7 activation (Pelkey et al., 2006). In contrast, low concentrations of L-AP4 that would have

preferentially activated mGluRs 4/8 did not decrease fluorescence in filopodia terminals (Pelkey et al., 2006). These findings demonstrate the presence of mGluR 7 at MF input to str. lucidum interneurons in addition to the presence of mGluR 7 on filopodial extensions when the identitiy of the postsynaptic neuron is unknown and could potentially be an L-Mi.

Though our data indicate that the N-type VGCC is a downstream target of mGluRs 4/8 activation, since the complement of VGCCs linked to release is variable, it is likely that inhibition of the N-type VGCC is not the only effect of mGluRs 4/8 activation (Scanziani et al., 1995; Anwyl, 1999). Indeed, application of ω-CgTx to block N-type VGCCs only partially occludes the actions of L-AP4 at the MF – L-Mi synapse. Consequently, it is possible that application of low concentrations L-AP4 would not result in a detectable change in calcium signal within the filopodial extensions. Furthermore, as discussed in the previous chapter, it may be that L-Mi are preferentially targeted by *en passant* boutons rather than filopodia, and as yet, calcium imaging experiments have not investigated *en passant* boutons of the MF system.

Because perforant path (PP) synaptic responses are sensitive to both group II and group III mGluRs, it could be argued that electrical stimulation applied to MF_{SDG} could activate the PP, rather than dentate gyrus granule cells. This is unlikely for the following reasons. First, the medial and lateral perforant paths are modulated by complementary sets of mGluRs, the medial by group II and the lateral by group III, but not both (Macek et al., 1996). The postsynaptic responses that were evoked from MF_{SDG} stimulation were highly sensitive to agonists of both group II and group III mGluRs. Furthermore, the frequency, but not amplitude of asynchronous EPSCs were also affected by both L-AP4 and DCG-IV, indicating that the fibers from which these aEPSCs were evoked are sensitive to both L-AP4 and DCG-IV, and that it is not a disynaptic connection. Additionally, when the MF was stimulated within the str. lucidum

activating synapses far from the str. lacunosum-moleculare (Cosgrove et al., 2009), the sensitivity to L-AP4 was identical to stimulation at the MF_{SDG} (Table 5). Together, these data support the claim that glutamate release from MF onto L-Mi is modulated by mGluRs 4/8. This novel finding indicates the presence of high affinity group III mGluRs at MF terminals targeting a specific feedforward inhibitory interneuron, suggesting that L-Mi serve unique functional roles in the CA3 neural network.

In addition to the published data specifically concerning MF input to CA3 interneurons, the documented anatomical localization of group III mGluRs in the hippocampus (Shigemoto et al., 1997; Bradley et al., 1999; Corti et al., 2002) also needs to be addressed. Anatomically, the immunolocalization of mGluR 4 on presynaptic terminals forming asymmetric synapses in CA3 is diffuse and prominent only in the inner and middle one-third of the dentate gyrus moleculare layer (Shigemoto et al., 1997; Bradley et al., 1999; Corti et al., 2002). In contrast, the distribution of mGluR 8 is pronounced in the str. lacunosum moleculare of CA3 and has been attributed to the axon terminals of the lateral perforant path (Shigemoto et al., 1997; Ferraguti et al., 2005) because lesions to the entorhinal cortex decrease (though do not eliminate) this staining (Shigemoto et al., 1997). However, we have previously demonstrated spatial overlap between MF and PP synapses on L-Mi within the str. lacunosum moleculare of area CA3 (Cosgrove et al., 2009), making it possible that some of the mGluR 8 staining in the previous work may be due to granule cell axons *en route* to the str. lucidum. Supporting our contention that MF input to L-Mi is modulated by mGluRs 4/8 is the finding that mRNA for mGluRs 4 and 8 are found within the dentate gyrus granule cells (Tanabe et al., 1993; Ohishi et al., 1995; Saugstad et al., 1997; Ferraguti et al., 2005).

4.3.2 MF input to L-Mi is regulated by mGluRs 4/8

These data demonstrate that MF input to L-Mi is sensitive to low concentrations of L-AP4, an agonist to group III mGluRs. Since mGluRs 4/8 and mGluR 7 have a tenfold difference in affinity for L-AP4 and glutamate (Conn and Pin, 1997), it is possible to selectively activate mGluRs 4/8 without activating mGluR 7 using a low (10 μM) concentration of L-AP4. MF input to L-Mi is highly sensitive to this concentration of L-AP4, decreasing the postsynaptic response by ~45%. This robust inhibition is presynaptically mediated as indicated by the increase in failure rate, paired-pulse ratio and coefficient of variation of the postsynaptic response. Though the stimulation protocol was not minimal, the stimulation intensity was low and failures were evident in many of the recordings. L-AP4 application increased the frequency of these failures indicating that activation of mGluRs 4/8 decreases the probability of release. In order to provide a direct indication that mGluRs 4/8 are present presynaptically on the MF bouton and activation of these receptors decreases the probability of release, EPSCs were desynchronized into putative single quanta and the effects of L-AP4 on frequency and amplitude of the asynchronous response were monitored. Since there was no change in the amplitude of the response, an effect at the level of the postsynaptic AMPAR can be ruled out. Additionally, since the frequency of the response was reversibly decreased with L-AP4 application, it can be concluded that activation of mGluRs 4/8 result in a decrease in the probability of release. Adding further support to the claim that mGluRs 4/8 are presynaptically located is the finding that the RC input was not affected by application of L-AP4 and that ω-CgTx partially occludes the actions of L-AP4. Together, these data provide a convincing demonstration that MF terminals contacting L-Mi express mGluRs 4/8.

5.0 FUNCTIONAL IMPLICATIONS OF TARGET-SPECIFIC EXPRESSION OF GROUP III MGLURS AT MF INPUT TO L-M INTERNEURONS

5.1 INTRODUCTION

The differential distribution of a presynaptic protein is only important if the expression of that protein confers specialization of the synaptic communication at that synapse. Though I have demonstrated that MF express mGluRs 4/8 in a seemingly target-specific manner, and that activation through use of the agonist L-AP4 decreases the probability of transmitter release from those boutons, I have not yet provided evidence of the endogenous function of the receptor. This chapter will address the impact of the presynaptic high affinity group III mGluR on the function of the MF to L-Mi connection.

5.1.1 Agonists are insufficient to determine endogenous receptor function

Use of the agonist L-AP4 to investigate the functional role of group III mGluRs has been shown to not effectively mimic activation of the receptor by synaptic activity (Pinheiro and Mulle, 2008). For example, at the calyx of Held, L-AP4 application produces a robust inhibition of transmitter release (Barnes-Davies and Forsythe, 1995; Takahashi et al., 1996; Billups et al., 2005). Use of the group III antagonist to prevent endogenous activation of the receptor at the calyx of Held, however, reveals a much more subtle effect with little to no impact on the

synaptic amplitude and short term plasticity characteristics of the synapse (von Gersdorff et al., 1997; Billups et al., 2005). A similar pattern has been noted in the nucleus tractus solitarius (Chen et al., 2002) and cerebellar cortex (Lorez et al., 2003). Thus, though use of an agonist is useful for determining the presence and localization of a receptor, investigations into the function of a receptor cannot use the agonist because the effect of receptor activation is frequently overestimated. In order to get a true understanding of the role of a receptor, the antagonist must be used.

Use of the antagonist presents another problem, however, in that the investigator must then discover a pattern of activity sufficient to activate the receptor. Further, any activity pattern must be constrained by the known patterns of activity produced by the cell *in vivo* to gain an accurate understanding of the receptor's role at a synapse. Previous investigations into the role of the group III mGluR at the calyx of Held used long trains of high frequency stimulation to attempt to uncover the role of that receptor when activated by synaptic glutamate (von Gersdorff et al., 1997; Billups et al., 2005). The use of such a protocol at MF input to L-Mi, however, would be unrealistic as dentate gyrus granule cells do not tend to fire in prolonged (1 sec) bursts of high frequency activity (Jung and McNaughton, 1993; Henze et al., 2002). Instead, granule cells generally have a low firing frequency, occasionally firing in high frequency bursts in response to a relevant behavior by the rat (Jung and McNaughton, 1993; Henze et al., 2002).

Because the pattern of activity that would be sufficient to activate the high affinity group III mGluR at the MF to L-Mi connection was unknown, several frequencies were investigated. Further, in creating a hypothesis about the type of activity that might activate the receptor, it is of use to remember that the group III mGluR at MF input to L-Mi is a high affinity receptor, binding glutamate in at 3 to 38 μM allowing the receptor to be sensitive to small changes in the

concentration of glutamate as a result of synaptic activity. Additionally, these receptors are located within the active zone of the presynaptic terminal (Shigemoto et al., 1997), thus placing these receptors in close proximity to synaptically released glutamate from the MF. Turning to the literature, there are reports documenting the tonic activity of presynaptic mGluRs (Losonczy et al., 2003), the activation of presynaptic mGluRs during moderate frequencies of activity (Scanziani et al., 1997), and some evidence that short trains of frequencies within the gamma band are capable of activating presynaptic mGluRs (Chen et al., 2002).

Thus, in order to determine the role of the mGluRs 4/8 at MF input to L-Mi, I investigated whether the receptors were tonically active, activated by low to moderate frequencies (0.05 – 4 Hz) of activity, and high frequencies (20 or 40 Hz) of activity through use of the group III mGluR competitive antagonist MSOP (100 μM). Specifically, because MF input to L-Mi does not undergo frequency facilitation (Chapter 3), it was my hypothesis that moderate frequencies of activity would be sufficient to activate the receptor, decreasing glutamate release from the MF sufficiently to prevent frequency facilitation, such that when activation of mGluRs 4/8 is prevented through application of MSOP an underlying frequency facilitation would be revealed.

5.1.2 Spike transmission from MF to postsynaptic targets

In addition to understanding the role of the receptor in modulating glutamate release from the MF onto the L-Mi, as part of this series of experiments, I was interested in determining whether that change in transmitter release was meaningful to the L-Mi in such a way that the firing of the L-Mi in response to MF input was altered as a result of mGluRs 4/8 activation. L-Mi are accommodating interneurons (Calixto et al., 2008; Ascoli et al., 2009), and are reluctant to fire

action potentials (personal observation). This may be, in part, due to the small quantal amplitude of MF input to L-Mi. Another factor contributing to the reluctance of L-Mi firing could be the relatively hyperpolarized resting membrane potential of the cells (-67.78 ± 0.72 mV). An alternative possibility is that in the *in vitro* preparation where connections have been cut and stimulation intensity is low there are not enough inputs to the cell to effectively bring it to firing threshold. This property of the slice preparation is useful because studying synaptic currents is more tractable, but does limit our understanding of what a meaningful input to a cell is – if modulation of an input does not result in a shift in the cells output, it may not be functionally relevant. Thus, I was interested in determining whether activation of this receptor changed the probability of spike transmission between the MF and L-Mi.

A recent *in vivo* study was performed investigating the probability of spike transmission within CA3 as a result of a single dentate gyrus granule cell firing (Henze et al., 2002). Interestingly, it was noted that the probability of spike transmission for interneurons and pyramidal cells is not high in response to a single stimulus, but that through a short train the probability increases. For MF input to interneurons, however, the probability is always rather low (Henze et al., 2002). In keeping with this, an investigation into the probability of spike transmission at the MF to str. lucidum interneuron connection revealed that str. lucidum interneurons require short trains of MF input to reach firing threshold (Lawrence et al., 2004). Interestingly, however, it was also noted that str. lucidum interneurons have a relatively high probability of spontaneous action potentials (2.8 Hz; Lawrence et al., 2004), which was similar to what was seen *in vivo* (Henze et al., 2002). In contrast, L-Mi rarely, if ever fire spontaneously during a recording (personal observations), indicating that in order to bring L-Mi to firing threshold, trains of activity will be required. Thus, to determine the impact of mGluRs 4/8

activation on spike transmission at the MF to L-Mi connection, short trains of 10 stimuli at 20 and 40 Hz were delivered. These frequencies were chosen because they fall within the range of frequencies granule cells fire in vivo (Jung and McNaughton, 1993; Henze et al., 2002).

The goal of this chapter is to investigate the physiologic role of the presence of mGluRs 4/8 on MF terminals contacting L-Mi, including the pattern of activity required to activate the receptor endogenously and the impact of the receptor on the probability of spike transmission between the MF and L-Mi. Importantly, the antagonist will be used to reveal an activity pattern sufficient to activate the receptors. Additionally, test frequencies will fall within the documented range of activity patterns for dentate gyrus granule cells. These results will expand our understanding of control of feedforward interneurons in CA3 of the hippocampus.

5.2 RESULTS

Application of the agonist L-AP4 to synapses with high affinity group III mGluRs frequently overestimates the endogenous impact of this receptor on the system (Billups et al., 2003; von Gersdorff et al., 1997; Lorez et al., 2003). Thus, to determine the functional impact of this receptor at the MF to L-Mi connection, we used the competitive antagonist of group IIII mGluRs MSOP (100 μM) to prevent endogenous activation. To assess the pattern of activity that might physiologically activate the receptor, we investigated whether the receptor was tonically active and whether it could be activated by low or high frequencies of activity.

5.2.1 Group III mGluRs are not tonically active

To assess tonic activity, MSOP (100 μM) was applied and the effect on the amplitude of single postsynaptic responses (tested at 0.2 Hz) was determined. No effect on the initial amplitude of the postsynaptic response was seen (23.94 ± 2.69 pA control; 23.83 ± 3.14 pA MSOP; p = 0.950; N = 9). Further, when the effect of MSOP on the paired-pulse ratio was investigated, there was no significantly effect on the paired-pulse ratio at a 50 ms ISI (1.83 ± 0.24 control; 1.86 ± 0.23 MSOP; p = 0.498; N = 9; Fig. 15). This was also true for responses recorded in current clamp (amplitude: 1.59 ± 0.57 mV control; 1.48 ± 0.68 mV MSOP; N = 5; p = 0.279; PPR: 3.37 ± 0.59 control; 3.76 ± 0.77 MSOP; N = 5; p = 0.133; Fig. 15). These data indicate that the group III mGluRs are not tonically active on MF terminals contacting L-Mi, suggesting that ambient resting glutamate concentrations are insufficient to activate the receptor.

5.2.2 Group III mGluRs do not rescue frequency facilitation

Though I did not observe frequency facilitation in the control condition, it was my hypothesis that moderate frequencies of activity might be sufficient to activate mGluRs 4/8 and the lack of facilitation may result from that activation. Thus, I hypothesized that application of MSOP (100 μM) might reveal an underlying facilitation at moderate frequencies (Scanziani et al., 1997; Toth et al., 2000). To test this hypothesis, I stimulated the MF with alternate periods of 0.05 Hz and 2 Hz (Scanziani et al., 1997), a frequency that shows strong facilitation at both the MF to pyramidal cell and MF to str. lucidum interneuron connections (Toth et al., 2000). In contrast to my hypothesis, however, application of MSOP did not rescue frequency facilitation at the MF – L-Mi synapse when tested at 2Hz (normalized to 0.05 Hz: 1.21 ± 0.10 control; 1.11 ±

0.20 MSOP; N = 5; p = 0.677; Fig. 15C). Furthermore, EPSC amplitudes at 2 Hz were not significantly different than amplitudes at 0.05 Hz for either the control or MSOP condition (control: 28.71 ± 3.91 pA at 0.05 Hz; 34.79 ± 5.47 pA at 2 Hz; p = 0.108; N = 5; MSOP: 29.82 ± 5.46 pA at 0.05 Hz; 29.70 ± 2.83 pA at 2Hz; p = 0.972; N = 5) indicating that low and moderate frequencies are insufficient to activate this receptor. These results were surprising because frequency facilitation is conserved at the MF to pyramidal cell synapse and MF to str. lucidum interneuron synapse. Since frequency facilitation is a presynaptic form of short term plasticity (Henze et al., 2000; Lawrence and McBain, 2003), these results suggest that MF input to L-Mi is fundamentally different than MF input to either pyramidal cells or str. lucidum interneurons, and that the expression of the high affinity group III mGluR is not the only target specific difference in presynaptic physiology of the system.

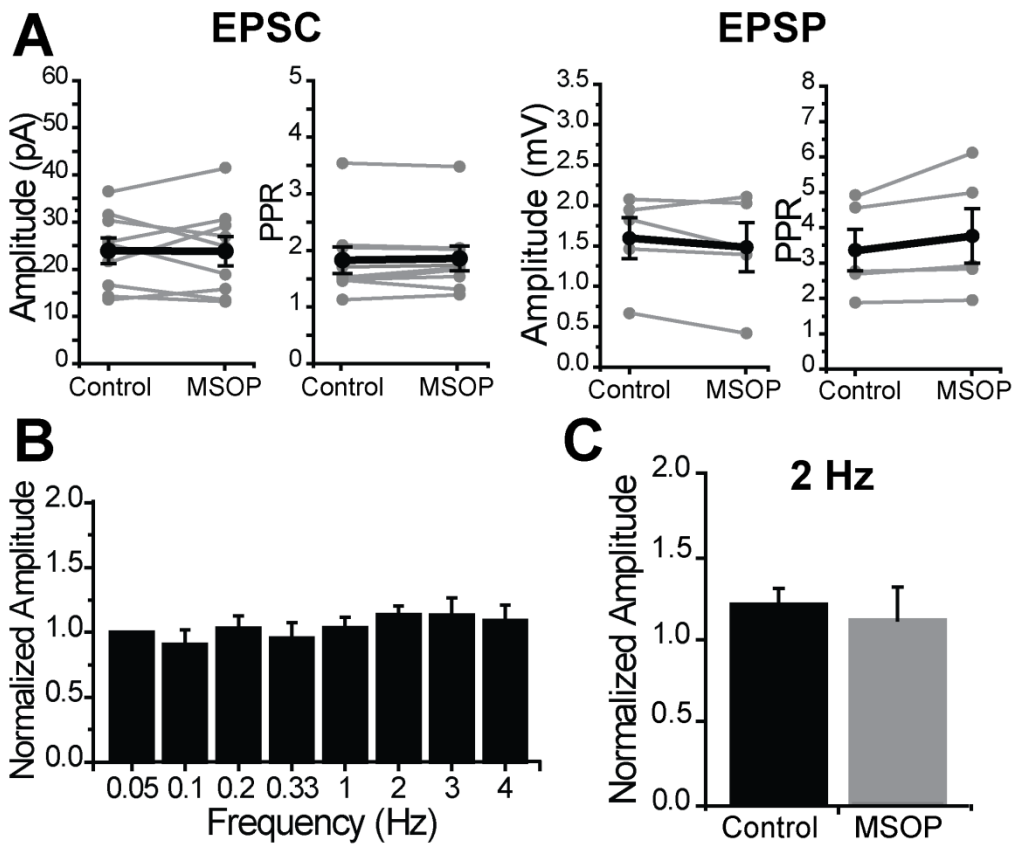

Figure 15. Group III mGluRs are neither tonically active nor activated by low frequency activity.

A) Effect of MSOP on the amplitude of single EPSCs (left, tested at 0.2 Hz) and EPSPs (right) and the paired-pulse ratio at a 50 ms ISI. MSOP does not change either the amplitude or the PPR of mossy fiber EPSCs or EPSPs. B) Plot of normalized amplitude of MF evoked EPSCs at 0.1, 0.2, 0.33, 1, 2, 3, and 4 Hz normalized to EPSCs evoked at 0.05 Hz (Reproduced from Chapter 3 for comparison.) C) Application of MSOP does not reveal frequency facilitation at 2 Hz. Plot of EPSC amplitude normalized to .05 Hz control under both control and MSOP conditions. No significant difference between control and MSOP (N = 5, p = 0.677) and no significant facilitation vs. 0.05 Hz (control: 1.21 ± .21, N = 5, p = .10; MSOP: 1.11 ± .44, N = 5, p = 0.597).

5.2.3 Spike transmission is inhibited by mGluRs 4/8 activation at the MF to L-Mi connection

The probability of spike transmission between the MF and interneurons is known to be low in response to single stimuli, and stimuli at low frequencies (Henze et al., 2002). Thus, in order to determine both the probability of spike transmission at MF input to L-Mi and the impact of mGluRs 4/8 activation on that probability, short trains of high frequency stimulation were used. Additionally since mGluRs 4/8 are neither tonically active nor activated by low and moderate frequencies of activity, it is my hypothesis that high frequencies of activity will be sufficient to activate the receptor.

5.2.3.1 Specific methods: Cell attached recording configuration.

Cell attached recordings were made as outlined by Perkins (2006). Cells were recorded from using the loose patch configuration, with seal resistances of 100 – 500 MΩ (Perkins, 2006). The internal pipette solution was ACSF and pipette resistance was 3 – 5 MΩ. Action currents were recorded in voltage clamp. Recordings were discarded if the seal spontaneously opened, and / or if spontaneous firing frequency increased, indicating that the cell was dying.

5.2.3.2 MSOP confers a small enhancement of facilitation in response to short trains of MF activity

Having demonstrated that mGluRs 4/8 are not tonically active at the MF to L-Mi connection, nor activated by low and moderate frequencies of activity, I was interested in determining the effect of the receptor at high frequencies of activity. Previous reports have demonstrated that short trains of high frequency activity are sufficient to activate high affinity group III mGluRs (Chen

et al., 2002; Losonczy et al., 2003). In order to determine whether short trains of high frequency activity were sufficient to activate mGluRs 4/8 at MF input to L-Mi, I recorded trains of five MF-evoked EPSCs at 20 and 40 Hz before and after application of MSOP.

Figure 16 presents the data from those experiments. MSOP revealed a small enhancement of facilitation at 20 Hz, and though there was a trend at 40 Hz, the effect was not significant at most points. Though there was significant enhancement in the 20Hz train, the lack of significance at all points in the 40 Hz train for these data is due to, in part, high variability of facilitation in the control condition, as well as in the MSOP condition, as demonstrated in the averaged traces in Fig. 16. Because the facilitation accommodates in the train ($EPSC_5 / EPSC_1 < EPSC_2 / EPSC_1$), the stimulus number at which that accommodation begins is highly variable. Thus, for some cells, the largest effect of MSOP was at stimulus #3, and for other at stimulus #5 (see averaged traces in Fig. 16A and 16D). To compensate for this difference, I aligned the data to the stimulus number at which the greatest difference was observed with application of MSOP. Using this method, enhanced facilitation is observed following application of 100 μM MSOP at both 20 ($EPSC_N / EPSC_1$: control, 1.32 ± 0.18; MSOP, 1.79 ± 0.24; N = 8; $p < 0.001$; Fig. 16C) and 40 Hz ($EPSC_N / EPSC_1$: control, 1.49 ± 0.17; MSOP, 2.05 ± 0.24; N = 7; $p < 0.05$; Fig. 16F).

It is interesting to note that, though there was no effect of MSOP on the PPR when the stimulus frequency was 0.2 Hz, there was an effect of MSOP on the second stimulus of the train of 5 stimuli at 20 Hz, which is the same ISI tested for the PPR. These data suggest that while pairs of stimuli do not result in enough glutamate to activate this receptor, trains of activity does result in sufficient glutamate release, and that the glutamate released in response to these longer trains is either not sufficiently cleared in the 30 sec inter-sweep interval, or that the internal cascade is not resolved in those 30 seconds.

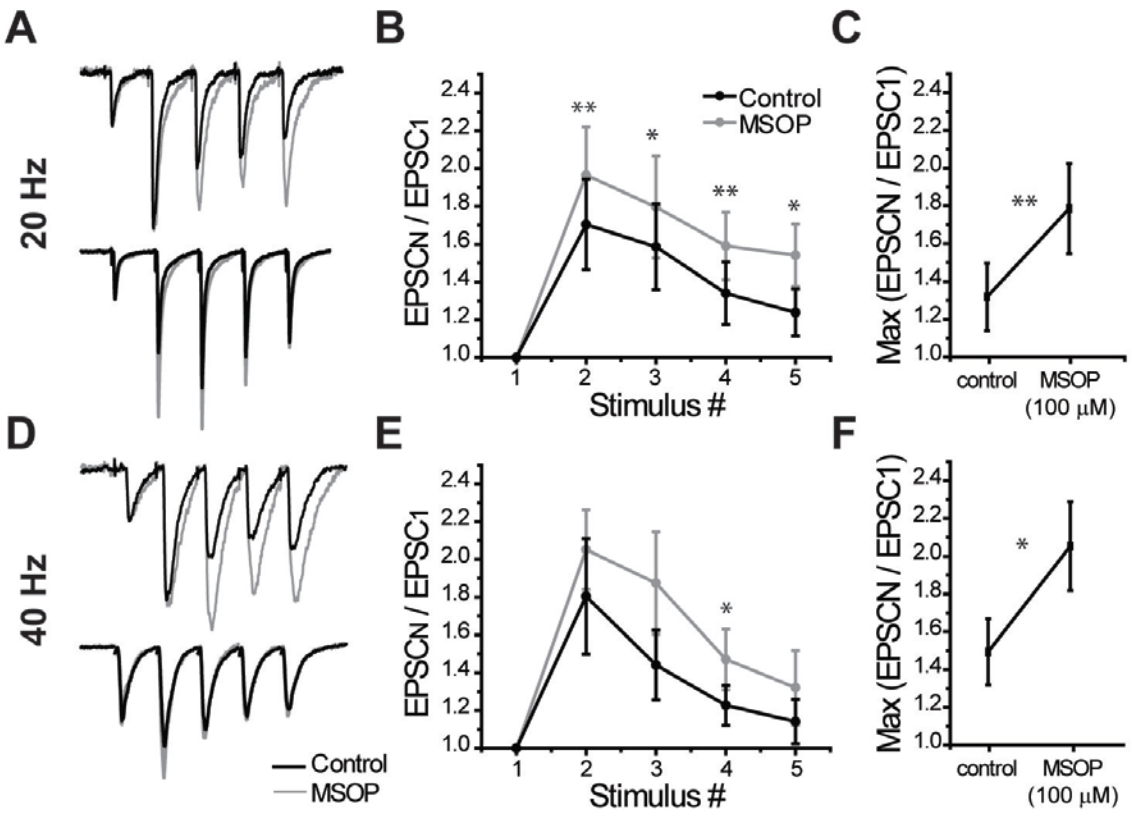

Figure 16. Relief of inhibition by mGluRs 4/8 reveals enhanced facilitation in short, high frequency trains.

EPSCs were recorded in response to short trains of MF stimulation at 20 Hz (A) and 40 Hz (D). Sample traces in A and D are average EPSCs (N = 10 - 15) from two representative cells before (black trace) and after (grey trace) MSOP application illustrating the variability in facilitation pattern and timing of the effect of MSOP. B and E) Summary plots of the ratio of EPSCN / EPSC1 for each stimulus before (black line and symbols) and after application of 100 μM MSOP (grey line and symbols). Traces were normalized to the first EPSC of the control condition for each cell in the average. C and F) Plot of the ratio of EPSCN / EPSC1 at the stimulus number that had the largest effect of MSOP (e.g. in A, top set of traces, EPSC5 / EPSC1, bottom set of traces, EPSC2 / EPSC1) **p < 0.01; *p < 0.05.

5.2.3.3 Activation of mGluRs 4/8 delays and decreases the probability of spike transmission

Though MSOP did not have a robust effect on the facilitation of EPSCs in a train, there was a trend indicating a relief of inhibition of facilitation in the train. Furthermore, since it is likely that these synapses occur on distal dendrites (Chapter 3), there may be problems with my ability to clamp the responses such that subtle differences in EPSC cannot be effectively measured. Additionally, since the fundamental question is how this receptor alters feedforward inhibition in response to MF activity, I decided to determine the impact of the receptor on the probability of spike transmission between the MF and the L-Mi.

In vivo data show that short trains of high frequency MF activity are sufficient to elicit action potentials in CA3 interneurons (Henze et al., 2002). Because we were also interested in determining the effect of mGluRs 4/8 activation on the CA3 network, and specifically the ability of MF to elicit action potentials in the L-Mi, we determined the probability of spike transmission before and after application of the group III mGluR antagonist MSOP (100 μM). I hypothesized that activation of mGluRs 4/8 during high frequency MF activity would modulate the MF to L-Mi connection such that the L-Mi would require more input to achieve action potential threshold. Using frequencies that fall within the range of granule cell firing as a rat traverses a place field (Henze et al., 2002; Jung and McNaughton, 1993) we applied trains of ten stimuli to the MF at 20 and 40Hz before and after the application of MSOP. We then determined whether the group III receptor had an effect on the probability of action potential generation, and whether it changed the latency to the first action potential in response to the train. In these experiments, L-Mi were recorded in current clamp conditions, and the MF input was stimulated as described above. Once a stable EPSP amplitude was obtained, the V_h was adjusted from rest (~ -67 mV) to

between -60 mV and -55 mV to allow for a low probability of firing (P(AP) = ~0.1) in response to 10 stimuli at 20 Hz. This adjustment was made to avoid a "floor effect" where the initial probability of AP firing might be zero, thus making even nominal increases seem disproportionately large. 30 trials of 10 stimuli at 20 and 40 Hz, delivered at 20 second intervals were then collected before and after the application of MSOP (100 μM). Fig. 17A shows several overlapping, consecutive sweeps from a representative cell, and Fig. 17B depicts the raster plot of action potentials during the train before and after MSOP application. From these data, the probability of firing in response to each stimulus in the train was calculated and the summary data plotted in Figs. 17C. We found that the overall probability of action potential firing in response to both frequencies was significantly higher in the presence of MSOP (20 Hz: 0.08 ± 0.02 control to 0.20 ± 0.05 MSOP, $N = 5$, $p < 0.05$; 40Hz: 0.16 ± 0.02 control to 0.21 ± 0.03 MSOP; $N = 5$; $p < 0.05$; Fig. 19B). At the end of the experiment, DCG-IV (2.5 μM) was applied to confirm MF origin (EPSP amplitude: 30.00 ± 6.67% of control, $N = 5$, $p < 0.001$).

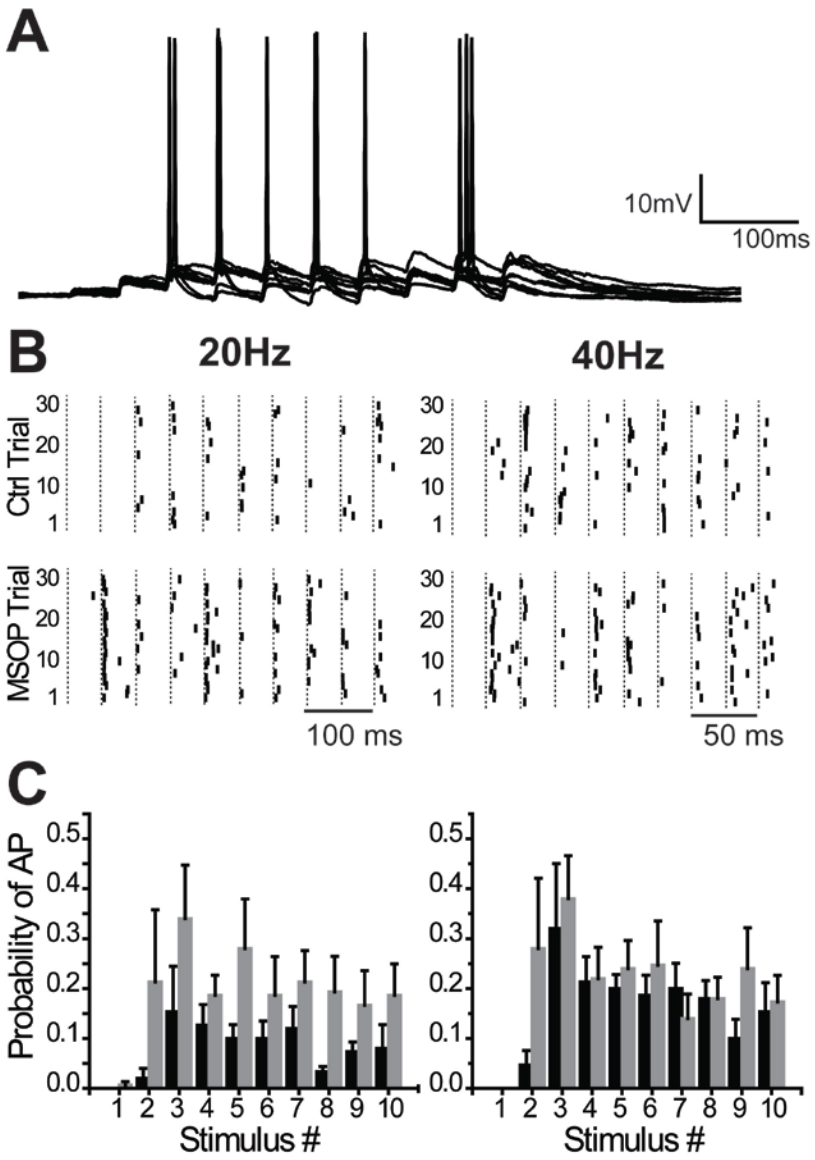

Figure 17. Activation of high affinity group III mGluRs decreases the probability of spike transmission.

A) Overlapping, consecutive sweeps from a representative interneuron to demonstrate the stimulation protocol delivered to the MF. B) Raster plots showing the raw timing of action potentials in response to the trains at 20 (left) and 40 (right) Hz. Vertical, dashed lines indicate the timing of each stimulus, and the rows across are each trial (N = 30). Each tick mark represents a single action potential. C) Summary plot showing the overall probability of action potential firing in response to each stimulus before (black bars) and after (grey bars) MSOP application.

More importantly, the time to first action potential was shorter in the presence of MSOP, indicating that activation of the group III mGluRs delays the firing of the postsynaptic L-M interneuron in response to MF input. This was determined by calculating the latency to the first action potential in response to the train of MF input for each trial before and after MSOP (Fig. 20). These data were then binned by stimulus number and plotted as a cumulative scatterplot, which was fit with a Boltzmann function. MSOP application significantly decreased the time to first action potential in response to stimuli at both 20 Hz (50% control: 192.24 ± 12.0 ms; 50% MSOP: 102.02 ± 13.7 ms; $p < 0.05$; Fig. 20A) and 40 Hz (50% control: 79.71 ± 3.32 ms; 50% MSOP: 51.71 ± 1.46ms; $p < 0.05$; Fig. 20A). This delay in L-Mi firing caused by an mGluRs 4/8-mediated decrease in MF glutamate release means that additional synaptic input is required before summation of the inputs in the L-Mi is sufficient to elicit an action potential. Specifically, activation of mGluRs 4/8 delays L-Mi firing for tens to hundreds of milliseconds which, when a granule cell is firing at 20 or 40 Hz, corresponds to the requirement of several additional sequential synaptic events to fire the postsynaptic cell (e.g. time difference between MSOP and control conditions at 20Hz = ~90 ms, which at 20 Hz results in ~2 additional events). Thus, if two MF synaptic events are sufficient to elicit an action potential in the L-Mi without mGluRs 4/8, the activation of this receptor necessitates further granule cell activity before threshold is reached in the L-Mi – possibly three or four synaptic events. It is important to note that in some of the trials, the L-Mi never fired and so these numbers are, if anything, an underestimate of the shift in the timing of L-Mi firing. Of equal importance is that these changes occurred without any significant change in action potential threshold (-38.26 ± 1.36 mV control; -39.28 ± 1.73 mV MSOP; $N = 5$; $p = 0.134$; Fig. 19C).

Because we were concerned that intracellular dialysis of whole-cell recordings may be affecting the threshold for action potential elicitation, we repeated this experiment using the cell-attached configuration in voltage clamp (seal resistance ~100 to 500 MΩ) (Perkins, 2006). Nearly identical results were obtained in cell attached for both 20 Hz (probability of AP: 0.12 ± 0.01 to 0.34 ± 0.05; $p < 0.001$; N = 7; time to first AP: 150.67 ± 88.6 ms to 93.98 ± 8.93 ms; $p < 0.05$; N = 7) and 40 Hz (probability of AP: 0.25 ± 0.06 to 0.44 ± .06; $p < 0.05$; N = 7; time to first AP: 174.55 ± 5.49 ms to 47.34 ± 3.32 ms; $p < 0.05$; N = 7) confirming that this effect is due to activation of the group III mGluRs, and not a byproduct of the recording conditions (Figs. 18, 19A and 20B). Together these data demonstrate that activation of the presynaptic high affinity group III mGluRs significantly impacts the timing of feedforward inhibition from L-Mi onto pyramidal cells in CA3.

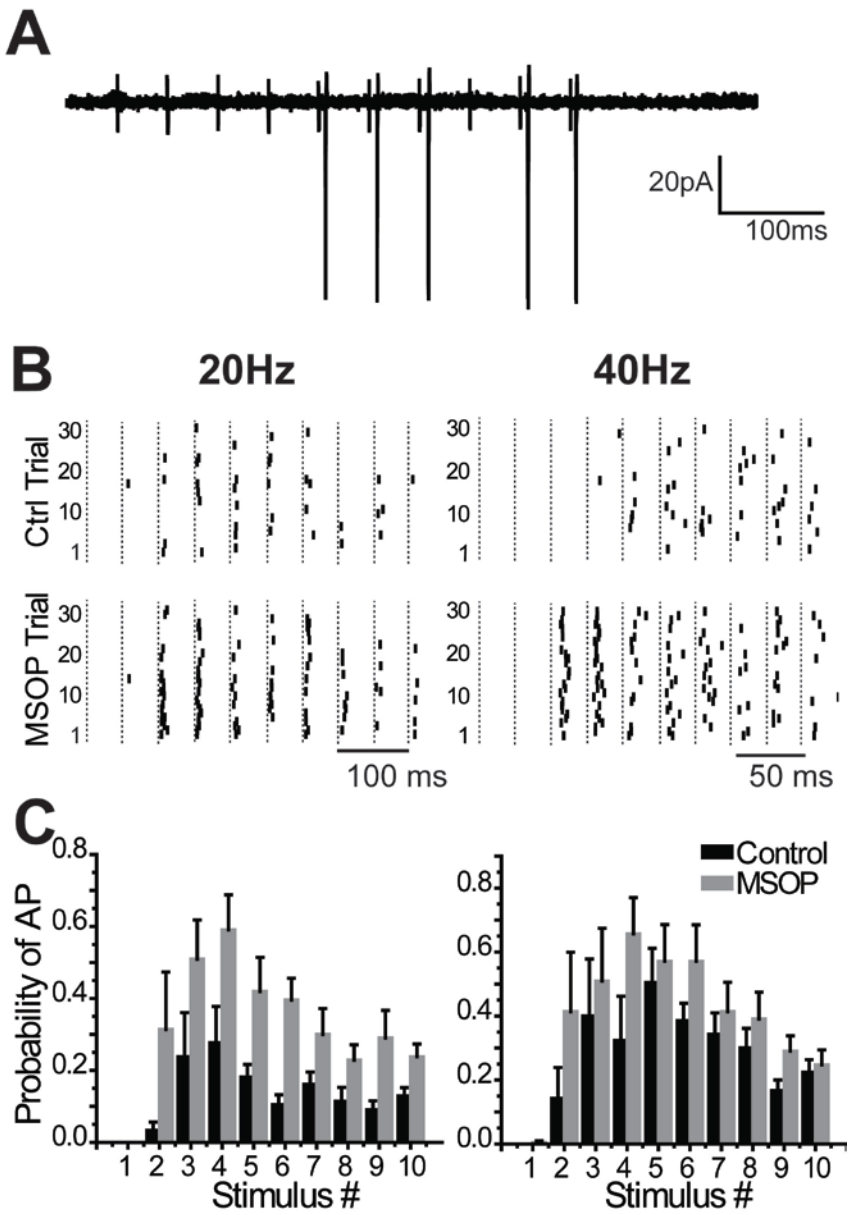

Figure 18. Activation of mGluRs 4/8 delays and decreases the probability of action currents.

A) Several consecutive, overlapping sweeps recorded from an L-Mi in cell attached patch configuration to demonstrate the stimulation and recording configuration. B) Raster plots demonstrating the timing of individual action currents in response to MF stimuli. Vertical, dashed lines indicate the time of stimulation and horizontal rows indicate each trial. C) Summary plot showing the overall probability of action current firing in response to each stimulus before (black bars) and after (grey bars) application of 100 μM MSOP.

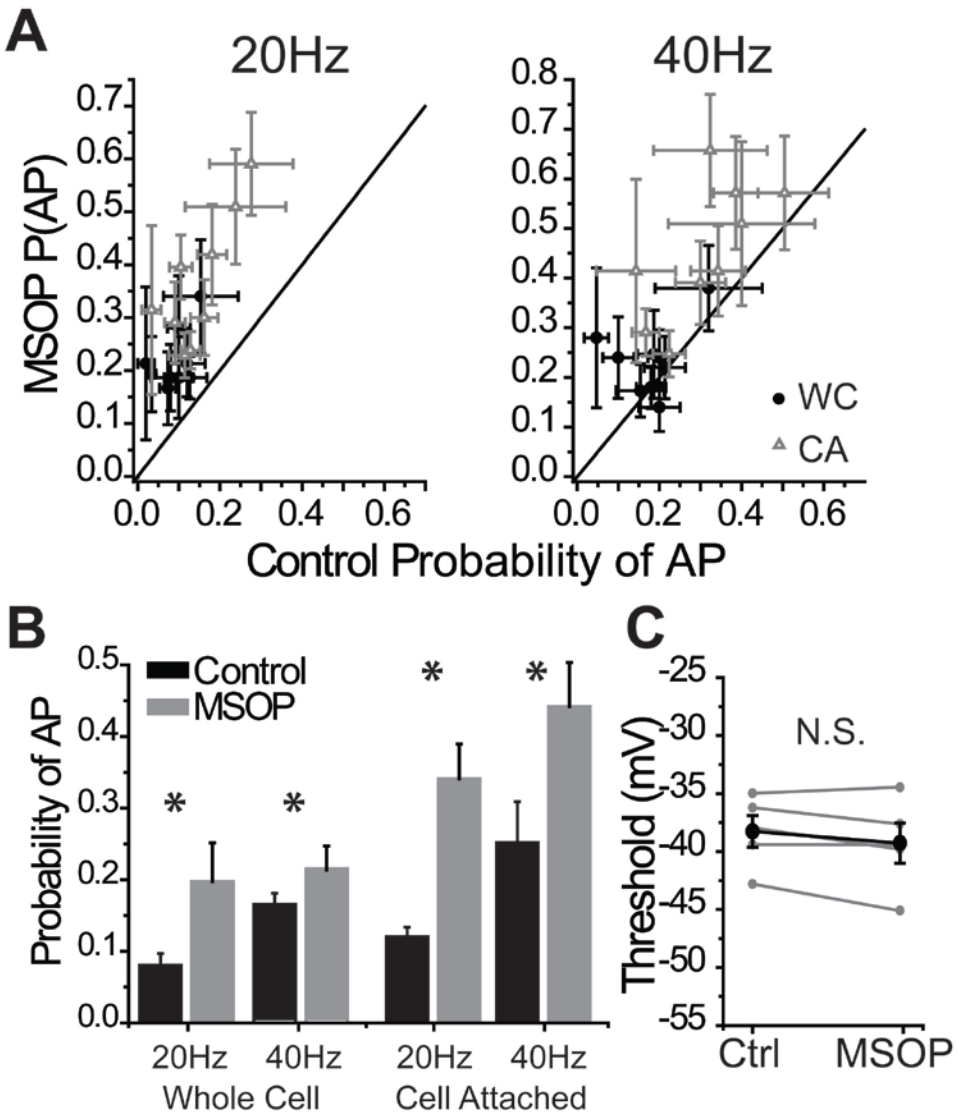

Figure 19. Activation of mGluRs 4/8 decrease probability of spike transmission.

A) Probability of spike transmission before (x-axis) and after (y-axis) application of MSOP with a unity line. (•) indicates whole-cell recording configuration and (Δ) indicated cell-attached recording configuration. Whole cell and cell-attached recording configurations largely overlap one another, and fall to the left of the unity line indicating that the probability of the L-Mi firing an action potential is higher in the MSOP condition for almost every point tested at both 20 Hz (left) and 40 Hz (right). B) Summary plot of the overall probability of firing an action potential before (black bars) and after (grey bars) MSOP application for both 20 Hz and 40Hz in the whole cell and cell attached configuration. C) Plot showing action potential threshold for the L-Mi before and after MSOP application. Grey symbols & lines indicate individual cell data, black symbols and lines are mean ± SEM. * $p < 0.05$

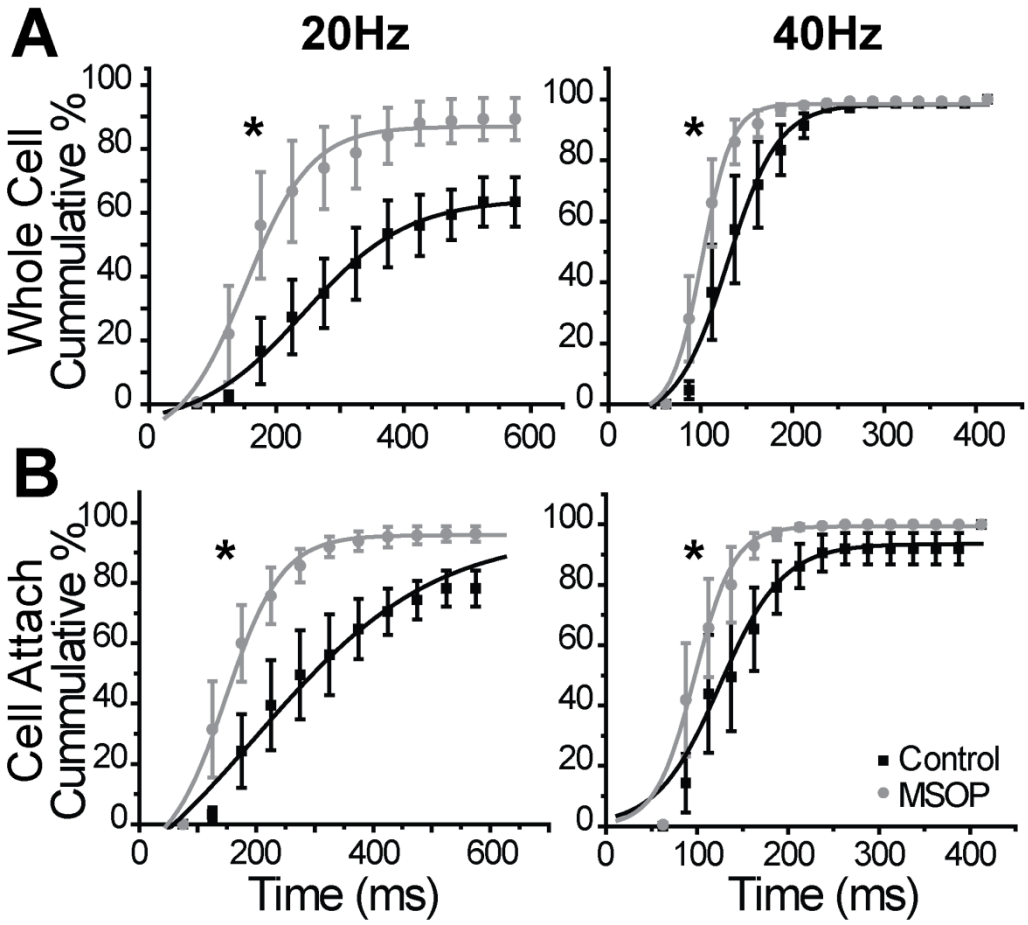

Figure 20. Activation of mGluRs 4/8 delays L-Mi action potential firing in response to MF input.

A) Summary data plotting the cumulative probability of the latency to the first AP in each train at 20 and 40 Hz for whole cell and cell attach (B) condition before (black dots and fits) and after (grey dots and fits) MSOP application at both 20 (left) and 40 Hz (right). Scatter plots were then fit with a Boltzmann function. *$p < 0.05$

5.3 DISCUSSION

These data convincingly demonstrate the importance of the target-cell specific distribution of mGluRs 4/8 at MF input to L-Mi. The expression of this receptor on MF terminals contacting L-Mi delays L-Mi firing in response to MF input and decreases the overall probability of spike transmission. Consequently, this receptor high-pass filters MF input to L-Mi, requiring trains of input that are of a sufficiently high frequency and sufficiently long duration before eliciting APs in the L-Mi. Thus, this receptor is a regulator of feedforward inhibition in CA3 of the hippocampus.

5.3.1 High-pass filtering of MF input to L-Mi by mGluRs 4/8 activation

Previous reports have noted that interneurons do not tend to fire in response to a single input from MF granule cells but that the probability of spike initiation increases throughout a train of high frequency input (Henze et al., 2002; Lawrence et al., 2004). In keeping with these observations, L-Mi did not fire in response to a single MF input but required a train of MF input before reaching threshold. This finding is consistent with my interpretation that individual MF inputs to L-Mi do not drive the interneuron because of the small quantal amplitude (Chapter 3). Instead, convergence and summation of several MF inputs is required to elicit firing from the cell (Cosgrove et al., 2009).

When activation of mGluRs 4/8 was prevented by application of the competitive antagonist MSOP, the probability of spike transmission was higher, and the latency to first action potential was shorter. Therefore, activation of mGluRs 4/8 imposes a high pass filter on spike transmission by requiring trains of MF input that are longer and at a higher frequency before

eliciting spiking in the L-Mi. It is interesting to note that the effect of MSOP is attenuated in the 40 Hz condition vs. the 20 Hz trials both for tests of spike transmission and questions of short term facilitation. Presynaptically expressed short term facilitation is thought to rely on insufficient clearing of residual calcium from the terminal before the next action potential (and subsequent opening of VGCCs) occurs (Katz and Miledi, 1968; Zucker and Regehr, 2002; Xu et al., 2007). Since mGluRs 4/8 have the N-type VGCC as a downstream target (see 4.2.3), activation of the receptor, and subsequent inhibition of the N-type channel is in a balancing act with the buildup of residual calcium as a result of the high frequency activity (Billups et al., 2005). It is possible, therefore, that there are frequencies where the effectiveness of mGluRs 4/8 is overshadowed by other presynaptic conditions. Thus, it is my hypothesis that activation of this receptor will have the largest impact during short bursts of high frequency activity, but that the effect may taper at the highest frequencies granule cells achieve (~100 Hz; Jung and McNaughten, 1993; Henze et al., 2002).

5.3.2 Functional implications of mGluRs 4/8 expression on MF terminals contacting L-Mi

Feedforward inhibition provided by interneurons to pyramidal cells narrows the time window for integration of excitatory inputs by the pyramidal cell (Pouille and Scanziani, 2001). L-Mi provide feedforward inhibition onto the apical dendrite of CA3 pyramidal cells (McBain and Fisahn, 2001; Romo-Parra et al., 2008; Ascoli et al., 2009), where RC input also converges (Wittner et al., 2007). The positioning of these inputs suggests that the inhibition provided by the L-Mi occurs through axodendritic shunting (Ascoli et al., 2009). Since activation of the high affinity group III mGluRs on MF terminals delays L-Mi firing for tens to hundreds of milliseconds, several additional sequential MF synaptic events reach the pyramidal cell before

the L-Mi becomes active. Since pyramidal cells fire action potentials in response to MF input sooner than interneurons (Henze et al., 2002; Lawrence et al., 2004), the recurrent collateral pathway may become active before the L-Mi. Thus, the feedforward inhibition imparted by the L-Mi to the pyramidal cell may, in fact, be acting to temper the excitation provided by the RC pathway, rather than the MF input itself. Thus, activation of mGluRs 4/8 and subsequent delay in L-Mi firing may shift the function of the L-Mi from inhibiting the summation of MF input by the pyramidal cell to shunting away RC input.

Furthermore, a recent computational study has shown that feedforward inhibition alters the relationship between synaptic input and action potential firing (Ferrante et al., 2009). In the absence of inhibition, the input/output (I/O) relationship of the pyramidal cell can be modeled by a single sigmoid function, with the lower limit set by the frequency of input required to reach action potential threshold, and the upper limit set by the maximum firing frequency of the cell. Because the activity of the interneuron can also be modeled by a sigmoid I/O function, when inhibition is added to the system the overall transfer function of the pyramidal cell is represented by the sum of both I/O curves (pyramidal cell and interneuron). The resultant biphasic sigmoid function has a plateau range at which the pyramidal cell could maintain a consistent output firing frequency across a wide range of input frequencies (Ferrante et al., 2009). By increasing the latency for eliciting spiking in the L-Mi, activation of mGluRs 4/8 shifts the I/O curve of the interneuron to the right. This rightward shift in the interneuron's I/O function effectively shifts the CA3 pyramidal cell I/O function to the right without changing the output frequency (Ferrante et al., 2009). This would allow a population of CA3 pyramidal cells receiving inhibitory input from interneurons with similar shifted I/O properties to fire at similar average frequencies regardless of input frequency ranges. Because the generation of oscillatory activity requires a

rather homogeneous neuronal firing rate, activation of mGluRs 4/8 at MF terminals on feedforward interneurons could to promote ensemble synchronization within the CA3 neural network, by ensuring a constant pyramidal cell firing rate in spite of shifts in the MF input.

6.0 SUMMARY AND CONCLUSIONS

6.1 GENERAL OVERVIEW

The data presented in this thesis increase our understanding of the mossy fiber system and regulation of feedforward inhibition in the CA3 network. Furthermore, these data highlight the precise matching in synaptic physiology between pre and postsynaptic partners, and the specializations that can and do occur. Overall, these data indicate a unique role of the L-M interneuron, which has largely been overlooked as a player in the CA3 network, one that may serve to enhance lateral inhibition and increase the signal to noise ratio at the level of the pyramidal cell through feedforward inhibition (Lacaille and Schwartzkroin, 1988; Pouille and Scanziani, 2001).

The work presented here identifies a phenomenon, offers a mechanism through which the phenomenon is effected, and provides evidence of the physiologic and functional implications of that phenomenon. Specifically, the main findings of this work are that the mossy fiber differentially expresses presynaptic group III mGluRs based on the identity of the target neuron, and that expression of this receptor in conjunction with the short term plasticity characteristics of the synapse, imposes the requirement of a barrage of high frequency granule cell activity before the L-Mi is able to reach action potential threshold (schematized in Fig. 21). This arrangement is unique to the L-Mi as the receptor is absent on terminals contacting other targets (Pelkey et al.,

2005). Furthermore, other targets are sensitive to moderate changes in frequency, and thus respond to a broader range of input frequencies (Salin et al., 1996; Toth et al., 2000). This indicates that inhibition from the L-Mi may be recruited only during the high frequencies of granule cell that are observed in response to exploratory behavior and memory consolidation (Hughes, 2008).

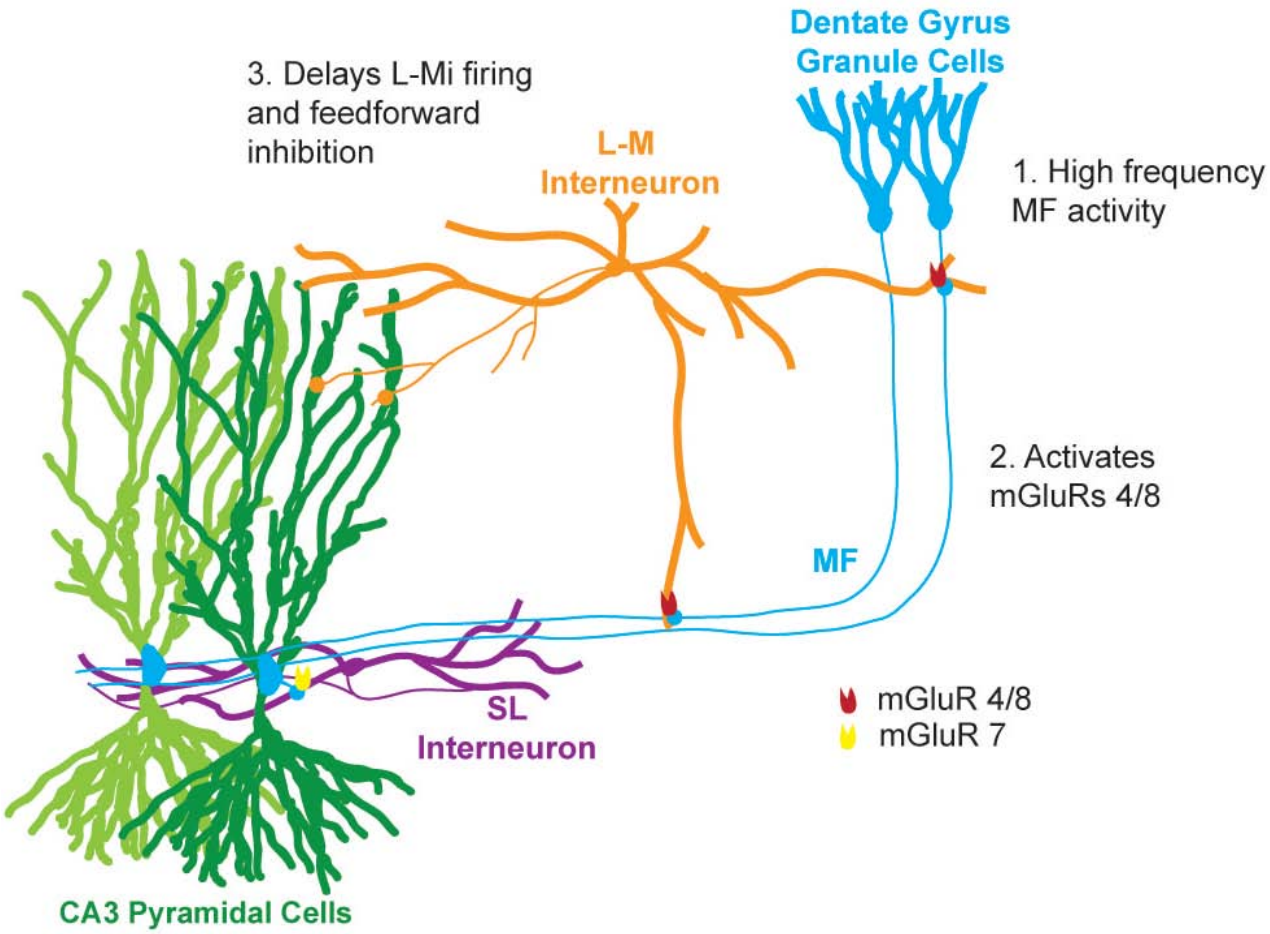

Figure 21. Summary schematic of regulation of MF input to L-Mi by mGluRs 4/8

Schematic demonstrating the target specific expression of mGluR 4/8 (red symbols) on MF (blue) terminals contacting L-Mi (orange) vs. MF terminals contacting str. lucidum interneurons (purple) which express mGluR 7 (yellow symbols) via a filopodial extension from the giant MF bouton. Short bursts high frequency activity in dentate gyrus granule cells (blue) activates mGluRs 4/8 on MF terminals contacting L-Mi, which delays spike transmission at that synapse. Thus, feedforward inhibition onto CA3 pyramidal cells (green) is delayed.

6.1.1 MF input to L-Mi: balancing short term plasticity and activation of mGluR

The synaptic profile of MF input to L-Mi is different than what has been observed at MF input to other targets. Previous work has demonstrated that MF input to L-Mi undergoes bidirectional long term plasticity, with the predominant form being LTP (Galvan et al., 2008). This is in contrast to what is seen at MF input to str. lucidum interneurons, which undergo LTD unless mGluR 7 is internalized (Maccaferri et al., 1998; Pelkey et al., 2005). With the work presented here, we now know that MF input to L-Mi also undergoes short term facilitation at 20 and 40 Hz, though the facilitation attenuates through the train. This short term facilitation may be a result of a relatively low probability of release at the MF to L-Mi connection, as extrapolated from the quantal and bulk stimulation data (Chapter 3).

Perhaps most surprising, however, is the finding that MF input to the L-Mi does not undergo frequency facilitation, a short term plasticity property that is conserved at other targets of the MF system (Salin et al., 1996; Toth et al., 2000; Lysetskiy et al., 2005). Frequency facilitation at MF input to CA3 pyramidal cells seems to be the byproduct of tonic inhibition by adenosine receptors (Moore et al., 2003; Klausnitzer and Manahan-Vaughan, 2008). Tonic activation of presynaptic A1 adenosine receptors functions to decrease the probability of release so dramatically that moderate increases in frequency can bring about 400 to 1000% increases in EPSC amplitudes. Interestingly, this may not fully explain the frequency facilitation seen at MF input to str. lucidum interneurons as the initial probability of release is found to be relatively high at that synapse (~0.40; (Lawrence and McBain, 2003; Lawrence et al., 2004). Furthermore, at MF input to L-Mi, the probability of release is quite low and yet frequency facilitation is absent. This indicates that the correlation between A1 receptor activation and low probability of

release at MF input to pyramidal cells is not the only mechanism contributing to the expression of frequency facilitation at MF synapses.

In spite of the lack of frequency facilitation, the short term and paired-pulse facilitation demonstrate the capability of MF input to L-Mi to undergo facilitation. This facilitation is tempered by the expression of the presynaptic mGluRs 4/8 that become active during high frequency stimulation and dampens any facilitation that might arise. The timing of L-Mi firing as a result of MF input, and thus feedforward inhibition onto pyramidal cells by L-Mi is regulated by the presence of this receptor. By delaying firing in the L-Mi by tens to hundreds of milliseconds, the receptor imposes the demand for high frequency input of a sufficient duration, creating a high pass filter. Without this receptor, the probability of L-Mi firing in response to MF input is much higher. One question that could be investigated further is whether regulation of the expression of mGluRs 4/8 on MF terminals contacting L-Mi is possible as a mechanism for regulating short and / or long term plasticity at the synapse.

G-protein coupled receptors undergo activity dependent desensitization and internalization (Ferguson, 2001). It has been shown that mGluR 7 undergoes internalization via the protein that interacts with protein kinase C (PICK1) (Dev et al., 2001), and at MF synapses onto str. lucidum interneurons, prolonged L-AP4 application results in mGluR7 internalization (Pelkey et al., 2005). It has also been found that mGluRs 4 and 8 bind PICK1 (El Far et al., 2000; Ferraguti and Shigemoto, 2006), glutamate receptor interacting protein (GRIP) and syntenin (Hirbec et al., 2002) making it possible that the surface expression of these receptors is regulated by a similar process. Of these, syntenin is a presynaptic protein found to be necessary for presynaptic clustering of the active zone cytoskeletal matrix (Ziv and Garner, 2004; Ko et al., 2006) and PICK1 is responsible for the surface expression of the proteins bound to it (Xu and

Xia, 2006). Thus, the surface expression and / or phosphorylation state of mGluRs 4 and 8 on MF terminals contacting L-Mi may serve as a point of regulation for adjusting the strength of the connection between the MF and L-Mi. It can be hypothesized that high frequencies of MF activity could desensitize or internalize mGluRs 4/8, thus resulting in a relief of inhibition of spike transmission between the MF and L-Mi, thus increasing feedforward inhibition to CA3 pyramidal cells.

Alternatively, mGluRs 4/8 could simply be a filter that is overcome by sufficiently high frequencies of synaptic activity. The inhibition of spike transmission created by activation of mGluRs 4/8 was attenuated at trains of 40 Hz compared to 20 Hz. Though the effect of the antagonist, MSOP, was still significant, the impact of the antagonist was smaller. It is possible that at high enough frequencies of MF activity, the short term plasticity characteristics of the MF will overcome the inhibition exerted by mGluRs 4/8, such that there is a ceiling to the frequencies affected by activation of mGluRs 4/8. Together, these potential mechanisms provide alternatives to adjusting the gain of feedforward inhibition that do not rely on the expression of long term plasticity. Thus, the feedforward inhibition provided by the L-Mi can be dynamically regulated at varying frequencies of MF input without the requirement of long term changes to the network.

Another question that would be interesting to investigate is whether mGluRs 4/8 are activated by homosynaptic glutamate release, thus operating as autoreceptors, or whether they can be activated by neighboring glutamatergic inputs. Another layer to this question would be whether the neighboring inputs are MF inputs, or PP inputs if near the suprapyramidal blade of the dentate gyrus. There is evidence that these interneurons integrate input from the PP and MF through supralinear summation at short interstimulus intervals (Calixto et al., 2008), and as PP

provides feedforward excitation with respect to MF input onto both L-Mi and CA3 pyramidal cells, it is likely that these inputs interact. If PP input were capable of activating the heterosynaptic mGluRs 4/8 on MF terminals, this would increase the limit of the high pass filter, increasing the demand of MF input to elicit spiking in the L-Mi. Similarly, if neighboring granule cells could activate mGluRs 4/8 on a MF bouton, lateral inhibition could be effected at the level of the L-Mi, which would then change the pattern of feedforward inhibition from this population of cells. Because of anatomical location of the mGluRs 4/8 within active zones (Shigemoto et al., 1997; Bradley et al., 1999; Corti et al., 2002), it is likely, however, that these receptors do act as autoreceptors as they would be exposed to synaptically released glutamate, and possibly sheltered from heterosynaptic sources of glutamate.

It should be noted that the high affinity group III mGluR is not the only presynaptic receptor playing a role at this synapse and determining the release characteristics of MF input to L-Mi. Notably, another presynaptic metabotropic receptor is present on MF terminals targeting L-Mi, the mGluR 2/3. Though this receptor likely affects MF release characteristics, since it is not located within the active zone, and rather distributed in the preterminal region of the bouton (Shigemoto et al., 1997), the source of glutatmate activating the group II mGluR is probably not the same as the group III mGluR. With its location in the preterminal region, activation of mGluRs 2/3 may be a result of neighboring synaptic activity or only under extremely high frequencies of activity that produce robust spillover (Shigemoto et al., 1997). Thus, for the patterns of stimulation considered in this thesis, mGluRs 2/3 are probably not activated, though the role of these receptors in the physiology of the connection is an open question, and an interesting one.

6.1.2 Assessing the importance of inhibition from L-M interneurons onto CA3 pyramidal cells

In order to assess the relative impact of inhibition from L-Mi onto CA3 pyramidal cells, several factors should be addressed including the number of L-Mi present in CA3, the number of pyramidal cells each L-Mi might target and the strength of the connection between L-Mi and pyramidal cells. It has been estimated that interneurons make up ten percent of the cell population in the hippocampus (Amaral and Lavenex, 2007). Within CA3, there are approximately 250,000 pyramidal cells(Rapp and Gallagher, 1996), giving an estimate of ~ 25,000 interneurons within CA3, encompassing all of the subtypes. Of these, it can be estimated that approximately seven percent have soma in the str. lacunosum moleculare, resulting in an estimate of ~ 1,700 L-Mi in CA3 of the hippocampus (Nomura et al., 1997). This may be a slight underestimate, as markers for individual subtypes of interneurons were used to get the count, thus leaving open the possibility that a subtype of interneuron was not counted, but does provide a useful estimate of the relative number of L-Mi in CA3. Furthermore, greater than 90% of cells with soma in the str. lacunosum moleculare are GABAergic (Woodson et al., 1989).

Though there is no direct evidence through paired recordings that CA3 L-Mi contact CA3 pyramidal cells, work has been performed in CA1 to show the connection (Bertrand and Lacaille, 2001), and the anatomy of L-Mi in CA3 is very similar to that of CA1, with axons of L-Mi undergoing wide arborization in the str. radiatum of CA3 near the apical dendrites of pyramidal cells (Ascoli et al., 2009). Additionally, it has been shown that puffs of GABA in the str. lacunosum moleculare relieve inhibition on CA3 pyramidal cells, indicating that a population of cells with dendrites in the str. lacunosum moleculare provides inhibition to CA3 pyramidal cells (Perkins, 2002). Since L-Mi have wide reaching dendritic arbors that extend throughout the str.

lacunosum moleculare and axons that target the region of pyramidal cell apical dendrites, and these cells are known to target pyramidal cells in CA1, L-Mi are likely synapsing on CA3 pyramidal cells. Additionally, the work done in CA1 demonstrates that the connectivity rate of L-Mi to pyramidal cells was approximately 11%, though it is likely an significant underestimate resulting from the slicing procedure (Bertrand and Lacaille, 2001). When the cells are coupled, however, the inhibition provided by L-Mi onto pyramidal cells is quite robust, with large amplitude responses when the holding potential is depolarized to -40 mV (Bertrand and Lacaille, 2001). Additionally, it is likely that the type of inhibition provided is shunting, as the chloride reversal potential was near rest (Bertrand and Lacaille, 2001). Though it will certainly be important in future studies to confirm that L-Mi in CA3 synapse on CA3 pyramidal cells, the anatomical evidence indicates that this is the case, and that my assumption that L-Mi provide inhibition onto CA3 pyramidal cells is a safe one.

6.2 ALTERNATE METHODS AND INTERPRETATIONS

6.2.1 Minimal stimulation

An initial point of criticism of this thesis may be my decision to not use minimal stimulation to investigate MF input to L-Mi. At the beginning of every new experiment, the question of minimal vs. bulk stimulation was considered. I chose to perform these experiments using bulk stimulation for the following reasons.

As the strontium quantal analysis data demonstrate, the amplitudes recorded using minimal stimulation would have been quite small, less than 10 pA, though these data also readily demonstrate that those values are sufficiently larger than the noise of my recordings (Fig. 6). The problem arises when the failure rate data are considered. In spite of having failures in the recordings, the recorded EPSC amplitudes were still several times larger than the calculated quantal amplitudes, indicating that several fibers were being stimulated. Additionally, these average amplitudes did not exclude failures, making the average amplitudes, if anything, an underrepresentation of the numbers of fibers being stimulated. Figure 22 shows an example of one such recording, albeit an extreme one to more clearly illustrate the point.

Though the control recording for this cell had all-or-none EPSCs evoked from MF stimulation and a failure rate of ~ 50%, this stimulation intensity is clearly not minimal, as application of both L-AP4 (red) and DCG-IV (blue) reveal intermediate amplitudes, as well as an increasd failure rate. Because of this potential for false positives with minimal stimulation, it was decided that making claims that would rely upon a minimal stimulation protocol would not be useful or accurate. To compensate for not using minimal stimulation, paired-pulse stimulation was used to demonstrate the presynaptic locus of mGluRs 4/8. Additionally, strontium was used to desynchronize release into putative single quanta to ensure that activation of mGluRs 4/8 was affecting the presynaptic terminal through a decrease in release probability and not a postsynaptic effect at the receptor.

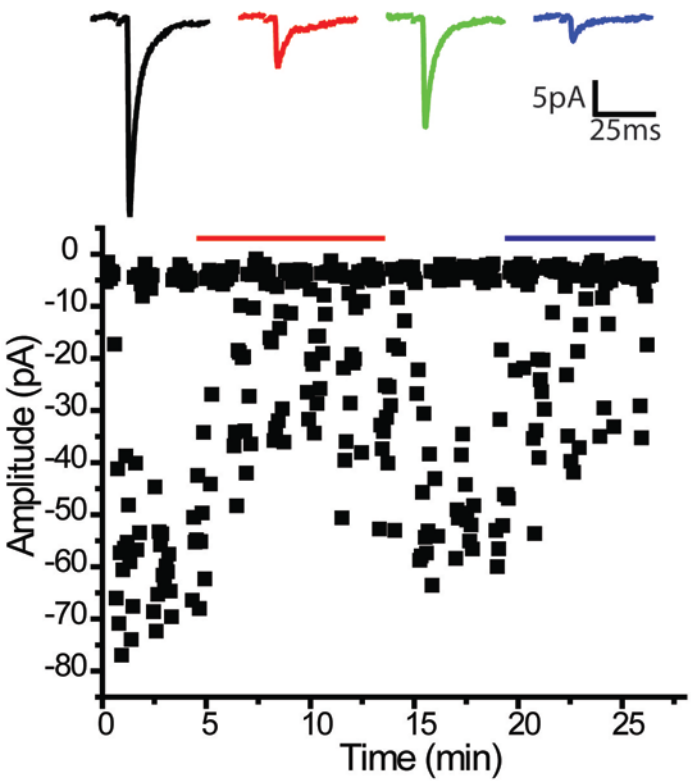

Figure 22. Illustration of problems with minimal stimulation at MF input to L-Mi

Averaged traces (N = 15-30; top) and scatter plot (bottom) of EPSC amplitudes during control period (black trace), L-AP4 application (red bar and trace), washout (green trace), and application of DCG-IV (blue bar and trace). In the control period, EPSCs were roughly all-or-none, with a failure rate of ~50% as is seen with minimal stimulation. Both L-AP4 and DCG-IV increased failure rates, but also demonstrate that this stimulation was not minimal, as intermediate amplitudes were revealed.

Furthermore, through the use of low intensity bulk stimulation, I gained insight into the convergence rate of granule cell input onto the L-Mi. The MF makes multiple contacts with each L-Mi. In some recordings where both the MF_{SDG} and MF_{SL} inputs could be stimulated, each evoking EPSCs with amplitudes of ~35 pA, it is possible to make estimates of 7 to 10 individual contacts from the MF onto the L-Mi from those two stimulation locations alone.

In considering the quantal amplitude, relatively negative resting membrane potential of ~ -67 mV, and the reluctance of the L-Mi to fire in response to MF input, it would seem that the L-Mi requires converging, summating input at least from the MF to achieve action potential threshold. It is unlikely that a single granule cell input would ever bring an L-Mi to fire, as the connection has a small quantal amplitude, low probability of release. Even considering the short term facilitation seen in response to trains at high frequency, it would seem that multiple inputs would be required to reach action potential threshold, thus making bulk stimulation perhaps a more physiologic stimulation protocol. For these reasons, my decision to use bulk stimulation instead of minimal does not undermine the interpretation of these data, and may have added additional information about the connection between the MF and L-Mi that would not have otherwise been appreciated.

6.2.2 Spike transmission protocol

Another methods decision worth addressing is the construction of the protocol to investigate the probability of spike transmission at the MF to L-Mi connection. First, I acknowledge that minimal stimulation was not used (see above) and thus, the results and interpretation reflect MF input to the L-Mi, not that of an individual granule cell. I would defend this decision as

elaborated above, with emphasis on the convergence rate of granule cell input to the L-Mi indicating that individual granule cells do not detonate L-Mi.

The other aspect of the protocol that bears discussion is the decision to slightly depolarize the cells above rest. This decision was made when pilot studies without this depolarization were performed and recordings were made where the L-Mi did not fire once in thirty trials of 20 Hz stimulation in the control condition, but did fire following application of MSOP. Though those results were certainly dramatic, going from a "silent" circuit to one where feedforward inhibition is possible, based on the *in vivo* data recorded by Henze et al. (2002), it was likely those results were an overestimate of the impact of the receptor on the connection. Thus, because I could not replicate the *in vivo* condition, I could attempt to match the control probabilities observed. In order to do this, there were two options: to either increase stimulation intensity until spikes were elicited (Mistry and Mellor, 2008), or to depolarize the postsynaptic cell slightly until low intensity stimulation could evoke action potentials (Fricker and Miles, 2000). The latter was chosen because increasing the stimulation intensity could potentially recruit the neighboring PP for the MF_{SDG} location or the RC pathway neighboring the MF_{SL} stimulation location. Furthermore, the resting membrane potential of the postsynaptic neuron is already somewhat altered by the *in vitro* recording condition as the concentrations of ions in the ACSF and internal pipette solution likely do not exactly match *in vivo* conditions. In this way, I aimed to gain a physiologic understanding of the role of mGluRs 4/8 in gating spike transmission at MF input to L-Mi.

6.2.3 Potential for space clamp problems

The functional anatomy data demonstrating that the kinetics of MF inputs to L-Mi are similar from the MF_{SDG} and MF_{SL} stimulation locations can provide some clues as to the location of these inputs on the dendritic arbor. Since it is my hypothesis that the MF_{SL} input to L-Mi impinges on dendrites that cross into the str. lucidum, one can estimate that the synapse is ~ 200 µm away from the soma of the interneuron. Since the kinetics are similar for both MF_{SDG} and MF_{SL} inputs, it may be that both of these inputs impinge on distal dendrites of the L-Mi. If this is the case, my ability to effectively voltage clamp the recording using a potassium based internal solution may be compromised. Use of a cesium based internal solution would have increased this capability, by decreasing leak conductances from potassium channels, and was implemented for the experiments using strontium to de-synchronize release into putative single quanta. For the majority of experiments, however, a potassium based internal solution was used because I needed to verify the action potential firing pattern of each interneuron I recorded. Since CA3 interneurons have not been subject to a full characterization, as in CA1, the properties that are available to categorize interneurons are somal location, action potential firing pattern, and post-hoc anatomical reconstruction. Thus, every interneuron (with exception of the interneurons recorded for the experiments using a cesium based internal) was tested with a depolarizing current step to confirm that the interneuron had an accommodating firing pattern in an effort to record from a homogenous population of intereneurons. Furthermore, since the recording conditions were consistent, any problems with space clamp would be the same across recordings and thus not affect the qualitative results of these experiments.

6.3 IMPLICATIONS FOR THE NETWORK PROPERTIES OF CA3

6.3.1 CA3 has several sources of feedforward inhibition

Granule cell firing *in vivo* is generally low (~1 Hz) (Jung and McNaughton, 1993; Henze et al., 2002), with occasional bursts of higher frequencies up to instantaneous frequencies of 100s of Hz as the rat traverses a place field (Jung and McNaughton, 1993; Henze et al., 2002). The question of what amount of input is sufficient to allow spike transmission at granule cell to pyramidal and interneuron targets has been addressed previously (Miles, 1990; Henze et al., 2002; Lawrence et al., 2004; Mori et al., 2004). The importance of this question cannot be underestimated. The function of the CA3 network is thought to be consolidation of memory through the use of lateral inhibition provided by feedforward interneurons across pyramidal cells (Leutgeb and Leutgeb, 2007), facilitating pattern separation (Kullmann and Lamsa, 2007). Critical to this hypothesis is the precise timing of interneuron and pyramidal cell action potentials in response to an excitatory input (Pouille and Scanziani, 2001).

Henze et al. (2002) performed an *in vivo* experiment where a single granule cell was stimulated and the probability of spike transmission was measured in both pyramidal cells and interneurons. In contrast to the assumed role of MF input to pyramidal cells serving as a "detonator" synapse, it was found that the probability of spike transmission in response to a single granule cell action potential was quite low (Henze et al., 2000). Similarly, though *in vitro* work has demonstrated the ability of the MF to elicit action potentials in interneurons with a single stimulus (Miles, 1990), the *in vivo* results indicated a very low probability of spike transmission (Henze et al., 2000). For both cell types, the probability of spike transmission increased with trains of stimuli at high frequencies, though the probability was higher in

pyramidal cells than interneurons (Henze et al., 2000), which has also been demonstrated *in vitro* (Lawrence et al., 2004).

Coupled with these data describing the probability of spike transmission is the anatomical finding that mossy fibers target interneurons ~ ten times more often than pyramidal cells (Acsady et al., 1998). Furthermore, the postsynaptic densities in apposition to filopodial extensions are longer than those found in apposition to giant bouton active zones, and they are frequently perforated (Acsady et al., 1998) indicating a higher concentration of AMPAR, and thus a stronger synaptic connection (Ganeshina et al., 2004). The number of active zones (functional transmitter release sites) however, evens the numbers as there are approximately thirty active zones per giant mossy fiber bouton targeting pyramidal cells vs. one active zone per contact with interneurons (Acsady et al., 1998). Thus, the postsynaptic potentials recorded in pyramidal cells in response to stimulation of a single granule cell axon are larger than those recorded in interneurons (Lawrence et al., 2004; Mori et al., 2004).

The interpretation of these results was the hypothesis that, at low frequencies of activity, the overall output of the mossy fiber system would be inhibition, but that at higher frequencies, the ratio of inhibition to excitation would flip, allowing pyramidal cells to become active (Lawrence and McBain, 2003). Recent experiments recording intracellularly from pairings of granule cells, pyramidal cells and str. lucidum interneurons in hippocampal slice culture have confirmed this hypothesis, demonstrating that as granule cell stimulation frequency is increased from 10 Hz to 40 Hz, the compound EPSP / IPSP recorded from a CA3 pyramidal cell shifts from a predominantly inhibitory response at 10 Hz to predominantly excitatory at 40 Hz (Mori et al., 2004). Maintenance of this strong inhibitory component at low frequencies has relied on the relatively high probability of release and large quantal amplitude of MF input to str. lucidum

interneuron (Lawrence et al., 2004), as well as the high convergence rate of interneurons onto CA3 pyramidal cells (Vida and Frotscher, 2000; Lawrence and McBain, 2003; Mori et al., 2004). Because the hypothesized basis of this feature of the CA3 network relies so heavily on connectivity ratios and relative synaptic strengths, modulation is only possible through long term plasticity of the individual synaptic strengths to coordinate a change in the overall output of the pyramidal cell. This may be enhanced by the observation that a group of interneurons targeted by the same granule cell converge their inhibitory input onto a pyramidal cell also targeted by that granule cell (Mori et al., 2007). This would imply that the lateral inhibition required by models of pattern separation would be created by recurrent collateral input to other subgroups of interneurons targeting neighboring CA3 pyramidal cells.

All of this work, however, ignores the existence of other feedforward interneurons in CA3 of the hippocampus. The work presented here presents a group of interneurons with soma in the str. lacunosum moleculare that receive input from many granule cells throughout their dendritic arbors that then provide inhibitory input to the apical dendrite of CA3 pyramidal cells. These interneurons may, in fact, be a crucial aspect to the feedforward inhibition required by CA3, possibly by serving a complementary role to the str. lucidum interneurons. Since there is evidence that interneurons receiving MF input from a single granule cell converge on the pyramidal cell also receiving input from that granule cell (Mori et al., 2007), it would seem that another population that targets divergent pyramidal cells would be required. It is possible that these interneurons serve that purpose. Furthermore, since MF input to str. lucidum interneurons undergoes short term and long term depression, the discovery of a population of feedforward interneurons that facilitate in response to MF input, as L-Mi do, indicates they may serve a complementary function.

6.3.2 Hypothesized role of L-Mi in the CA3 network

Having presented my data and discussed many aspects of MF input to L-Mi, I will present a simple model of the role of the L-Mi in the CA3 network. L-Mi receive input from the PP and the MF. There is evidence that both of these inputs have relatively small quantal amplitudes, and as a result, it is my hypothesis that these interneurons rely on convergence of inputs to achieve action potential threshold. Thus, as the entorhinal cortex becomes active, the PP synapses on the L-Mi, dentate gyrus granule cells and CA3 pyramidal cells. Though the PP input is insufficient to elicit firing in the pyramidal cells and interneurons, granule cells becomes active, and the MF synapses onto L-Mi and CA3 pyramidal cells, as well as str. lucidum interneurons. If the MF input is at a low frequency, only CA3 pyramidal cells and str. lucidum interneurons will become active, and as a result of the network properties, the overall result will be inhibition mediated by the str. lucidum interneurons (Lawrence and McBain, 2003; Mori et al., 2004).

If, on the other hand, the MF input is a burst of high frequency input, the pyramidal cell, str. lucidum interneuron and L-Mi will become active, though at different time points. The str. lucidum interneuron and CA3 pyramidal cells have a similar latency to first firing, though the probability of firing is generally higher in the pyramidal cell (Henze et al., 2002; Lawrence et al., 2004). Thus, the RC pathway will also become active, setting off a ripple of pyramidal cell activity and str. lucidum activity throughout CA3. With a timing delay because of activation of the mGluRs 4/8 on MF terminals, L-Mi will also become active, and exert strong inhibition along the apical dendrites of CA3 pyramidal cells, where RC input also converges (Lacaille and Schwartzkroin, 1988; Bertrand and Lacaille, 2001; Ascoli et al., 2009). In this way, the L-Mi provides feedforward inhibition from the MF and PP to the CA3 pyramidal cell that modulates the feedback excitation of the RC pathway.

Though the model is simplistic, it provides testable hypotheses as to the role of the L-Mi in the CA3 network and is a starting point for a more general model of CA3 function that incorporates inhibition from multiple sources. Furthermore, it allows for modulation of the circuit on short time scales, using patterns of activity that are physiologic, rather than imposing requirements of long tetani to modulate the system. As a result, these data and the model I have put forth, provide new leads into understanding the function of the CA3 network. Furthermore, these data highlight how observations of the details of synaptic physiology can translate into a better understanding of network properties.

BIBLIOGRAPHY

Acsady L, Kamondi A, Sik A, Freund T, Buzsaki G (1998) GABAergic cells are the major postsynaptic targets of mossy fibers in the rat hippocampus. J Neurosci 18:3386-3403.

Ali AB, Nelson C (2006) Distinct Ca2+ Channels Mediate Transmitter Release at Excitatory Synapses Displaying Different Dynamic Properties in Rat Neocortex. Cereb Cortex 16:386-393.

Alle H, Jonas P, Geiger JRP (2001) PTP and LTP at a hippocampal mossy fiber-interneuron synapse. Proceedings of the National Academy of Sciences of the United States of America 98:14708-14713.

Amaral D, Lavenex P (2007) Hippocampal Neuroanatomy. In: The hippocampus book (Andersen P, ed), pp 37 - 114. New York: Oxford University Press.

Amaral DG (1979) Synaptic extensions from the mossy fibers of the fascia dentata. Anat Embryol (Berl) 155:241-251.

Amaral DG, Ishizuka N, Claiborne B (1990) Neurons, numbers and the hippocampal network. Prog Brain Res 83:1-11.

Andersen P, Bliss T, Skrede K (1971) Lamellar organization of hippocampal excitatory pathways. Experimental Brain Research 13:222-238.

Anwyl R (1999) Metabotropic glutatmate receptors: electrophysiological properties and role in plasticity. Brain Research Reviews 29:83-120.

Ascoli GA, Brown KM, Calixto E, Card JP, Galván EJ, Perez-Rosello T, Barrionuevo G (2009) Quantitative morphometry of electrophysiologically identified CA3b interneurons reveals robust local geometry and distinct cell classes. The Journal of Comparative Neurology 515:677-695.

Avoli M, D'Antuono M, Louvel J, Köhling R, Biagini G, Pumain R, D'Arcangelo G, Tancredi V (2002) Network and pharmacological mechanisms leading to epileptiform synchronization in the limbic system in vitro. Progress in Neurobiology 68:167-207.

Barnes-Davies M, Forsythe ID (1995) Pre- and postsynaptic glutamate receptors at a giant excitatory synapse in rat auditory brainstem slices. The Journal of Physiology 488:387-406.

Bekkers JM, Clements JD (1999) Quantal amplitude and quantal variance of strontium-induced asynchronous EPSCs in rat dentate granule neurons. The Journal of Physiology 516:227-248.

Bertrand S, Lacaille J-C (2001) Unitary synaptic currents between lacunosum-moleculare interneurones and pyramidal cells in rat hippocampus. The Journal of Physiology 532:369-384.

Betz WJ (1970) Depression of transmitter release at the neuromuscular junction of the frog. The Journal of Physiology 206:629-644.

Billups B, Graham BP, Wong AYC, Forsythe ID (2005) Unmasking group III metabotropic glutamate autoreceptor function at excitatory synapses in the rat CNS. The Journal of Physiology 565:885-896.

Bliss TVP, Lomo T (1973) Long-lasting potentiation of synaptic transmission in the dentate area of the anaesthetized rabbit following stimulation of the perforant path. The Journal of Physiology 232:331-356.

Bradley SR, Levey AI, Hersch SM, Conn PJ (1996) Immunocytochemical localization of group III metabotropic glutamate receptors in the hippocampus with subtype-specific antibodies. J Neurosci 16:2044-2056.

Bradley SR, Standaert DG, Rhodes KJ, Rees HD, Testa CM, Levey AI, Conn PJ (1999) Immunohistochemical localization of subtype 4a metabotropic glutamate receptors in the rat and mouse basal ganglia. The Journal of Comparative Neurology 407:33-46.

Breustedt J, Vogt KE, Miller RJ, Nicoll RA, Schmitz D (2003) alpha1E-Containing Ca2+ channels are involved in synaptic plasticity. Proceedings of the National Academy of Sciences of the United States of America 100:12450-12455.

Buhl EH, Halasy K, Somogyi P (1994) Diverse sources of hippocampal unitary inhibitory postsynaptic potentials and the number of synaptic release sites. Nature 368:823-828.

Calixto E, Galvan EJ, Card JP, Barrionuevo G (2008) Coincidence detection of convergent perforant path and mossy fibre inputs by CA3 interneurons. J Physiol 586:2695-2712.

Cartmell J, Schoepp DD (2000) Regulation of Neurotransmitter Release by Metabotropic Glutamate Receptors. Journal of Neurochemistry 75:889-907.

Castillo PE, Weisskopf MG, Nicoll RA (1994) The role of Ca2+ channels in hippocampal mossy fiber synaptic transmission and long-term potentiation. Neuron 12:261-269.

Catterall WA, Few AP (2008) Calcium Channel Regulation and Presynaptic Plasticity. Neuron 59:882-901.

Chen C-Y, Ling E-h, Horowitz JM, Bonham AC (2002) Synaptic transmission in nucleus tractus solitarius is depressed by Group II and III but not Group I presynaptic metabotropic glutamate receptors in rats. The Journal of Physiology 538:773-786.

Chitwood RA, Jaffe DB (1998) Calcium-dependent spike-frequency accommodation in hippocampal CA3 nonpyramidal neurons. J Neurophysiol 80:983-988.

Claiborne BJ, Amaral DG, Cowan WM (1986) A light and electron microscopic analysis of the mossy fibers of the rat dentate gyrus. J Comp Neurol 246:435-458.

Conn PJ, Pin JP (1997) Pharmacology and functions of metabotropic glutamate receptors. Annual Review of Pharmacology and Toxicology 37:205-237.

Cope DW, Maccaferri G, Marton LF, Roberts JD, Cobden PM, Somogyi P (2002) Cholecystokinin-immunopositive basket and Schaffer collateral-associated interneurones target different domains of pyramidal cells in the CA1 area of the rat hippocampus. Neuroscience 109:63-80.

Corti C, Aldegheri L, Somogyi P, Ferraguti F (2002) Distribution and synaptic localisation of the metabotropic glutamate receptor 4 (mGluR4) in the rodent CNS. Neuroscience 110:403-420.

Cosgrove KE, Galván EJ, Meriney SD, Barrionuevo G (2009) Area CA3 interneurons receive two spatially segregated mossy fiber inputs. Hippocampus 9999:NA.

de Jong AP, Verhage M (2009) Presynaptic signal transduction pathways that modulate synaptic transmission. Current Opinion in Neurobiology 19:245-253.

Dev KK, Nakanishi S, Henley JM (2001) Regulation of mglu7 receptors by proteins that interact with the intracellular C-terminus. Trends in Pharmacological Sciences 22:355-361.
Doherty J, Dingledine R (1998) Differential Regulation of Synaptic Inputs to Dentate Hilar Border Interneurons by Metabotropic Glutamate Receptors. J Neurophysiol 79:2903-2910.
Doherty J, Dingledine R (2001) Reduced Excitatory Drive onto Interneurons in the Dentate Gyrus after Status Epilepticus. J Neurosci 21:2048-2057.
Dudek SM, Bear MF (1992) Homosynaptic long-term depression in area CA1 of hippocampus and effects of N-methyl-D-aspartate receptor blockade. Proceedings of the National Academy of Sciences of the United States of America 89:4363-4367.
El Far O, Airas J, Wischmeyer E, Nehring RB, Karschin A, Betz H (2000) Interaction of the C-terminal tail region of the metabotropic glutamate receptor 7 with the protein kinase C substrate PICK1. European Journal of Neuroscience 12:4215-4221.
Evans RM, Zamponi GW (2006) Presynaptic Ca2+ channels - integration centers for neuronal signaling pathways. Trends in Neurosciences 29:617-624.
Ferguson SSG (2001) Evolving Concepts in G Protein-Coupled Receptor Endocytosis: The Role in Receptor Desensitization and Signaling. Pharmacological Reviews 53:1-24.
Ferraguti F, Shigemoto R (2006) Metabotropic glutamate receptors. Cell and Tissue Research 326:483-504.
Ferraguti F, Klausberger T, Cobden P, Baude A, Roberts JDB, Szucs P, Kinoshita A, Shigemoto R, Somogyi P, Dalezios Y (2005) Metabotropic Glutamate Receptor 8-Expressing Nerve Terminals Target Subsets of GABAergic Neurons in the Hippocampus. J Neurosci 25:10520-10536.
Ferrante M, Migliore M, Ascoli GA (2009) Feed-forward inhibition as a buffer of the neuronal input-output relation. Proceedings of the National Academy of Sciences 106:18004-18009.
Freund TF, Buzsáki G (1996) Interneurons of the hippocampus. Hippocampus 6:347-470.
Fricker D, Miles R (2000) EPSP Amplification and the Precision of Spike Timing in Hippocampal Neurons. Neuron 28:559-569.
Galvan EJ, Calixto E, Barrionuevo G (2008) Bidirectional Hebbian Plasticity at Hippocampal Mossy Fiber Synapses on CA3 Interneurons. J Neurosci 28:14042-14055.
Ganeshina O, Berry RW, Petralia RS, Nicholson DA, Geinisman Y (2004) Differences in the expression of AMPA and NMDA receptors between axospinous perforated and nonperforated synapses are related to the configuration and size of postsynaptic densities. The Journal of Comparative Neurology 468:86-95.
Geiger JRP, Jonas P (2000) Dynamic Control of Presynaptic Ca2+ Inflow by Fast-Inactivating K+ Channels in Hippocampal Mossy Fiber Boutons. Neuron 28:927-939.
Goda Y, Stevens C (1994) Two components of transmitter release at a central synapse. Proceedings of the National Academy of Sciences of the United States of America 91:12942-12946.
Gulyás AI, Miettinen R, Jacobowitz DM, Freund TF (1992) Calretinin is present in non-pyramidal cells of the rat hippocampus--I. A new type of neuron specifically associated with the mossy fibre system. Neuroscience 48:1-27.
Guo J, Ikeda SR (2005) Coupling of Metabotropic Glutamate Receptor 8 to N-Type Ca2+ Channels in Rat Sympathetic Neurons. Molecular Pharmacology 67:1840-1851.

Harris EW, Cotman CW (1986) Long-term potentiation of guinea pig mossy fiber responses is not blocked by N-methyl d-aspartate antagonists. Neuroscience Letters 70:132-137.
Henze DA, Urban NN, Barrionuevo G (2000) The multifarious hippocampal mossy fiber pathway: a review. Neuroscience 98:407-427.
Henze DA, Wittner L, Buzsaki G (2002) Single granule cells reliably discharge targets in the hippocampal CA3 network in vivo. Nat Neurosci 5:790-795.
Hirbec Hln, Perestenko O, Nishimune A, Meyer G, Nakanishi S, Henley JM, Dev KK (2002) The PDZ Proteins PICK1, GRIP, and Syntenin Bind Multiple Glutamate Receptor Subtypes. Journal of Biological Chemistry 277:15221-15224.
Hughes JR (2008) Gamma, fast, and ultrafast waves of the brain: Their relationships with epilepsy and behavior. Epilepsy & Behavior 13:25-31.
Inchauspe CG, Martini FJ, Forsythe ID, Uchitel OD (2004) Functional Compensation of P/Q by N-Type Channels Blocks Short-Term Plasticity at the Calyx of Held Presynaptic Terminal. J Neurosci 24:10379-10383.
Jonas P, Major G, Sakmann B (1993) Quantal components of unitary EPSCs at the mossy fibre synapse on CA3 pyramidal cells of rat hippocampus. J Physiol 472:615-663.
Jones MV, Westbrook GL (1996) The impact of receptor desensitization on fast synaptic transmission. Trends in Neurosciences 19:96-101.
Jung MW, McNaughton BL (1993) Spatial selectivity of unit activity in the hippocampal granular layer. Hippocampus 3:165-182.
Kamiya H, Zucker RS (1994) Residual Ca2 + and short-term synaptic plasticity. Nature 371:603-606.
Kamiya H, Shinozaki H, Yamamoto C (1996) Activation of metabotropic glutamate receptor type 2/3 suppresses transmission at rat hippocampal mossy fibre synapses. J Physiol 493 (Pt 2):447-455.
Katz B, Miledi R (1968) The role of calcium in neuromuscular facilitation. The Journal of Physiology 195:481-492.
Khazipov R, Congar P, Ben-Ari Y (1995) Hippocampal CA1 lacunosum-moleculare interneurons: modulation of monosynaptic GABAergic IPSCs by presynaptic GABAB receptors. J Neurophysiol 74:2126-2137.
Klausberger T, Somogyi P (2008) Neuronal Diversity and Temporal Dynamics: The Unity of Hippocampal Circuit Operations. Science 321:53-57.
Klausnitzer J, Manahan-Vaughan D (2008) Frequency Facilitation at Mossy Fiber-CA3 Synapses of Freely Behaving Rats Is Regulated by Adenosine A1 Receptors. J Neurosci 28:4836-4840.
Ko J, Yoon C, Piccoli G, Chung HS, Kim K, Lee J-R, Lee HW, Kim H, Sala C, Kim E (2006) Organization of the Presynaptic Active Zone by ERC2/CAST1-Dependent Clustering of the Tandem PDZ Protein Syntenin-1. J Neurosci 26:963-970.
Koester HJ, Johnston D (2005) Target Cell-Dependent Normalization of Transmitter Release at Neocortical Synapses. Science 308:863-866.
Kullmann DM, Lamsa KP (2007) Long-term synaptic plasticity in hippocampal interneurons. Nat Rev Neurosci 8:687-699.
Kunkel DD, Lacaille J-C, Schwartzkroin PA (1988) Ultrastructure of stratum lacunosum moleculare interneurons of hippocampal CA1 region. Synapse 2:382-394.

Lacaille JC, Schwartzkroin PA (1988) Stratum lacunosum-moleculare interneurons of hippocampal CA1 region. II. Intrasomatic and intradendritic recordings of local circuit synaptic interactions. J Neurosci 8:1411-1424.

Laezza F, Doherty JJ, Dingledine R (1999) Long-Term Depression in Hippocampal Interneurons: Joint Requirement for Pre- and Postsynaptic Events. Science 285:1411-1414.

Lawrence JJ, McBain CJ (2003) Interneuron Diversity series: Containing the detonation - feedforward inhibition in the CA3 hippocampus. Trends in Neurosciences 26:631-640.

Lawrence JJ, Grinspan ZM, McBain CJ (2004) Quantal transmission at mossy fibre targets in the CA3 region of the rat hippocampus. The Journal of Physiology 554:175-193.

Lee D, Lee K-H, Ho W-K, Lee S-H (2007) Target Cell-Specific Involvement of Presynaptic Mitochondria in Post-Tetanic Potentiation at Hippocampal Mossy Fiber Synapses. J Neurosci 27:13603-13613.

Lei S, McBain CJ (2002) Distinct NMDA Receptors Provide Differential Modes of Transmission at Mossy Fiber-Interneuron Synapses. Neuron 33:921-933.

Lei S, McBain CJ (2004) Two Loci of Expression for Long-Term Depression at Hippocampal Mossy Fiber-Interneuron Synapses. J Neurosci 24:2112-2121.

Leutgeb JK, Leutgeb S, Moser M-B, Moser EI (2007) Pattern Separation in the Dentate Gyrus and CA3 of the Hippocampus. Science 315:961-966.

Leutgeb S, Leutgeb JK (2007) Pattern separation, pattern completion, and new neuronal codes within a continuous CA3 map. Learning & Memory 14:745-757.

Li L, Bischofberger J, Jonas P (2007) Differential Gating and Recruitment of P/Q-, N-, and R-Type Ca2+ Channels in Hippocampal Mossy Fiber Boutons. J Neurosci 27:13420-13429.

Lisman JE (1999) Relating Hippocampal Circuitry to Function: Recall of Memory Sequences by Reciprocal Dentate-CA3 Interactions. Neuron 22:233-242.

Lorez M, Humbel U, Pflimlin M-C, Kew JNC (2003) Group III metabotropic glutamate receptors as autoreceptors in the cerebellar cortex. British Journal of Pharmacology 138:614-625.

Losonczy A, Somogyi P, Nusser Z (2003) Reduction of Excitatory Postsynaptic Responses by Persistently Active Metabotropic Glutamate Receptors in the Hippocampus. J Neurophysiol 89:1910-1919.

Lysetskiy M, Földy C, Soltesz I (2005) Long- and short-term plasticity at mossy fiber synapses on mossy cells in the rat dentate gyrus. Hippocampus 15:691-696.

Maccaferri G, Toth K, McBain CJ (1998) Target-specific expression of presynaptic mossy fiber plasticity. Science 279:1368-1370.

Macek TA, Winder DG, Gereau RW, Ladd CO, Conn PJ (1996) Differential involvement of group II and group III mGluRs as autoreceptors at lateral and medial perforant path synapses. J Neurophysiol 76:3798-3806.

Malenka RC (1993) Long-term depression: not so depressing after all. Proceedings of the National Academy of Sciences of the United States of America 90:3121-3123.

Manzoni OJ, Castillo PE, Nicoll RA (1995) Pharmacology of metabotropic glutamate receptors at the mossy fiber synapses of the guinea pig hippocampus. Neuropharmacology 34:965-971.

Markram H, Wang Y, Tsodyks M (1998) Differential signaling via the same axon of neocortical pyramidal neurons. Proceedings of the National Academy of Sciences of the United States of America 95:5323-5328.

McBain CJ, Fisahn A (2001) Interneurons unbound. Nat Rev Neurosci 2:11-23.
McNaughton BL, Morris RGM (1987) Hippocampal synaptic enhancement and information storage within a distributed memory system. Trends in Neurosciences 10:408-415.
Miles R (1990) Synaptic excitation of inhibitory cells by single CA3 hippocampal pyramidal cells of the guinea-pig in vitro. The Journal of Physiology 428:61-77.
Millan C, Lujan R, Shigemoto R, Sanchez-Prieto J (2002) Subtype-specific Expression of Group III Metabotropic Glutamate Receptors and Ca2+ Channels in Single Nerve Terminals. Journal of Biological Chemistry 277:47796-47803.
Millán C, Sánchez-Prieto J (2002) Differential coupling of N- and P/Q-type calcium channels to glutamate exocytosis in the rat cerebral cortex. Neuroscience Letters 330:29-32.
Mistry R, Mellor JR (2008) Bidirectional activity-dependent plasticity of membrane potential and the influence on spiking in rat hippocampal dentate granule cells. Neuropharmacology 54:290-299.
Miyazaki K, Ishizuka T, Yawo H (2005) Synapse-to-synapse variation of calcium channel subtype contributions in large mossy fiber terminals of mouse hippocampus. Neuroscience 136:1003-1014.
Moore KA, Nicoll RA, Schmitz D (2003) Adenosine gates synaptic plasticity at hippocampal mossy fiber synapses. Proceedings of the National Academy of Sciences of the United States of America 100:14397-14402.
Mori M, Gahwiler BH, Gerber U (2007) Recruitment of an inhibitory hippocampal network after bursting in a single granule cell. Proceedings of the National Academy of Sciences 104:7640-7645.
Mori M, Abegg MH, Gahwiler BH, Gerber U (2004) A frequency-dependent switch from inhibition to excitation in a hippocampal unitary circuit. Nature 431:453-456.
Nicoll RA, Schmitz D (2005) Synaptic plasticity at hippocampal mossy fibre synapses. Nat Rev Neurosci 6:863-876.
Nomura T, Fukuda T, Aika Y, Heizmann CW, Emson PC, Kobayashi T, Kosaka T (1997) Laminar distribution of non-principal neurons in the rat hippocampus, with special reference to their compositional difference among layers. Brain Research 764:197-204.
Ohishi H, Akazawa C, Shigemoto R, Nakanishi S, Mizuno N (1995) Distribution of the mRNAs for L-2-amino-4-phosphonobutyrate-sensitive metabotropic glutatmate receptors, mGluR4 and mGluR7, in the rat brain. Journal of Comparative Neurology 360:555-570.
Patenaude C, Massicotte G, Lacaille J-C (2005) Cell-type specific GABA synaptic transmission and activity-dependent plasticity in rat hippocampal stratum radiatum interneurons. European Journal of Neuroscience 22:179-188.
Pelkey KA, Topolnik L, Lacaille JC, McBain CJ (2006) Compartmentalized Ca2+ Channel Regulation at Divergent Mossy-Fiber Release Sites Underlies Target Cell-Dependent Plasticity. Neuron 52:497-510.
Pelkey KA, Lavezzari G, Racca C, Roche KW, McBain CJ (2005) mGluR7 is a metaplastic switch controlling bidirectional plasticity of feedforward inhibition. Neuron 46:89-102.
Pelletier JG, Lacaille J-C, Wayne S. Sossin J-CLVFCaSB (2008) Chapter 14 Long-term synaptic plasticity in hippocampal feedback inhibitory networks. In: Progress in Brain Research, pp 241-250: Elsevier.
Penttonen M, Kamondi A, Sik A, Acsády L, Buzsáki G (1997) Feed-forward and feed-back activation of the dentate gyrus in vivo during dentate spikes and sharp wave bursts. Hippocampus 7:437-450.

Perkins KL (2002) GABA Application to Hippocampal CA3 or CA1 Stratum Lacunosum-Moleculare Excites an Interneuron Network. J Neurophysiol 87:1404-1414.
Perkins KL (2006) Cell-attached voltage-clamp and current-clamp recording and stimulation techniques in brain slices. Journal of Neuroscience Methods 154:1-18.
Pinheiro PS, Mulle C (2008) Presynaptic glutamate receptors: physiological functions and mechanisms of action. Nat Rev Neurosci 9:423-436.
Poncer JC, McKinney RA, Gahwiler BH, Thompson SM (2000) Differential control of GABA release at synapses from distinct interneurons in rat hippocampus. The Journal of Physiology 528:123-130.
Pouille F, Scanziani M (2001) Enforcement of temporal fidelity in pyramidal cells by somatic feed-forward inhibition. Science 293:1159-1163.
Price CJ, Karayannis T, Pál BZ, Capogna M (2005) Group II and III mGluRs-mediated presynaptic inhibition of EPSCs recorded from hippocampal interneurons of CA1 stratum lacunosum moleculare. Neuropharmacology 49:45-56.
Rapp PR, Gallagher M (1996) Preserved neuron number in the hippocampus of aged rats with spatial learning deficits. Proceedings of the National Academy of Sciences of the United States of America 93:9926-9930.
Regehr WG, Delaney KR, Tank DW (1994) The role of presynaptic calcium in short-term enhancement at the hippocampal mossy fiber synapse. J Neurosci 14:523-537.
Reid CA, Clements JD, Bekkers JM (1997) Nonuniform Distribution of Ca2+ Channel Subtypes on Presynaptic Terminals of Excitatory Synapses in Hippocampal Cultures. J Neurosci 17:2738-2745.
Reuter H (1995) Measurements of exocytosis from single presynaptic neurve-terminals reveal heterogeneous inhibition by Ca2+ channel blockers. Neuron 14:773-779.
Reyes A, Lujan R, Rozov A, Burnashev N, Somogyi P, Sakmann B (1998) Target-cell-specific facilitation and depression in neocortical circuits. Nat Neurosci 1:279-285.
Romo-Parra H, Trevino M, Heinemann U, Gutierrez R (2008) GABA Actions in Hippocampal Area CA3 During Postnatal Development: Differential Shift From Depolarizing to Hyperpolarizing in Somatic and Dendritic Compartments. J Neurophysiol 99:1523-1534.
Rozov A, Burnashev N, Sakmann B, Neher E (2001) Transmitter release modulation by intracellular Ca2+ buffers in facilitating and depressing nerve terminals of pyramidal cells in layer 2/3 of the rat neocortex indicates a target cell-specific difference in presynaptic calcium dynamics. The Journal of Physiology 531:807-826.
Rusakov DA, Wuerz A, Kullmann DM (2004) Heterogeneity and Specificity of Presynaptic Ca2+ Current Modulation by mGluRs at Individual Hippocampal Synapses. Cereb Cortex 14:748-758.
Salin PA, Scanziani M, Malenka RC, Nicoll RA (1996) Distinct short-term plasticity at two excitatory synapses in the hippocampus. Proceedings of the National Academy of Sciences of the United States of America 93:13304-13309.
Saugstad JA, Kinzie JM, Mulvihill ER, Segerson TP, Westbrook GL (1994) Cloning and expression of a new member of the L-2-amino-4-phosphonobutyric acid-sensitive class of metabotropic glutamate receptors. Molecular Pharmacology 45:367-372.
Saugstad JA, Kinzie JM, Shinohara MM, Segerson TP, Westbrook GL (1997) Cloning and Expression of Rat Metabotropic Glutamate Receptor 8 Reveals a Distinct Pharmacological Profile. Molecular Pharmacology 51:119-125.

Savic N, Pedarzani P, Sciancalepore M (2001) Medium afterhyperpolarization and firing pattern modulation in interneurons of stratum radiatum in the CA3 hippocampal region. J Neurophysiol 85:1986-1997.

Scanziani M, Gahwiler BH, Thompson SM (1995) Presynaptic inhibition of excitatory synaptic transmission by muscarinic and metabotropic glutamate receptor activation in the hippocampus: are Ca2+ channels involved? Neuropharmacology 34:1549-1557.

Scanziani M, Gahwiler BH, Charpak S (1998) Target cell-specific modulation of transmitter release at terminals from a single axon. Proceedings of the National Academy of Sciences of the United States of America 95:12004-12009.

Scanziani M, Salin PA, Vogt KE, Malenka RC, Nicoll RA (1997) Use-dependent increases in glutamate concentration activate presynaptic metabotropic glutamate receptors. Nature 385:630-634.

Scharfman HE (2007) The CA3 "backprojection" to the dentate gyrus. Progress in Brain Research 163:627-637.

Schoepp DD (2001) Unveiling the Functions of Presynaptic Metabotropic Glutamate Receptors in the Central Nervous System. Journal of Pharmacology and Experimental Therapeutics 299:12-20.

Semyanov A, Kullmann DM (2000) Modulation of GABAergic signaling among interneurons by metabotropic glutamate receptors. Neuron 25:663-672.

Shigemoto R, Kinoshita A, Wada E, Nomura S, Ohishi H, Takada M, Flor PJ, Neki A, Abe T, Nakanishi S, Mizuno N (1997) Differential presynaptic localization of metabotropic glutamate receptor subtypes in the rat hippocampus. J Neurosci 17:7503-7522.

Soriano E, Frotscher M (1993) Spiny nonpyramidal neurons in the CA3 region of the rat hippocampus are glutamate-like immunoreactive and receive convergent mossy fiber input. The Journal of Comparative Neurology 333:435-448.

Spruston N, Lübke J, Frotscher M (1997) Interneurons in the stratum lucidum of the rat hippocampus: An anatomical and electrophysiological characterization. The Journal of Comparative Neurology 385:427-440.

Stricker C, Field AC, Redman SJ (1996) Statistical analysis of amplitude fluctuations in EPSCs evoked in rat CA1 pyramidal neurones in vitro. The Journal of Physiology 490:419-441.

Takahashi T, Forsythe I, Tsujimoto T, Barnes-Davies M, Onodera K (1996) Presynaptic calcium current modulation by a metabotropic glutamate receptor. Science 274:594-597.

Tamamaki N, Nojyo Y (1993) Projection of the entorhinal layer II neurons in the rat as revealed by intracellular pressure-injection of neurobiotin. Hippocampus 3:471-480.

Tanabe Y, Nomura A, Masu M, Shigemoto R, Mizuno N, Nakanishi S (1993) Signal transduction, pharmacological properties, and expression patterns of two rat metabotropic glutamate receptors, mGluR3 and mGluR4. J Neurosci 13:1372-1378.

Tang F (2005) Agonists and antagonists of metabotropic glutamate receptors: anticonvulsants and antiepileptogenic agents? Current Neuropharmacology 3:299-307.

Thomson AM (1997) Activity-dependent properties of synaptic transmission at two classes of connections made by rat neocortical pyramidal axons in vitro. The Journal of Physiology 502:131-147.

Toth K, McBain CJ (1998) Afferent-specific innervation of two distinct AMPA receptor subtypes on single hippocampal interneurons. Nat Neurosci 1:572-578.

Toth K, McBain CJ (2000) Target-specific expression of pre- and postsynaptic mechanisms. The Journal of Physiology 525:41-51.

Toth K, Suares G, Lawrence JJ, Philips-Tansey E, McBain CJ (2000) Differential mechanisms of transmission at three types of mossy fiber synapse. J Neurosci 20:8279-8289.
Treves A, Rolls ET (1992) Computational constraints suggest the need for two distinct input systems to the hippocampal CA3 network. Hippocampus 2:189-199.
Treves A, Rolls ET (1994) Computational analysis of the role fo the hippocampus in memory. Hippocampus 4:374-391.
Urban NN, Barrionuevo G (1998) Active summation of excitatory postsynaptic potentials in hippocampal CA3 pyramidal neurons. Proc Natl Acad Sci U S A 95:11450-11455.
Vida I, Frotscher M (2000) A hippocampal interneuron associated with the mossy fiber system. Proceedings of the National Academy of Sciences of the United States of America 97:1275-1280.
Vida I, Bartos M, Jonas P (2006) Shunting Inhibition Improves Robustness of Gamma Oscillations in Hippocampal Interneuron Networks by Homogenizing Firing Rates. Neuron 49:107-117.
von Gersdorff H, Schneggenburger R, Weis S, Neher E (1997) Presynaptic Depression at a Calyx Synapse: The Small Contribution of Metabotropic Glutamate Receptors. J Neurosci 17:8137-8146.
Williams S, Samulack DD, Beaulieu C, LaCaille JC (1994) Membrane properties and synaptic responses of interneurons located near the stratum lacunosum-moleculare/radiatum border of area CA1 in whole-cell recordings from rat hippocampal slices. J Neurophysiol 71:2217-2235.
Witter MP (1993) Organization of the entorhinal-hippocampal system: a review of current anatomical data. Hippocampus 3:33-44.
Wittner L, Henze D, Záborszky L, Buzsáki G (2007) Three-dimensional reconstruction of the axon arbor of a CA3 pyramidal cell recorded and filled in vivo. Brain Structure and Function 212:75-83.
Woodson W, Nitecka L, Ben-Ari Y (1989) Organization of the GABAergic system in the rat hippocampal formation: A quantitative immunocytochemical study. The Journal of Comparative Neurology 280:254-271.
Wu L-G, Saggau P (1997) Presynaptic inhibition of elicited neurotransmitter release. Trends in Neurosciences 20:204-212.
Xu J, Xia J (2006) Structure and Function of PICK1. Neurosignals 15:190-201.
Xu J, He L, Wu L-G (2007) Role of Ca2+ channels in short-term synaptic plasticity. Current Opinion in Neurobiology 17:352-359.
Ylinen A, Soltész I, Bragin A, Penttonen M, Sik A, Buzsáki G (1995) Intracellular correlates of hippocampal theta rhythm in identified pyramidal cells, granule cells, and basket cells. Hippocampus 5:78-90.
Yoshino M, Sawada S, Yamamoto C, Kamiya H (1996) A metabotropic glutamate receptor agonist DCG-IV suppresses synaptic transmission at mossy fiber pathway of the guinea pig hippocampus. Neuroscience Letters 207:70-72.
Zalutsky RA, Nicoll RA (1990) Comparison of Two Forms of Long-Term Potentiation in Single Hippocampal Neurons. Science 248:1619-1624.
Ziv NE, Garner CC (2004) Cellular and molecular mechanisms of presynaptic assembly. Nat Rev Neurosci 5:385-399.
Zucker RS, Regehr WG (2002) Short-term synaptic plasticity. Annual Review of Physiology 64:355-405.